

Polarizing versus depolarizing blood cardioplegia

An experimental study of myocardial function, metabolism and
ultrastructure following cardiopulmonary bypass and cardioplegic arrest

Terje Aass

Thesis for the Degree of Philosophiae Doctor (PhD)
University of Bergen, Norway
2019

UNIVERSITY OF BERGEN



Polarizing versus depolarizing blood cardioplegia

An experimental study of myocardial function,
metabolism and ultrastructure following
cardiopulmonary bypass and cardioplegic arrest

Terje Aass



Thesis for the Degree of Philosophiae Doctor (PhD)
at the University of Bergen

Date of defence: 11.01 2019

© Copyright Terje Aass

The material in this publication is covered by the provisions of the Copyright Act.

Year: 2019

Title: Polarizing versus depolarizing blood cardioplegia

Name: Terje Aass

Print: Skipnes Kommunikasjon / University of Bergen

'Of the heart... This moves of itself and does not stop unless forever.'
Dell' anatomia, fogli B by Leonardo da Vinci (1452–1519).

TABLE OF CONTENTS

1. ACKNOWLEDGEMENT	7
2. SCIENTIFIC ENVIRONMENT	9
3. ABSTRACT	10
4. LIST OF PAPERS	12
5. ABBREVIATIONS	13
6. INTRODUCTION	15
6.1 Background	15
6.2 Myocardial energy and oxygen consumption	15
6.3 Cardioplegic mechanisms	18
6.3.1 Depolarized cardioplegic arrest	18
6.3.2 Polarized cardioplegic arrest	20
6.4 Esmolol	21
6.5 Adenosine	21
6.6 Magnesium	22
6.7 Procaine	22
6.8 Blood	23
6.9 Temperature	23
7. AIM OF THE PROJECT	24
8. METHODS	25
8.1 Animals and anesthesia	25
8.2 Surgical protocol and instrumentation	26
8.3 Cardiopulmonary bypass	27
8.4 Cardioplegia	28
8.5 Pressure-volume conductance catheter	30
8.5.1 Pressure-volume loops	31

8.5.2 Acquisition	32
8.5.3 Load-independent indices of LV systolic and diastolic function	33
8.5.4 Analysis	35
8.6 Epicardial echocardiography	35
8.6.1 Strain and strain rate	36
8.6.2 Tissue Doppler Imaging	37
8.6.3 Speckle Tracking Echocardiography	37
8.6.4 Acquisition	38
8.6.5 Analysis	39
8.7 Myocardial tissue samples	39
8.7.1 Apoptosis	41
8.7.2 β -receptor activity	42
8.7.3 Oxidative stress	43
8.7.4 Metabolism	43
8.7.5 Ultrastructure	44
8.7.6 Regional tissue blood flow and water content	46
8.8 Left ventricular mechanical efficiency	47
8.9 Blood chemistry	47
8.10 Experimental protocols	48
8.10.1 Paper I	48
8.10.2 Paper II	48
8.10.3 Paper III	49
8.11 Statistical analysis	49
9. SUMMARY OF RESULTS	50
9.1 Paper I	50
9.2 Paper II	51
9.3 Paper III	52

10. DISCUSSION	53
10.1 Polarizing cardioplegia	53
10.2 Esmolol and adenosine for myocardial protection	53
10.2.1 Esmolol	53
10.2.2 Adenosine	55
10.3 Polarized vs. depolarized cardioplegic arrest	56
10.4 Energy metabolism	57
10.5 Ultrastructure	59
10.6 Weaning from cardiopulmonary bypass	59
10.7 General hemodynamics	60
10.8 Systolic and diastolic function	61
10.9 Myocardial injury	62
10.10 Myocardial dysfunction	64
10.11 Methodological considerations	65
10.11.1 Animal model	65
10.11.2 Study design	67
10.11.3 Conductance catheter	68
10.11.4 Epicardial echocardiography	71
10.11.5 Myocardial oxygen consumption and mechanical efficiency	74
10.11.6 Metabolism	75
10.11.7 Ultrastructure	76
11. FUTURE PERSPECTIVE	77
12. CONCLUSION	78
13. ERRATUM	79
14. REFERENCES	80
15. PAPERS I - III	95

1. ACKNOWLEDGEMENT

This thesis is the result of an extensive collaboration with outstanding co-workers, colleagues and staff whom all have been most supportive on a scientific, practical and/or personal level.

First of all, I want to express my deepest gratitude to my main supervisor, professor Ketil Grong. He gave me the golden opportunity to be a part of his scientific group at the Vivarium and was the initiator of this PhD-project. His superb experience and knowledge in research using experimental *in-vivo* models, together with a never-ending enthusiasm and perfectionism has without exception been motivating and exceedingly essential in all processes of the project. By always sharing his expertise in an educational and altruistic manner, his supervision has been outstanding. Furthermore, I am very grateful to my co-supervisor professor Knut Matre, who has a profound knowledge in assessment of myocardial function by echocardiography. Matre has been a fundamental mentor in teaching me echocardiography, both practical skills required during the experiments as well as in the analysis and the interpretation of data. His positive attitude and continuing interest for scientific discussions have been greatly appreciated. I would express my gratitude to professor Rune Haaverstad for giving me the opportunity to combine experimental research with clinical practice. As co-supervisor and Chief of Section of Cardiothoracic Surgery, he has been very important in both my scientific and clinical advancement. His consistently hard work and dedication in the field of cardiothoracic surgery have always been inspiring.

I am very grateful for the collaboration with David J. Chambers (BSc, PhD) at the Rayne Institute (King's College London), St Thomas' Hospital, London, United Kingdom. He has an extensive knowledge in this field of basic research and is one of the inventors of the novel cardioplegic solution investigated in this thesis. The collaboration in this project has been of mutual benefit and hopefully of great importance for the future implementation of the novel cardioplegic method into clinical practice. I would also thank Thomais Markou (PhD) at the Rayne Institute for the cooperation in Paper I. Additionally, I appreciate the collaboration in Paper II with

professor Seth Hallström and Christine Rossmann (PhD), Medical University of Graz, Austria and professor Bruno K. Podesser, Medical University of Vienna, Austria.

Professor emeritus Lodve Stangeland has been an exceptional loyal co-worker during all experimental studies and I am in grateful debt to him for all his support. I would also thank my fellow researchers and colleagues Christian Arvei Moen (MD, PhD), Geir Olav Dahle (MD, PhD), Pirjo-Riitta Salminen (MD, PhD) and Atle Solholm (MD) for their contributions in many aspects of the project. Despite their own busy workday of research and clinical practice, they have all been incredibly forthcoming and helpful. Accomplishing the experiments have been thoroughly reliant on the perfusionists responsible for the management of the heart-lung machine. I would like to thank Finn Eliassen (CCP), Malte Urban (CCP) and Knut Nesheim (MSc, CCP) for their positive manner, flexibility and professional influence on our team. The technical assistance from Lill-Harriet Andreassen, Cato Johnsen, Kjersti Milde and Rune Grøvdal has been exceptional during long and extensive experiments. I do not take their help for granted but really appreciate all their efforts. Likewise, I would like to thank Gry-Hilde Nilsen, Anne Aarsand and Randi Sandvik for handling and analyzing a considerable amount of tissue samples.

I would express my gratitude to the Western Norway Regional Health Authority, the Bergen University Heart Fund, the Norwegian Health Association, the Grieg Foundation, the Norwegian Research School in Medical Imaging and the Department of Heart Disease at Haukeland University Hospital for funding the project. Their generous financial support made this project achievable.

Finally, I am sincerely grateful to my family for their patience and support during both my scientific and clinical working day. To my wife Kari and our children Margrethe, Nikolai and Daniel, you give me perspective to what matters most in life!

2. SCIENTIFIC ENVIRONMENT

The present PhD-thesis is based on experimental studies conducted from 2013 until 2016 at the Department of Clinical Science, Faculty of Medicine, University of Bergen in collaboration with Section of Cardiothoracic Surgery, Department of Heart Disease, Haukeland University Hospital.

Main supervisor Professor Ketil Grong
Department of Clinical Science, Faculty of Medicine
University of Bergen

Co-supervisor Professor Knut Matre
Department of Clinical Science, Faculty of Medicine
University of Bergen

Co-supervisor Professor Rune Haaverstad
Department of Clinical Science, Faculty of Medicine
University of Bergen

Section of Cardiothoracic Surgery
Department of Heart Disease
Haukeland University Hospital

3. ABSTRACT

In cardiothoracic surgery, the use of the heart-lung machine for cardiopulmonary bypass (CPB) and induced cardiac arrest, cardioplegia, is required for performing the majority of the surgical procedures. Myocardial protection is essential during the ischemic period of cardioplegia. The aim of this project is to evaluate and verify if a recently developed routine for myocardial protection is feasible, safe and suited for use in clinical practice. This pre-clinical translational animal research project is designed to bridge the gap between basic research and new routines that may benefit the patient. In three different protocols, two groups of animals (10 in each group) are randomized to polarized or depolarized cardioplegic arrest. The novel and unexplored cardioplegic solution with esmolol, adenosine and magnesium; St Thomas' Hospital polarizing cardioplegia (STH-POL) is compared with today's gold standard; potassium-based St Thomas' depolarizing solution (STH-2), both administered as repeated, cold, oxygenated blood. Left ventricular regional and global function in the early hours after weaning from CPB are evaluated together with myocardial ultrastructure and metabolism. Our hypothesis is that STH-POL improves myocardial protection demonstrated as better preserved postoperative cardiac function in a large animal translational model. This knowledge is essential before initiating clinical studies and implementation. An optimal myocardial protection is important when performing cardiac surgery in an ageing population with increased occurrence of more complex heart diseases and comorbidity.

Paper I demonstrated improved regional and global contractility following 60 min of cardioplegic arrest with STH-POL compared to STH-2 blood cardioplegia. After weaning from CPB and following reperfusion, left ventricular dP/dt_{max} , Preload Recrutable Stroke Work and radial peak systolic strain rate were maintained 180 min after declamping in the group with polarized arrest and decreased with depolarized arrest.

Paper II focused on energy metabolism and ultrastructure with the STH-POL compared to the STH-2 cardioplegia during 60 min of cardiac arrest and at early reperfusion. The study demonstrated increased levels of creatine phosphate in left ventricular myocardial tissue samples at the end of the period of cardioplegic arrest and early after reperfusion in the STH-POL compared to the STH-2 group. Furthermore, the adenosine triphosphate content was increased and the mitochondrial surface-to-volume ratio decreased with polarizing compared to depolarizing cardioplegia 20 min after reperfusion. However, at 180 min after reperfusion these group differences were negligible.

Paper III addressed myocardial function after prolonged cardioplegic arrest for 120 min. A temporary increase in the load-independent contractility variable Preload Recruitable Stroke Work was seen in the STH-POL compared to the STH-2 group 150 min after declamping. Neither regional nor global left ventricular function differed between groups up to 240 min after declamping. However, compared to the STH-2 group, the left ventricular myocardial tissue blood flow rate decreased in the STH-POL group at 150 and 240 min compared to 60 min after declamping. The relationship between the left ventricular total pressure-volume area and blood flow rate was maintained after declamping in the STH-POL group and decreased in the STH-2 group. Thus, cardioplegic arrest with STH-POL alleviated the mismatch between myocardial function and perfusion after weaning from CPB compared to STH-2.

Conclusion: In a porcine model, cardioplegic arrest with St. Thomas' Hospital polarizing solution offered comparable myocardial protection and improved myocardial function (Paper I), preserved energy status (Paper II) and enhanced contractile efficiency (Paper III) in the early hours after weaning from cardiopulmonary bypass compared to St. Thomas' Hospital No 2 blood cardioplegia.

4. LIST OF PAPERS

I Aass T, Stangeland L, Moen CA, Salminen PR, Dahle GO, Chambers DJ, Markou T, Eliassen F, Urban M, Haaverstad R, Matre K, Grong K.
Myocardial function after polarizing versus depolarizing cardiac arrest with blood cardioplegia in a porcine model of cardiopulmonary bypass.
Eur J Cardiothorac Surg 2016; 50:130-139.

II Aass T, Stangeland L, Chambers DJ, Hallström S, Rossmann C, Podesser BK, Urban M, Nesheim K, Haaverstad R, Matre K, Grong K.
Myocardial energy metabolism and ultrastructure with polarizing and depolarizing cardioplegia in a porcine model.
Eur J Cardiothorac Surg 2017; 52:180-188.

III Aass T, Stangeland L, Solholm A, Moen CA, Dahle GO, Chambers DJ, Urban M, Nesheim K, Haaverstad R, Matre K, Grong K.
Left ventricular dysfunction after two hours of polarizing or depolarizing cardioplegic arrest in a porcine model.
Perfusion 2019; 34:67-75.

5. ABBREVIATIONS

ATP/ADP/AMP	Adenosine tri-, di- and monophosphate
β	The logarithmic regression coefficient of LV compliance
cAMP	Cyclic adenosine monophosphate
CA	Cardioplegic arrest
CI	Cardiac index (L/min/m ²)
CPB	Cardiopulmonary bypass
CPT-I/II	Carnitine palmitoyltransferase-I/II
CrP	Creatine phosphate
CVP	Central venous pressure (mmHg)
ECG	Electrocardiography
EDP	End-diastolic pressure (mmHg)
EDPVR	End-diastolic pressure-volume relation (mmHg/mL)
EDV	End-diastolic volume (mL)
EF	Ejection fraction (%)
ESPVR	End-systolic pressure-volume relation (mmHg/mL)
GRK2	G protein-coupled receptor kinases 2
HLM	Heart-lung machine
HPLC	High-performance liquid chromatography
HR	Heart rate (beats/min)
(i)	Value indexed for body surface area
ICC	Intraclass Correlation Coefficient
J	Joule, unit of energy
LV	Left ventricle
LV-dP/dt _{max}	Peak positive first derivate of LV pressure (mmHg/s)
LV-dP/dt _{min}	Peak negative first derivate of LV pressure (mmHg/s)
MAP	Mean arterial pressure (mmHg)
MDA	Malondialdehyde
MVO ₂	Myocardial oxygen consumption (mL/min/g)
PAP	Pulmonary artery pressure (mmHg)

PE	Potential energy
PRSW	Preload Recrutable Stroke Work (mmHg)
PVA	Pressure-volume area (mmHg*mL or Joule)
RM-ANOVA	Analysis of variance for repeated measurements
ROI	Region of interest
RV	Right ventricle
SL	Strain length (mm)
STE	Speckle Tracking Echocardiography
STH-2	St. Thomas' Hospital cardioplegic solution No 2
STH-POL	St. Thomas' Hospital polarizing cardioplegic solution
SV	Stroke volume (mL)
S_{vmit}	Mitochondrial surface density
$S_{vratio_{mit}}$	Mitochondrial surface-to-volume ratio
SW	Stroke work (mmHg*mL)
τ	Tau, time constant of isovolumic relaxation (ms)
TDI	Tissue Doppler Imaging

6. INTRODUCTION

6.1 Background

In open heart surgery, the use of cardiopulmonary bypass (CPB) with a heart-lung machine (HLM) and cardioplegic arrest (CA) is required for the majority of the surgical procedures to be done in a motion- and bloodless field.¹ In recent years, equipment and techniques have been developed to perform certain procedures without the use of CPB (off-pump surgery) together with less invasive catheter-based therapies for coronary artery disease, valve disorders and aortic diseases.²⁻⁵ Simultaneously, the need for support by heart-lung machine and cardiopulmonary bypass in modern cardiac and thoracic surgery has been further strengthened. Improved treatment routines and procedures for myocardial infarction and other cardiac life-threatening events have increased the chances of surviving the acute phase.⁶ This, together with increased life expectancy, has increased the age of the patient population that currently is offered cardiothoracic surgery.^{7,8} Furthermore, many of today's patients present reduced cardiac function preoperatively and/or are in need for concomitant coronary artery bypass surgery (CABG) and valve surgery or other combined procedures which require prolonged cardioplegic arrest. At the same time, the proportion of patients with diabetes, lung- and kidney diseases and other co-morbidity has also increased.⁹ The importance of minimizing harmful effects from the use of HLM and optimal myocardial protection has therefore increased.

6.2 Myocardial energy and oxygen consumption

The heart is the most energy-consuming organ in the human body. About 6 kg of adenosine triphosphate (ATP) cycles every day, thus providing the biochemical energy allowing about 100.000 heartbeats following pumping of approximately 10 tons of blood through the body.¹⁰ Cardiac energy metabolism is complex and consists in principle of three main processes (Figure 1).¹¹ The first is substrate utilization, the use of chemical energy stored fuel that originates from food. This process involves cellular uptake of mainly fatty acids and glucose. Beta-oxidation and glycolysis result in

intermediary metabolites that enter the Krebs cycle. The second component is the production of energy by oxidative phosphorylation by the mitochondrial respiratory chain. Phosphorylation of ADP produces the high-energy phosphate compound ATP, which is the direct source of energy for all energy-consuming reactions in the heart. The last component is ATP transfer and utilization. The energy-transfer mechanism to the myofibrils is also termed the creatine kinase energy shuttle.¹² Failure to produce, transport or utilize an adequate amount of energy causes functional loss and failure of the contractile work of the myocardium.¹⁰

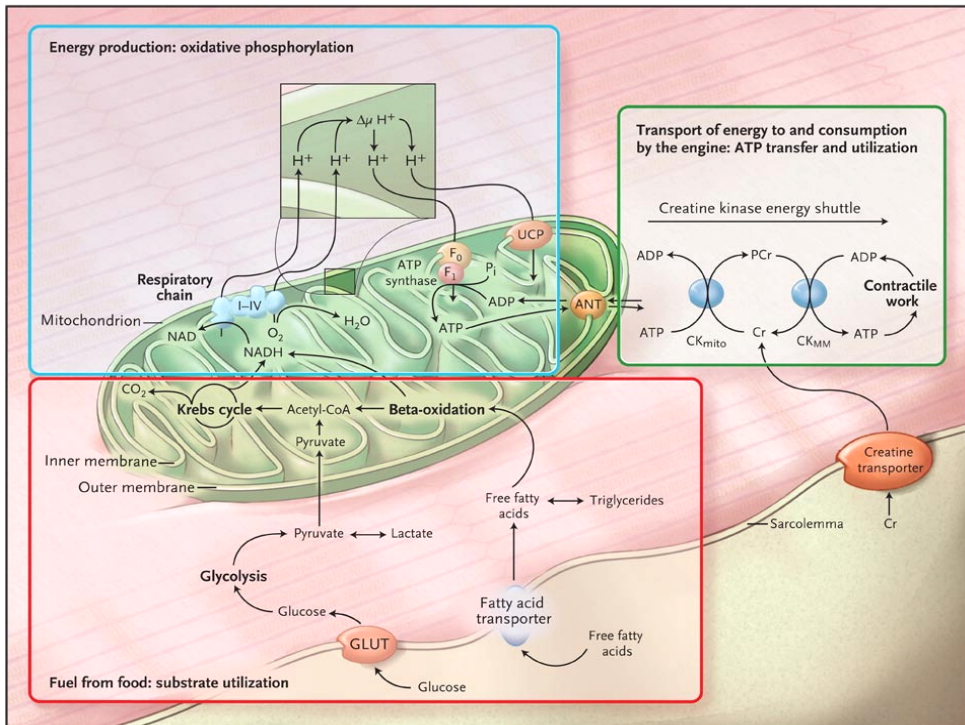


Figure 1. Myocardial energy metabolism. Reproduced with permission from Neubauer S. *The failing heart - an engine out of fuel.* NEJM 2007;356:1140-51, Copyright Massachusetts Medical Society.

The energy production is in demand for oxygen due to the aerobic oxidative phosphorylation mechanism. The relation between myocardial oxygen consumption (MVO₂) and the sum of potential energy (PE) and stroke work (SW) generated by one cardiac cycle, is schematically illustrated in Figure 2. The key element of myocardial protection during on-pump cardiac surgery, is to stop the contraction to reduce energy-

and oxygen consumption in the myocardium by inducing rapid heart arrest in diastole; cardioplegic arrest.¹³

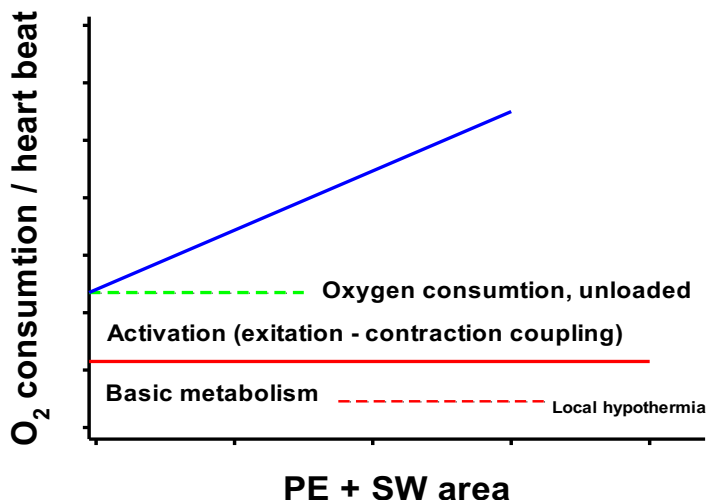


Figure 2. A schematic illustration of the relation between myocardial oxygen consumption (MVO_2) and the pressure-volume area, the sum of potential energy (PE) and stroke work (SW), demonstrating MVO_2 of the working heart (blue), the unloaded beating heart (dotted green) on CPB, the normothermic arrested heart (red) and the hypothermic arrested heart (dotted red). The pressure-volume area (PE + SW) is expressed in mmHg * mL or Joule on the x-axis (1 mmHg*mL is equal to 0.000133 Joule). On the y-axis oxygen consumption is expressed in mL O_2 per heartbeat.

The most widely used and clearly dominant form of cardioplegia the last four decades is perfusion of the myocardium with hyperkalemic solutions that evoke myocyte membrane depolarization and cardiac arrest.^{1,14,15} Perfusion with cold solutions also improves protection and contributes to reducing myocardial damage.^{16,17} Repeated perfusion with oxygenated cold blood cardioplegia is considered by many to provide the best protection of the myocardium and is used as a routine at Haukeland University Hospital and numerous other cardiac surgical centers worldwide.¹⁸⁻²⁰ In addition to cooling, blood cardioplegia also distributes oxygen to the myocardium in the cardioplegic phase. Upon reperfusion of the ischemic myocardium after CPB and CA, a transient decrease in heart function usually appears in the first hours after the procedure. This temporary decrease of function after reperfusion, may be due to myocardial stunning caused by reversible myocardial damage. Stunning, observed as a mismatch between myocardial function and blood flow rate, may last for hours and

days, this in spite of optimal myocardial protection and preservation.^{21,22} Also irreversible tissue damage in these situations can appear as stunning if increased function and remodeling in the remaining myocardium compensate for the loss of contractile tissue.^{23,24} Extended time on CPB and CA are factors that increase or prolong this temporary dysfunction. In patients with impaired cardiac function before the surgical procedure, this can be critical in terms of survival, especially for high-risk patients with additional factors of comorbidity.^{25,26} The use of cold, potassium-based blood cardioplegia implicates coronary perfusion with hyperkalemic, oxygenated solution approximately every 20 min. This procedure thus provides cooling of the myocardium and the possibility for reoxygenation. However, it is well documented that reperfusion and reoxygenation paradoxically can cause tissue damage in the myocardium.^{27,28} This detrimental effect has been shown in various animal models of acute coronary occlusion and reperfusion, as well as in experimental models of heart surgery with cardiopulmonary bypass and reperfusion after cardioplegic arrest.^{29,30} This tissue damage is called lethal reperfusion injury and can be prevented or limited by pharmacological interventions, such as beta-adrenergic blockers, oxygen-radical scavengers and anti-apoptotic interventions.^{21,31}

6.3 Cardioplegic mechanisms

6.3.1 Depolarized cardioplegic arrest

When the serum potassium concentration is ~10 mmol/L, the myocyte membrane potential will be about -65mV and the voltage-dependent fast Na^+ ion channels will be inactivated.^{32,33} The action potential will not be elicited, myocardial contraction ceases in diastole, electromechanical arrest is induced and the resting membrane potential will be at equilibrium at approximately -50 mV (Figure 3). At a higher concentration (~ 30 mmol/L) of extracellular potassium, the intended inactivation of the fast sodium channels will still be achieved, but also activate the voltage dependent slow calcium channels (threshold -35 mV) which is disadvantageous.^{34,35} The window of the optimal amount of potassium is narrow with an ideal concentration

between the voltage thresholds of the sodium and calcium channels, like the classic St Thomas Hospital solution 2 (Plegisol®) with a K^+ concentration of 16 mmol/L.³⁶ A prolonged depolarization of the myocyte membrane can be harmful due to mechanisms like inhabitation of Na/K-ATPase caused by ischemia and hypothermia, Na^+ window current and impaired Na^+/H^+ exchange. The net result is intracellular sodium loading. This effect pleads to a reversal of the sodium/calcium ion exchanger and the Ca^{2+} window current, with a resulting rise in intracellular calcium ions. The ion imbalance of Na^+ and Ca^{2+} activates energy demanding processes to correct the disparity.³⁷ If this alleviation fails, the result is aggravated reperfusion injury manifested as either reversible myocardial dysfunction, or irreversible contracture and cell death.³⁸⁻⁴³

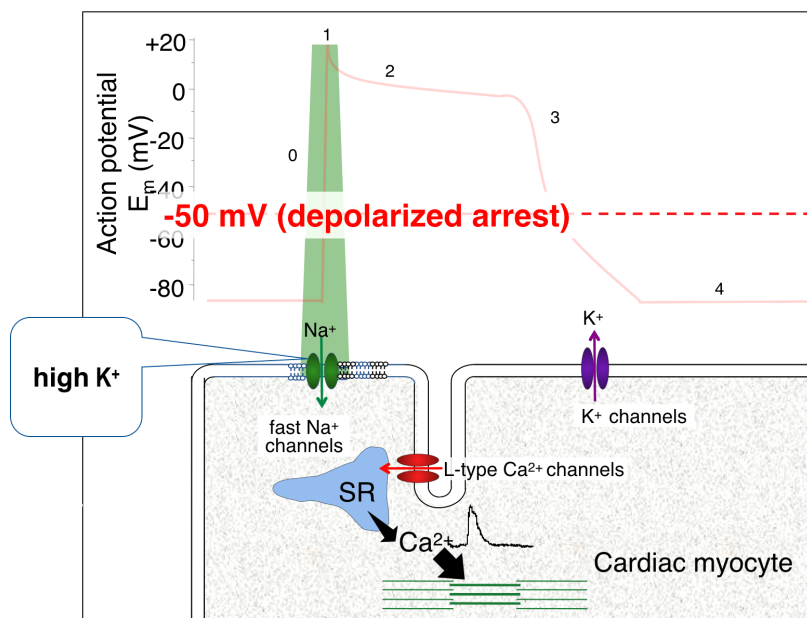


Figure 3. Excitation-contraction coupling and targets for depolarized arrest with potassium-based cardioplegic solution. The membrane potential of the resting myocyte is -85 mV. At high concentration of extracellular K^+ , the membrane potential changes towards a more positive value, by definition depolarization. At -65 mV, the voltage dependent fast sodium channels, which are responsible for the rapid, upstroke, phase zero towards action potential, are inactivated. The result is no action potential, no contraction and thereby diastolic arrest with myocyte membrane potential at -50 mV. Figure modified from Podesser BK, Chambers DJ; *New Solutions for the Heart. An Update in Advanced Perioperative Protection*, Springer Verlag/Wien;2001.

6.3.2 Polarized cardioplegic arrest

The alternative concept, polarized arrest, is to achieve rapid cardiac arrest with cardioplegic solutions, also keeping the myocyte membrane potential at or near the cell membrane resting potential (Figure 4). Such polarized cardiac arrest results in less myocyte sodium and calcium loading and consequently reduced activation of cellular ion channels/pumps and hence reduced energy consumption.^{37,44-46}

A number of different routines for improving myocardial protection have been studied, both experimentally and clinically.⁴⁷ Polarizing cardioplegic protocols using potassium channel openers (e.g. pinacidil, nicorandil, diazoxide, adenosine) or direct blockade of the fast sodium channel activation (e.g. tetrodotoxin, lidocaine, procaine, esmolol) have also been extensively studied.^{45,48-53} A combination of adenosine, lidocaine and magnesium (ALM[®]-cardioplegia) has gained some attention, also clinically.⁵²

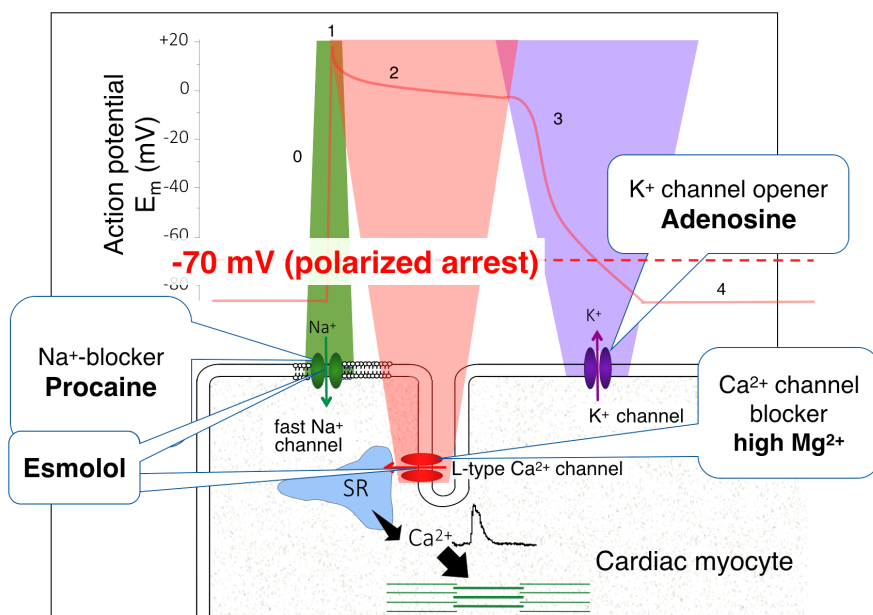


Figure 4. Excitation-contraction coupling and targets for polarized arrest with our modified version of the normokalemic St. Thomas' Hospital polarizing cardioplegic solution, STH-POL. The concept of polarized arrest is to maintain the membrane potential closer to the resting potential, which can be achieved in a number of ways. Relevant for this project is esmolol, adenosine, procaine and magnesium, which likely result in membrane potential at about -70 mV, polarized arrest, compared to -50 mV for the depolarized arrest (Figure 3). Figure modified from Podesser BK, Chambers DJ; *New Solutions for the Heart. An Update in Advanced Perioperative Protection*, Springer Verlag/Wien;2001.

A novel cardioplegia, the St. Thomas' Hospital polarizing cardioplegic solution (STH-POL), formulated with a mixture of esmolol, adenosine and Mg^{2+} , has been suggested after experimental research in both *ex-vivo* and *in-vivo* models.⁵⁴⁻⁵⁶ The solution combines the inhibition of the fast Na^+ - and L-type Ca^{2+} channels by esmolol, the K_{ATP} channel opener effect of adenosine and the reduced myocardial Ca^{2+} load caused by magnesium.^{33,57} Before implementation of a new routine for myocardial protection in clinical studies and practice, this routine must be compared and found non-inferior or superior to the current routine in a translational large animal *in-vivo* model.

6.4 Esmolol

Esmolol has a rapid onset by blocking the fast Na^+ channels, hence inhibiting the ion flux necessary to achieve the action potential.⁵⁸ Furthermore, esmolol is a cardio-selective direct β_1 adrenergic receptor antagonist, which blocks the sarcolemmal L-type Ca^{2+} channels and consequently inhibit calcium-activated mechanisms required for myocyte contraction.⁴³ In isolated perfused hearts (Langendorff) and isolated myocytes without catecholamine stimulation, additional negative inotropic effects of esmolol has been demonstrated, likely to not be mediated via its antagonism at the β -adrenoreceptors.⁵⁷ The overall result is cardioplegic arrest with the membrane potential closer to the resting membrane potential (E_m) compared to depolarized arrest (Figure 4).^{40,45} Esmolol has a short duration of effect ($T_{1/2} \sim 9$ min) due to degradation by esterase activity in erythrocytes. As a consequence, bradycardia and negative inotropic effect can be avoided as a clinical problem when weaning from CPB.⁵⁹⁻⁶³ Additionally, esmolol has antiarrhythmic properties and is protective in the vulnerable period of reperfusion.^{53,64,65}

6.5 Adenosine

Adenosine is an endogenous purine nucleoside from the metabolism of the high-energy phosphates. As a component in cardioplegic solutions, the foremost mechanism is binding to the A_1 -receptor which reduces cAMP by inhibiting adenylyl cyclase and

thereby acts as a K_{ATP} channel opener.⁶⁶ This effect causes outward K^+ flux and induces hyperpolarized heart arrest. This hyperpolarization effect is especially seen on myocardial conductive tissue such as the sinoatrial (SA) and atrioventricular (AV) nodes.⁶⁷ Additionally, adenosine may reduce K^+ induced Ca^{2+} overload.⁶⁸ Adenosine has a short half-life ($T_{1/2} < 10$ s) in blood.⁶⁹ However, the cardioprotective effect of adenosine is maintained, either by a prolonged activation of the A_1 -receptor or by the myocardial consequences of receptor activation similar to the mechanism of ischemic preconditioning.⁷⁰

The degradation of both adenosine and esmolol is independent from the liver- or kidney function, which improves clinical feasibility in patients with impaired organ function. These two cardiac arrest agents act synergistically resulting in a desired effect at relatively low but effective concentrations, while minimizing potential adverse effects.⁷¹

6.6 Magnesium

The effect of magnesium cations is antagonistic blockade of calcium channels in the myocyte membrane preventing Ca^{2+} , which is required for myocardial contraction, from entering the cell.⁷² Mg^{2+} as an additive to cardioplegic solutions, also reduces myocardial metabolism during ischemia and optimizes the intracellular Ca^{2+}/Mg^{2+} ionic hemostasis. Both mechanisms are important in preventing cell damage.⁷³⁻⁷⁵ Additionally, Mg^{2+} acts like an antiarrhythmic agent.^{76,77} Magnesium is an additive to the standard potassium-based blood cardioplegia used in our institution.

6.7 Procaine

Procaine is a local anesthetic substrate and is widely used as a low concentration additive to cardioplegic solutions.^{1,78} The mechanism is direct blocking of the fast sodium channel activation leading to cell membrane stabilization, which is a class 1A antiarrhythmic effect.⁷⁹ This is clinically relevant in the postischemic period of

reperfusion, especially after administration of hyperkalemic cardioplegic solutions.⁸⁰ In addition, procaine also prevents coronary artery constriction/spasm and has free radical scavenger properties.^{46,51} Procaine is included in the standard potassium-based blood cardioplegia used routinely in our institution and was therefore added in equal concentration to the St. Thomas' polarizing solution in this research project.

6.8 Blood

Cardioplegic arrest can be achieved by using a crystalloid solution or mixed with blood as vehicle.^{18,81} In general, crystalloid solutions are composed of arresting- and occasionally buffering agents, administered as a cold (4°C) solution, but without oxygen delivery during the period of ischemic arrest.^{44,82} Blood cardioplegia is a composition of a cardioplegia concentrate mixed with the patient's oxygenated blood derived from the HLM, thus oxygen can be provided to the ischemic myocardium during cardioplegic arrest.⁸³ Furthermore, blood acts like a natural buffer, has antioxidant qualities and is a free-radical scavenger.^{20,84} The osmolality of blood may reduce cellular edema compared to crystalloids.⁸⁵ Additionally, by using blood as a transport medium for the cardioplegic solution, hemodilution will be less compared to administration of crystalloid cardioplegia.⁸⁶ A potential disadvantage of using blood as an additive to the cardioplegic solution is the increased viscosity of blood, especially at low temperatures. This may alter the distribution of the cardioplegic solution and be of clinical importance both in patients with native narrow coronary arteries (e.g. neonatal/pediatric patients) or in adult patients with acquired, obstructive coronary disease (e.g. atherosclerosis).

6.9 Temperature

Cardioplegia can be administered as cold, tepid or normothermic infusate and will consequently influence the temperature of the myocardium after equilibration. Moderate topical and systemic cooling are also commonly used routines.⁴⁴ General hypothermia adds another component of myocardial protection additional to the

diastolic arrest, by decreasing the basal metabolism and oxygen consumption.⁸⁷ Hypothermia may also have detrimental effect due to negative influence on enzymatic and cellular reparative processes and shift in the oxygen-hemoglobin dissociation curve interfering with delivery of oxygen at the cellular level.⁸⁸ The optimal temperature, both during CPB and in the myocardium of the arrested heart, is still being questioned.⁴⁷

7. AIM OF THE PROJECT

The main objective of this project was to evaluate if cardioplegic arrest with adenosine/esmolol/magnesium, STH-POL, offers myocardial protection comparable to a standard depolarizing potassium-based cardioplegic solution, STH-2, both delivered as antegrade, repeated, cold, oxygenated blood cardioplegia. We hypothesized that repeated perfusions of the myocardium with the novel STH-POL cardioplegic solution, provided an equal or better myocardial protection compared to the standard STH-2 cardioplegic solution in a clinically relevant and translational animal model.

The specific aims of the three studies were to compare STH-POL and STH-2 cardioplegic regimes with respect to:

- Differences in regional and global cardiac function, β -adrenergic receptor desensitization and myocardial injury following weaning from CPB after 60 min of cardioplegic arrest, thus simulating a standard, single procedure of open heart surgery (Paper I).
- Differences in myocardial high-energy phosphate metabolism and myocardial ultrastructure following 60 min of cardioplegic arrest and after weaning from CPB (Paper II).
- Differences in left ventricular function and contractile efficiency after weaning from CPB after an extended cardioplegic arrest of 120 min, simulating a more complex or combined surgical procedure (Paper III).

8 METHODS

8.1 Animals and anesthesia

All experiments were performed in Norwegian Landrace pigs of either gender. Results from 60 young animals weighting 42 ± 3 kg were included in Paper I - III. All animal experiments were done in accordance with the European Communities Council Directive of 2010 (63/EU). The animal handling and research protocols were approved by the Norwegian State Commission for Laboratory Animals (Project 20135835) and the responsible veterinarian at the Vivarium, University of Bergen.

The pigs were brought to the animal facility at the Vivarium for acclimatization about one week before the experiments. Two ear veins were cannulated after premedication with intramuscular injection of a mixture of ketamine (20 mg/kg), diazepam (10 mg) and atropine (1 mg) and ventilation on mask with oxygen and 3% isoflurane (Rhodia, Bristol, UK). Loading doses of intravenous (IV) fentanyl (0.02 mg/kg), midazolam (0.3 mg/kg), pancuronium (0.063 mg/kg) and sodium pentobarbital (15 mg/kg) were given, followed by a continuous infusion of fentanyl (0.02 mg/kg/h), midazolam (0.3 mg/kg/h) and pancuronium (0.2 mg/kg/h). A separate infusion (to prevent precipitation) with sodium pentobarbital (4 mg/kg/h) in Ringer's acetate with 20 mmol/L KCl added, was administrated. This pentobarbital infusion also constituted the basic fluid substitution of 15 mL/kg/h throughout the experiments. After tracheotomy for airway intubation, the animals were ventilated (Julian, Drägerwerk, Lübeck, Germany) with a mixture of nitrous oxide (56-58%) and oxygen. The tidal volume was set to 11 mL/kg and the frequency adjusted aiming at an end-tidal pCO₂ of 5.0 to 5.6 kPa. Prophylactic antibiotic therapy with Cefalotin 1g dissolved in saline, was given IV initially, followed by 0.5 g during CPB and 1.0 g after weaning (Paper I + III). In addition, intravenous Ringer's acetate, 5 mL/kg/h, was provided after weaning from CPB. The anesthetic protocol has previously been evaluated by the research group allowing the use of neuromuscular blocking agents in young pigs.⁸⁹

8.2 Surgical protocol and instrumentation

The right femoral artery and vein were cannulated for blood sampling and infusion by surgical cut-down in the groin. An early arterial blood gas analysis determined the need for ventilator adjustments. Rectal temperature was monitored and an open suprapubic cystostomy with insertion of a catheter measured diuresis. A midline sternotomy and pericardiotomy exposed the heart and heparin (125 IU/kg) was given IV to prevent catheter clotting. A continuous cardiac output catheter (CCO/EDV 177HF 75, Edwards Lifesciences Inc, Irvine, CA) was advanced from the left internal mammary vein into the pulmonary artery for monitoring cardiac output, right ventricular end-diastolic volume (EDV), central venous pressure (CVP) and pulmonary artery pressure (PAP) (Vigilance II[®] and TruWave[®] transducers, Edwards Lifescience Inc) (Figure 5). A microtip pressure catheter (Millar MPC-500, Houston, TX) was inserted into the proximal aorta through the left internal mammary artery. An identical catheter through the apex of the heart monitored left ventricular pressure in Paper II. A dual-field pressure-conductance catheter (CA71083-PL, CDLeycom, Hengelo, the Netherlands) connected to a Sigma-M signal conditioner (CDLeycom) was inserted through the apex and into the left ventricle in Paper I + III. The distal part was positioned just above the aortic valve, verified by epicardial echocardiography (Vivid E9, GE Vingmed Ultrasound, Horten, Norway). An infant feeding tube allowing microsphere injections was inserted into the left atrium and a tourniquet was placed around the inferior vena cava (IVC) for short-term intermittent dynamic preload reductions (Paper I + III). After two-point sensor calibration on the day of the experiment, all hemodynamic parameters were sampled by a 16-channel Ponemah ACQ-7700 system (Data Sciences International, St. Paul, MN), and later analyzed (Ponemah Physiology Platform v. 5.2, Data Sciences International).

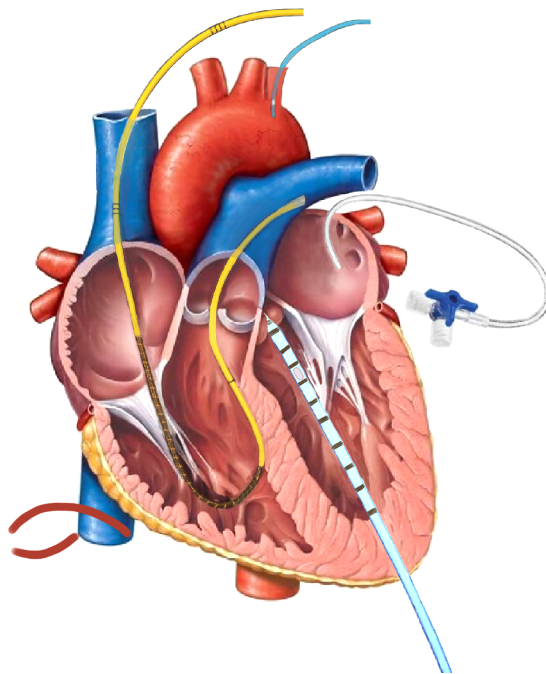


Figure 5. Baseline instrumentation in Paper I + III. Millar pressure catheter (blue) through the left internal mammary artery for monitoring central aortic pressure. Edwards CCO-catheter/Swan Ganz (yellow) through the left internal mammary vein for monitoring CVP, PAP and CCO. Baby feeding tube (grey) into the left atrium for injection of fluorescent microspheres. CDLeycom dual-field pressure-conductance catheter (light blue) through the apex of the left ventricle for monitoring left ventricular volume and pressure. Tourniquet (red) around the IVC for intermittent preload reductions.

8.3 Cardiopulmonary bypass

The heart-lung machine (Stöckert SIII, Munich, Germany) was primed with 1200 mL Ringer's acetate in the circuit. Systemic heparinization (heparin 500 IU/kg) was followed by cannulation of the brachiocephalic artery (EOPA 18 Fr, Medtronic Inc., Minneapolis, MN) and right atrial appendage (MC2 28/36 Fr, Medtronic Inc.) (Figure 6). CPB was established with a flow of 90 mL/min/kg and water temperature of 32°C in the heat exchanger. The time period of aortic cross-clamping was 60 min (Paper I + II) and 120 min (Paper III). A left heart vent catheter (DLP 13, Medtronic Inc.) was introduced in the left atrial appendix and advanced through the mitral valve into the left ventricle for passive drainage of the heart during cardioplegic arrest (Paper I). An alternative method for unloading the left ventricle, was a similar vent catheter

temporarily placed through the apex into the ventricle (Paper II + III). The body temperature was allowed to drift towards 34°C and CPB flow was reduced to 72 mL/min/kg when rectal temperature reached 35°C or after 20 min. After 40 min (Paper I + II) or 100 min (Paper III) of aortic cross-clamping, systemic rewarming was commenced with reset of CPB flow to 90 mL/min/kg and water temperature at 40°C. Arterial blood gases were acquired before cross-clamping, at half time during the cardioplegic period (Paper I + III) and prior to declamping. During CPB, the tidal volume of the ventilator was reduced to 50% to prevent atelectasis. Additional heparin (250 IU/kg) was given at half time during aortic cross-clamping. Defibrillation was the only allowed antiarrhythmic intervention in these research protocols and was used if ventricular fibrillation occurred after declamping. After 10 min of reperfusion, the animals were weaned from CPB. The residual blood in the HLM circuit was infused followed by decannulation. Protamine sulfate (1 mg/kg Paper I, 1,5 mg/kg Paper II, 2 mg/kg Paper III) was slowly injected IV for heparin reversal.

8.4 Cardioplegia

Cardioplegia was given as either the normokalemic St. Thomas' Hospital polarizing solution (STH-POL) formulated with a mixture of esmolol, adenosine and Mg²⁺, or the hyperkalemic St. Thomas' Hospital cardioplegic solution 2 (STH-2). Both solutions were pre-prepared as concentrate, modified by adding procaine and administered as cold (12°C), oxygenated, blood cardioplegia, freshly mixed by a dual-head pump and separate cooling on the HLM. The cardioplegia was given into the aortic root with a flow set to 7% of CPB flow, following a standardized protocol with an initial 'high-dose' (1:4 concentrate/blood) for 3 min and 2 min of 'low-dose' (1:8 concentrate/blood) given at 20 and 40 min after aortic cross-clamping (Paper I - III) and additionally at 60, 80 and 100 min in Paper III. The final molar concentrations of the key components in the cardioplegic solutions are presented in Table 1.

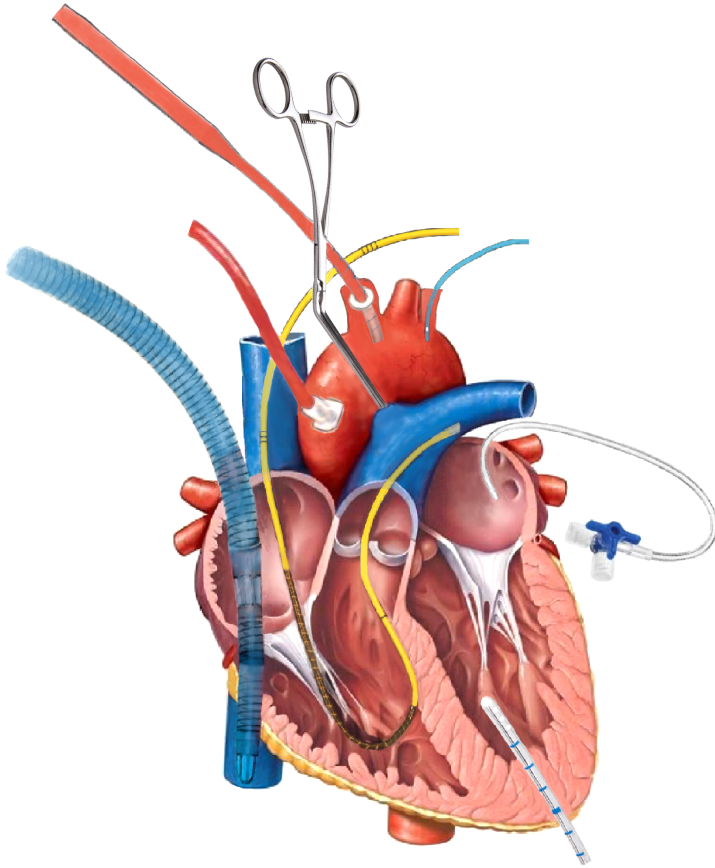


Figure 6. Instrumentation during CPB and CA in Paper III. Basic instrumentation as in Baseline situation (Figure 5). EOPA 18 Fr cannula (red) through the brachiocephalic artery and into to the ascending aorta for systemic return of oxygenated blood from the HLM. Two-stage 28/36 Fr venous cannula (blue) through the right atrial appendage for venous drainage into to the HLM from the right atrium and inferior vena cava. Cardioplegia needle in the proximal ascending aorta for antegrade delivery of STH-POL or STH-2 cold blood cardioplegic solution. Aortic cross-clamp in the distal ascending aorta. DLP 13 Fr left heart vent (grey) through the apex for unloading the left ventricle during cardioplegic arrest.

Table 1. Final molar concentrations in oxygenated blood cardioplegia.

	STH-POL		STH-2	
	high-dose 3 min	low-dose 2 min	high-dose 3 min	low-dose 2 min
Esmolol (mM)	1.35	0.68	-	-
Adenosine (mM)	0.50	0.25	-	-
Mg ²⁺ (mM)	20	10	16	9
K ⁺ (mM)	4.3	4.3	22	14
Cl ⁻ (mM)	106	106	134	120
Procaine-HCl (mM)	0.8	0.4	0.8	0.4

STH-POL = Modified St. Thomas' Hospital polarizing cardioplegic solution.

STH-2 = Modified St. Thomas' Hospital cardioplegic solution No 2.

8.5 Pressure-volume conductance catheter

The systolic left ventricular performance is depending on three principle factors; preload, afterload and the contractile state of the myocardium. The contractile function can be evaluated by a pressure versus volume plot. Experimentally, several methods have been used to obtain this relation. Since the early 1980s, the use of conductance catheter and continuous ventricular volume estimations has been an established method.⁹⁰ The principle of this method is a catheter with multiple electrodes generating an electrical field between the most distal and the most proximal electrode. Since the early 1990s, this method was improved by adding electrodes making two alternating electrical fields with opposite polarity (Figure 7) between the proximal and the distal pairs of electrodes.⁹¹ The result is a more homogeneous electric field and thereby a more linear relation between real volume in the heart chamber and estimated volume from the conductance signal. The dual-field conductance catheter is placed along the left ventricle (LV) long axis. Accessing the LV can either be through a retrograde approach from e.g. the right carotid artery or directly into the LV through the apex of the heart. The conductance catheter is designed with a soft pigtail for optimal position and stabilization.

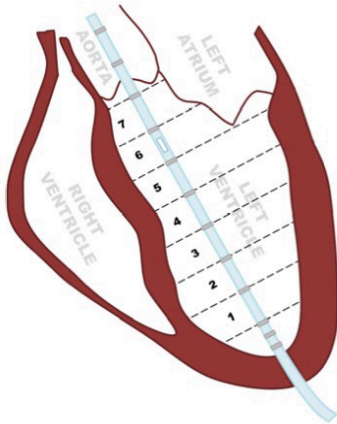


Figure 7. The two proximal and distal electrodes are driving electrodes for a dual electrical field along the ventricular axis. 7 segments are included for calculation of segmental volumes by measuring resistance between pairs of electrodes, cross sectional area and blood conductivity. The pressure sensor is located at segment 6. In addition, an 'internal' ECG signal is recorded.

By using a dual-field conductance catheter with multiple electrodes and a full-bridge solid-state pressure sensor in the LV, a plot can be presented as real-time pressure-volume loops (Figure 8).

8.5.1 Pressure-volume loops

Pressure-volume area (PVA) is a measure of total mechanical work, calculated as the sum of stroke work (SW) and potential energy (PE) (Figure 8). Other parameters, which can be calculated from a PV-loop, are e.g. stroke volume, end-systolic and end-diastolic volumes, ejection fraction and cardiac output (stroke volume * heart rate). From the pressure signal, variables like dP/dt_{\min} and dP/dt_{\max} (peak negative/positive derivate of LV pressure) and Tau (time constant of isovolumic relaxation) can be calculated. The electrical field generated by the conductance catheter is not only limited to the LV blood volume. The dual electrical field also passes through the ventricular wall. Other conductive tissues (e.g. myocardium, lungs) and fluids surrounding the LV cavity, e.g. blood in the right ventricle (RV), affect the measured conductance and introduce an offset in the relation between true LV volume and the volume derived from the catheter.

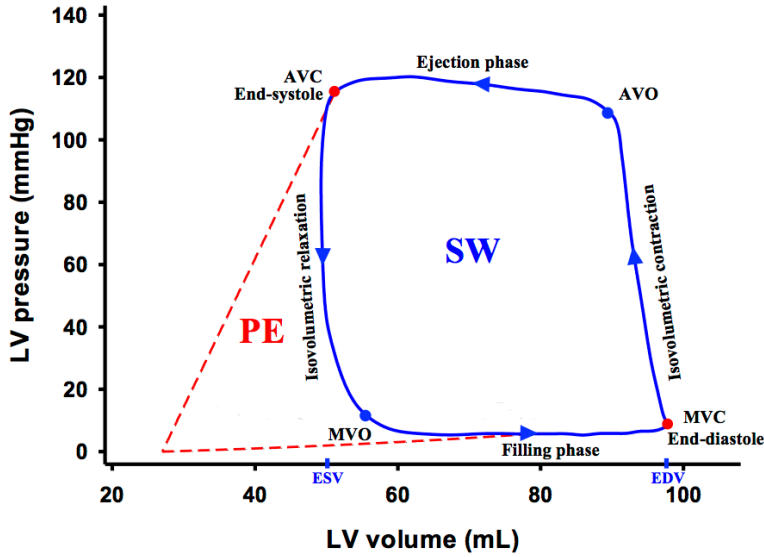


Figure 8. Real-time left ventricular pressure-volume loop (blue) from one single heart cycle. The loop turns counter-clockwise starting with mitral valve closure (MVC) at end-diastole, followed by isovolumic contraction before aortic valve opening (AVO) and start of the ejection of blood into the aorta. Aortic valve closing (AVC) defines end-systole followed by isovolumic relaxation, which ends in the mitral valve opening (MVO) initiating the passive filling phase. Stroke work (SW) is the area of the loop, stroke volume (SV) is $EDV - ESV$. Potential energy (PE) is the area (dotted red) defined by the end-systolic and the logarithmic end-diastolic pressure-volume relations together with descending part of the PV-loop. The total left ventricular mechanical work for one cardiac cycle is $PE + SW$.

This parallel conductance can be corrected for by injection of hypertonic saline into the pulmonary artery.⁹² Finally, the Baan equation is used for calculation of absolute volumes:

$$V(t) = 1/\alpha * \rho * L^2 * (G(t) - G_p)$$

where $V(t)$ is total intraventricular volume, α is alpha factor (derived from volume estimates from the Swan-Ganz catheter), ρ is blood resistance, L is distance between segmental electrodes, $G(t)$ is total conductance and G_p is parallel conductance.⁹³

8.5.2 Acquisition

In Paper I and III, a dual-field conductance-pressure catheter was inserted through the apex and into the left ventricle with the distal part including 2-3 electrodes in position just above the aortic valve (Figure 5). The remaining electrodes in the left ventricle allow assessments of conductance in up to 7 segmental electrical fields together with

pressure data. Following pre-oxygenation (short period of 100% O₂ ventilation) and ventilator shut-off in end-expirium, five to 10 heartbeats with stable hemodynamics and six to 12 consecutive cardiac cycles during IVC occlusion using a tourniquet, were sampled as a dynamic run (Figure 9). Arrhythmia or other interferences were not accepted, and a new run was obtained when aortic pressure (AOP) was stabilized at pre-run level. A total of four valid run acquisitions were sampled in all experiments. In addition, at each of these situations three bolus injections of 5 mL hypertonic (10%) saline were rapidly injected into the pulmonary artery through the CCO-catheter, for estimation of parallel conductance.

8.5.3 Load-independent indices of LV systolic and diastolic function

Pressure-volume loops obtained during an acute preload reduction makes it possible to calculate variables describing volume-/load-independent systolic and diastolic function. The slope of the end-systolic pressure-volume relationship (ESPVR) derived from a regression line through the end-systolic points of the PV-loops is one variable describing left ventricular systolic function (Figure 9). The slope of the linear ESPVR relation can be described using the equation:⁹⁴

$$ESP = E_{es} (ESV - V_0)$$

where ESP is end-systolic pressure, E_{es} is the slope of the linear relationship, ESV is end-systolic volume and V_0 is the x-axis intercept. The linear ESPVR and following calculation of $ESPVR_{slope}$ reflects the LV systolic function.⁹⁵ However, the relation is often more of a logarithmic character and altering loading conditions may affect ESPVR. Consequently, this variable is considered not be accurate.⁹⁶ Preload Recrutable Stroke Work (PRSW) is defined by the linear regression of stroke work (equivalent to the area of the PV-loop) on the y-axis, related to the end-diastolic volume (EDV) on the x-axis during a dynamic preload reduction (Figure 9). The relationship between stroke work and EDV is, for all practical purposes, linear and this load-independent index of myocardial contractility can be described using the equation:⁹⁷

$$M_w = SW / (EDV - V_w)$$

where M_w is the slope of PRSW, SW is stroke work, EDV is end-diastolic volume and V_w is the x-axis intercept.

The end-diastolic pressure-volume relationship (EDPVR) is derived from a regression line through the end-diastolic points of the PV-loop. As illustrated in Figure 9, this relationship is non-linear, hence the EDPVR is described as the slope (β) in a logarithmic equation:

$$EDP = a * e^{(\beta * EDV)}$$

where EDP is end-diastolic pressure, a is the y-axis intercept and β is the slope. The slope of EDPVR is a measure of left ventricular compliance and describes its passive function in diastole.⁹⁶ Peak negative first derivative of LV pressure (dP/dt_{min}) acquired from the pressure-conductance during stable preload conditions, describes the active relaxation of the left ventricle. Tau (τ), which is the time constant of isovolumic relaxation, is an additional variable describing the active effectiveness of LV during diastole.⁹⁸ Peak positive first derivative of intraventricular pressure (dP/dt_{max}) during isovolumic contraction (Figure 8) is a variable for LV contractility, but due to its pre- and afterload dependency the method is considered to be inaccurate compared to PRSW.

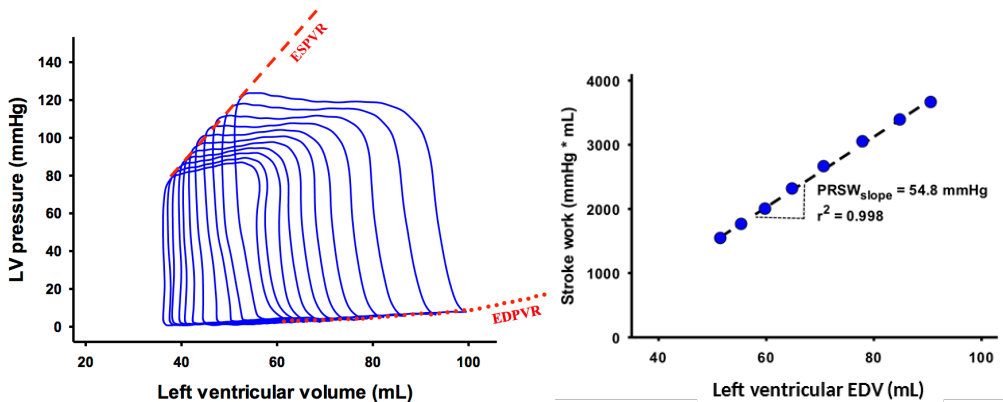


Figure 9. Pressure-volume loops at multiple time points during a sequence (= dynamic run) of 11 heartbeats simultaneously with preload reduction by occlusion of the IVC. The slope of end-systolic (ESPVR) and end-diastolic (EDPVR) pressure-volume relations are marked as red interrupted or dotted line, respectively. The slope of the regression line defined by the end-systolic points in each loop, defines the ESPVR, one variable reflecting the load-independent contractility. Additional figure (right) is pressure-volume loop areas (blue dots) from the left figure, plotted against end-diastolic volumes (EDV) of the corresponding cardiac cycles. Preload Recrutable Stroke Work (PRSW) is the linear relation between stroke work and EDV while the slope is termed $PRSW_{slope}$ and represents the load-independent contractility. The coefficient of determination = r^2 .

8.5.4 Analysis

Associated data files (1 for evaluation of function, 3-4 for parallel conductance) obtained by the pressure-conductance catheter were coded and analyzed as independent entities with custom-made software (MATLAB, MathWorks Inc., Natick, MA). The mean of 5-8 cardiac cycles during stable situations together with load-independent variables obtained during the dynamic preload reductions were calculated. Absolute volumes were estimated by correcting for parallel conductance and cardiac output. Volumes were indexed by body surface area (BSA) calculated as:

$$BSA (m^2) = (BW^{2/3} * k) / 100$$

where BW is body weight in kg and k for the pig is $9 \text{ m}^2/\text{kg}^{-2/3}$.⁹⁹

8.6 Epicardial echocardiography

The use of two-dimensional transthoracic echocardiography is an established method for evaluation of morphology and function of the heart in both experimental settings and clinical practice.¹⁰⁰ Echocardiography provides real-time imaging, is non-invasive, widely available and essential in the diagnosing and management of the majority of patients with cardiac conditions. New advances in echocardiographic technology incorporate three-dimensional techniques. Furthermore, a method for evaluation of cardiac function is the assessment of myocardial deformation either by Tissue Doppler Imaging (TDI) or Speckle Tracking Echocardiography (STE). Above all in an experimental laboratory setting, these two methods are essential for validation of minor, but significant changes of myocardial function. Epicardial echocardiography in an open chest model facilitates the use of ultrasound probes with higher frequency than in clinical practice. Consequently, the recordings enable data with high spatial and temporal resolution and thereby more reliable and reproducible measurements.

8.6.1 Strain and strain rate

Deformation in this context refers to the concept of strain. The definition is a fractional or percentage change in length compared to its original length. Additionally, positive strain is defined as lengthening or stretching, while negative strain is shortening.¹⁰¹

If the strain is linear it can be defined by the Lagrangian formula:

$$\varepsilon = \frac{L - L_0}{L_0}$$

where ε = strain, L = length at a specific time during the cardiac cycle, usually the peak systolic value, and L_0 the original length usually read at end-diastole giving peak systolic strain.¹⁰² The helical myocardial fiber orientation of the left ventricle is complex, and the motion and deformation following myocardial contraction can be measured in several directions during one heart cycle. The most commonly used arrangement for directional measurements is using the chamber axis, allowing assessment of deformation in the three main directions (Figure 10) of the LV.

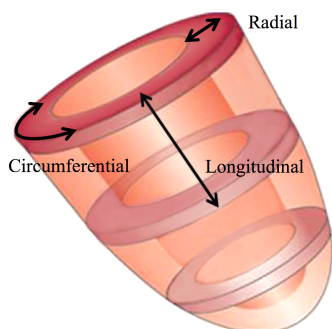


Figure 10. Strain assessment in three directions. Radial and circumferential deformation are evaluated using short-axis views. Longitudinal deformation is evaluated in the long-axis four-chamber direction from an apical view.

Strain rate (SR) is the first derivative of strain with respect to time, describing the speed of deformation. Peak ejection strain rate is correlated to dP/dt_{\max} derived from the pressure-conductance catheter (Ch. 8.5.3).¹⁰³ Strain and strain rate can be measured both as a regional and a global variable.

8.6.2 Tissue Doppler Imaging

Echocardiographic recordings using Tissue Velocity Imaging modality is the basis for subsequent processing and analyzing of Tissue Doppler Imaging strain (Figure 11A) and strain rate (Figure 11B).¹⁰⁴ In TDI, the displacement towards the scanner probe is normally color-coded red while blue denotes displacement in the opposite direction. Myocardial velocities (displacement per unit time) for each sample volume can be displayed as time curves. The basis for strain rate measurements is the velocity differences. In a selected region of interest (ROI), velocities can be analyzed off-line on a workstation and the strain rate can be estimated and displayed as time curves. By measurement of two different velocities (V1 and V2) at two different positions by a predefined distance (strain length), myocardial velocity gradient can be calculated which is proportional to strain rate. Strain is calculated by temporal integration of SR, usually over one cardiac cycle. The method of TDI is restricted to measure the myocardial deformation component along the ultrasound beam and is consequently limited by angle dependency (Ch. 10.11.4).

8.6.3 Speckle Tracking Echocardiography

An alternative non-Doppler method for evaluation of myocardial deformation is the use of Speckle Tracking Echocardiography, which uses the Brightness mode (B-mode) images of a cine-loop (Figure 12).¹⁰⁵ By speckles means acoustic markers produced at random by reflection, interference and scattering of the echo beam. Such speckles act as natural positional markers and is relatively stable during a part of the cardiac cycle (e.g. peak systole) and can be used for tracking the myocardial motion throughout a defined period of a heartbeat.¹⁰⁶ The post-processing software defines a cluster of speckles (called ‘kernel’) and tracks the kernels displacement frame by frame based on the user-defined ROI using a sum-of-absolute differences algorithm. Ultimately, off-line calculation of myocardial deformation parameters such as regional or global systolic strain (%) and strain rate (s^{-1}) can be performed. In contrast to TDI, STE can quantify strain and strain rate in two directions within the imaging plane and is often called two-dimensional (2D) strain.¹⁰⁴

Both TDI and STE have demonstrated to be reliable methods to measure left ventricular systolic function and are comparable to alternative techniques like sonomicrometry and MRI.¹⁰⁷⁻¹⁰⁹

8.6.4 Acquisition

In this project, regional myocardial function was evaluated in Paper I and III by 2D epicardial echocardiography (Vivid E9, GE Vingmed Ultrasound). Using a soft silicone pad ($4 \times 4 \times 3$ cm) as offset between the probe (6 MHz sector probe, GE Vingmed Ultrasound) and the epicardium, Pulsed Wave Doppler (PWD) spectral velocity traces with the sample volume in the aortic valve ostium obtained from the apex, was used to identify the aortic valve opening and the aortic valve closure for timing purposes. During B-mode recordings, the frequency was set to 6.5 MHz, and the anterior myocardial wall was focused by using a depth scale of 0-3 cm (Figure 11A). In the TDI mode, color gain was adjusted and frame rate set to obtain a high frame rate by reducing the image sector width to avoid aliasing. Mean frame rates for the TDI recordings were 544 (range 249-696) and 619 (range 327-749) frames/s in Paper I and Paper III, respectively. Accurate position of the probe was essential for a perpendicular image view in relation to the anterior wall for measurement of radial strain. Mean frame rates for the STE recordings in Paper III were 74 (range 63-88) frames/s in the short-axis view (SAX) and 74 (range 63-93) frames/s in the four-chamber apical view.

To avoid hemodynamic variations due to airway pressure alterations, the ventilator was disconnected during echocardiographic recordings, and 3-5 stable cardiac cycles were recorded at each situation. TDI of the anterior left ventricular wall was recorded in SAX in Paper I and Paper III, while STE was recorded in SAX and four-chamber views in Paper III. End-diastole was defined as the first deflection in the QRS complex in the ECG, while start and end of ejection (end-systole) were defined as the aortic valve clicks in the PWD velocity spectrum. The size of the ROI in the TDI analysis was set to 6×6 mm and the strain length (SL) to 6 mm (Figure 11). Care was taken not to place the ROI within a distance of $\frac{1}{2}$ SL from the epicardium and $\frac{1}{2}$ SL from the endocardium since the TDI recording extends outside the ROI display.¹¹⁰ The initial

ROI for each recording in the STE analysis was selected by manually tracing the endocardium lining in the reference frame. Care was taken to include the full thickness of the left ventricular wall by optimizing the width of ROI, but without sampling outside the epicardium. Myocardial deformation was assessed throughout the cycle with the software dividing the ROI into 6 preset segments (Figure 12). Both visual and automatic validation of adequate tracking was performed before approval and subsequent final analysis.

8.6.5 Analysis

All analyses were performed by using commercial software (EchoPAC BT12, GE Vingmed Ultrasound). One cardiac cycle was selected without any prior arrhythmia causing hemodynamic variations and used for analysis.

8.7 Myocardial tissue samples

In Paper I – III, myocardial tissue samples were acquired *ex-vivo* when the final measurements were completed and after the heart was explanted. Samples were obtained from the right ventricle, endo-, mid- and epicardium of the septum, and the anterior- and the posterior wall of the left ventricle. Samples snap frozen in liquid nitrogen (-196°C) were stored at -80°C for later analysis of β -receptor activity, carnitine palmitoyl-transferases, apoptotic activity and oxidative stress. Furthermore, in Paper II samples from the LV epi- and midmyocardium of the anterior wall were acquired *in-vivo*, both from the working and the cardioplegic heart. At the time of sampling, a 6 mm biopsy was snap-frozen in liquid nitrogen within 5 s while a 4 mm biopsy was cut and fixed directly in glutaraldehyde for morphometry (Figure 13).

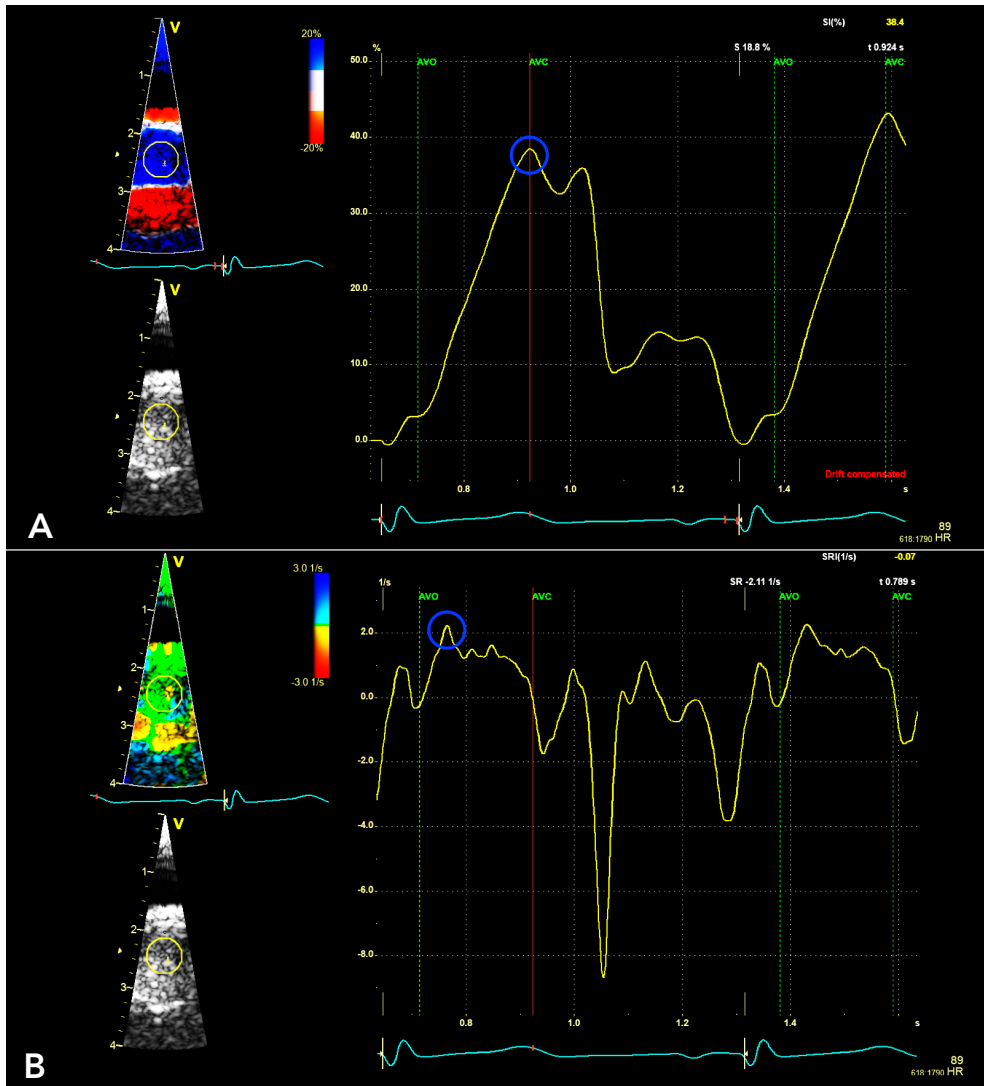


Figure 11A. Baseline analysis of a single layer TDI radial strain of the LV anterior wall in an experiment in Paper III. Circular ROI = 6 mm radius (yellow circle) with SL = 6 mm is positioned in the mid-myocardium (left) and tracked through one heart cycle, visualized in both color map (upper) and B-mode (lower). Yellow curve (right) is the corresponding radial strain curve during the heart cycle. Peak systolic strain value (blue circle) at Baseline (38.4%) is representative for mean values in Paper III. AVO = aortic valve opening (green vertical dotted lines), AVC = aortic valve closure (end-systole, red vertical line) from Pulsed Wave Doppler.

Figure 11B. Baseline analysis of a single layer TDI radial strain rate of the LV anterior wall at Baseline in the same experiment as above (A). ROI (yellow circle) is equally positioned in the mid-myocardium (left) and yellow curve (right) is the corresponding radial strain rate curve through one heart cycle. Peak ejection strain rate value (blue circle) at Baseline (2.11 s^{-1}) is representative for means in Paper III. AVO and AVC as in Figure 11A.

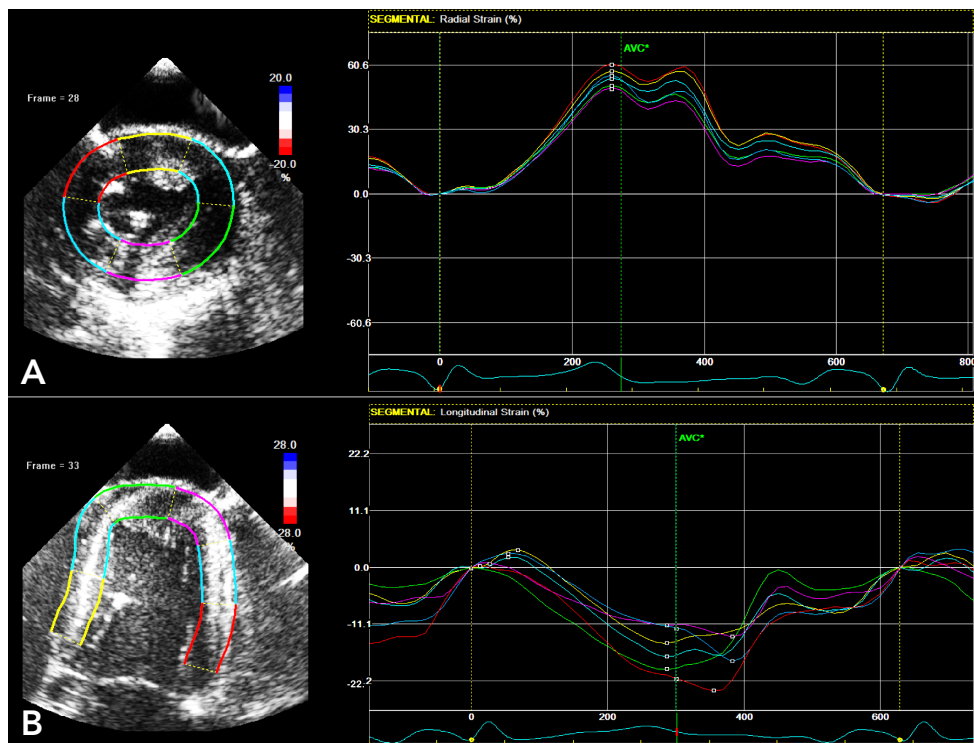


Figure 12A. Short-axis view of the LV, demonstrating Baseline analysis of STE radial strain in an experiment in Paper III. The left ventricle is divided into six preset segments (left). The corresponding colored curves of radial strain for each segment through one heart cycle are presented in the panel to the right. AVC = aortic valve closure (end-systole, green dotted vertical line) from Pulsed Wave Doppler.

Figure 12B. Long-axis four-chamber view of the LV in STE mode. The standard six segments of the left ventricle are illustrated in the panel to the left. The corresponding colored curves for regional longitudinal strain in each segment during one heart cycle, are presented in the panel to the right. The peak systolic strain value (active contraction) is negative (i.e. shortening) in the longitudinal direction. AVC as in Figure 12A.

8.7.1 Apoptosis

In the pathway of apoptosis, sequential activation of cysteine-aspartic acid proteases (i.e. caspases) is essential in the execution-phase of the cell apoptosis. Caspase-3 is one of the pro-enzymes that are inactive under normal conditions, but in the apoptotic cell caspase-3 is activated following a complex intrinsic and extrinsic signaling pathway.¹¹¹ In Paper I and III, caspase-3 activity was determined using the Caspase-3 Colorimetric Assay Kit (BioVision Inc., Milpitas, CA). Tissue was homogenized and

lysis performed according to the manufacturer's instructions. Triplet samples containing 400 μg of total protein, measured by the Quick Start™ Bradford Protein Assay (Bio-Rad Laboratories, Inc., Hercules, CA), were incubated for 2h before fluorometric readings.

8.7.2 β -receptor activity

Cardiopulmonary bypass and cardioplegic arrest cause adrenergic stress response.¹¹² A systemic inflammatory response syndrome is triggered by the surgical trauma and the contact of the blood components with the artificial surface of the bypass circuit during CPB. Leukocytes and endothelial cells are activated, and various pro- and anti-inflammatory mediators are released. Among others, the consequence of this complex acute phase reaction is an increased level of circulating catecholamines.¹¹³ Myocardial catecholamine levels are also upregulated during the cardioplegic arrest. This local catecholamine release is independent of the central sympathetic activation. Modulating mechanisms are activation of presynaptic receptors (α_2 -adrenoreceptors, adenosine A_1 -receptors), neuronal amine reuptake and metabolic alterations like hypoxia/anoxia, loss of high-energy phosphates, extracellular hyperkalemia and acidosis.¹¹⁴

The adrenergic stress response may lead to some degree of desensitization of myocardial β -adrenergic receptors. Impaired signaling through this pathway may play a significant role in the etiology of postoperative myocardial dysfunction and also cause less response if inotropic support is needed.¹¹² G protein-coupled receptor kinase-2 (GRK2) is a serine/threonine kinase, which is involved in this mechanism by phosphorylation and desensitization of agonist-occupied β -adrenergic receptors. In Paper I, the activation of GRK2 in the myocardium was assessed with immunoblotting using antibodies against phosphorylated GRK2 (LS-C199027, LifeSpan BioSciences Inc., Seattle, WA) and total GRK2 (CST3982, Cell Signaling, Boston, MA) according to manufacturer's instructions. The blots were quantified using scanning densitometry.

8.7.3 Oxidative stress

Reperfusion of the ischemic myocardium after cardioplegic arrest can be detrimental to the myocardium due to oxidative stress induced by reactive oxygen species (ROS). Furthermore, cardiopulmonary bypass also affects neutrophil activation, which is pro-inflammatory and essential in the mechanism of oxidative stress.¹¹⁵ Malondialdehyde (MDA) is a product formed from degrading polysaturated lipids by ROS. In Paper III, oxidative stress was evaluated by assessment of MDA by using a commercial fluorometric kit (K739-100, BioVision Inc., Milpitas, CA). Tissue samples obtained from the LV endo-, mid- and epicardium and the right ventricle were snap-frozen and stored in liquid nitrogen. Later the myocardial samples were homogenized, lysed and analyzed according to the manufacturer's instructions.

8.7.4 Metabolism

Fatty acids and glucose are the most important substrates for energy metabolism in the heart. Failure to produce, transport or utilize an adequate amount of energy causes functional loss and failure of the contractile work of the myocardium. Free fatty acids are transferred from the cytosol into the mitochondrion by the carnitine transport system. Carnitine palmitoyltransferase I and II (CPT-I, CPT-II) are enzymes essential for catalyzing the transport of carnitine from the cytosol through the outer- and inner membrane of the mitochondrion (Figure 1). The synthesis and catabolism of high-energy phosphates is the final step in the process of transforming chemical energy into mechanical work. In Paper I, assessment of CPT-I and CPT-II activity in the outer and inner mitochondrial membranes were evaluated. Each sample was homogenized after adding 500 μ l of ice-cold sucrose (0.25 M sucrose, 5 mM HEPES-buffer, 0.2 mM ethylene glycol tetraacetic acid, pH 7.4) and centrifuged at 4°C, 600 g for 12 min. The protein concentration in the supernatant (post-nuclear fraction) was measured (Bio-Rad Protein Assay, Bio-Rad Laboratories, Inc., Hercules, CA). In 150 μ g of protein, CPT-I and CPT-II were measured as described elsewhere.¹¹⁶

In Paper II, frozen tissues samples (averaging 65 mg) from the epi-/midmyocardium of the anterior left ventricular wall were homogenized with a micro-dismembrator and deproteinized with 500 μL of 0.4 mol/L perchloric acid. After centrifugation (12000 g) 200 μL of the acid extract was neutralized with 20-25 μL of 2 mol/L potassium carbonate (4°C). The supernatant (20 μL injection volume) obtained after centrifugation was used for high-performance liquid chromatography (HPLC) analysis. The pellets of the acid extract were dissolved in 1 mL of 0.1 mol/L sodium hydroxide and further diluted 1:10 with physiologic saline for protein determination (BCA Protein Assay, Pierce). High-energy phosphates (ATP, ADP, AMP and creatine phosphate), hypoxanthine and xanthine were measured by HPLC. Separation was performed on a Hypersil ODS column (5 μm , 250 mm x 4 mm I.D.) using a L-2200 autosampler, two L-2130 HTA pumps and a L-2450 diode array detector (all: VWR Hitachi, Radnor, PA). Detector signals (absorbance at 214 nm and 254 nm) were recorded and the program EZchrom Elite (VWR Hitachi) was used for data acquisition and analyzes. Energy charge (EC) was calculated as:¹¹⁷

$$EC = \frac{[ATP] + 0.5[ADP]}{[ATP] + [ADP] + [AMP]}$$

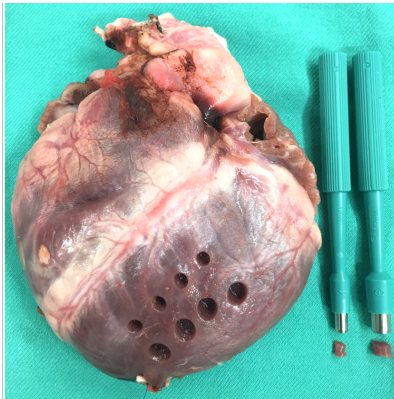


Figure 13. Explanted porcine heart with schematic illustration of multiple punch biopsies obtained from the left ventricular anterior wall at Baseline, during cardioplegic arrest and subsequent early and late during reperfusion in Paper II. In-vivo, the diagonal branches of the left anterior descending (LAD) artery were carefully avoided.

8.7.5 Ultrastructure

Morphological evaluation of the architecture of the myocyte in experimental models of myocardial ischemia has provided essential information on the pathogenesis of hypoxic heart injury.¹¹⁸ Transmission Electron Microscopy (TEM) produces a 2D

image with a maximum magnification of x 500.000. In heart muscle tissue, it visualizes cell structures like the nucleus, mitochondria, sarcoplasm system and the myofibrils.

In Paper I and II, myocardial tissue samples from the anterior left ventricular wall, were fixed overnight in 0.1 mol/L Na-cacodylate buffer with 2.5% glutaraldehyde, washed, post-fixated with 1% OsO₄, dehydrated and stored in 70% ethanol, sectioned and stained with uranyl acetate. Sections were visualized by TEM (JEM-1230, Jeol, Tokyo, Japan), and images acquired using a 1 MP Gatan camera. The scanning electron microscopy images (x15 000) were acquired with microscope (JSM-7400F, Jeol). By morphometry, the myocyte volume fraction of mitochondria (V_{Vmit}), myofibrils (V_{Vmyo}) and cytosol (V_{Vcyt}) were calculated as the number of overlaying points within the cellular structure related to the total number of points included in the extranuclear space on each micrograph with a grid of 81 points with random offset (Figure 14, left). With a random offset Merz grid (Figure 14, right) the mitochondrial surface-to-volume ratio was calculated as:

$$Sv_{ratio_{mit}} (\mu m^2 / \mu m^3) = (2 * Mx) / (Mp * l/p)$$

where Mx = the total number of outer mitochondrial membrane line-crossings, Mp = total number of points encircled by outer mitochondrial membranes and l/p is a constant for the applied Merz grid. The mitochondrial surface density was calculated:

$$Sv_{mit} (\mu m^2 / \mu m^3) = (2 * Mx) / l$$

where Mx = the total number of outer mitochondrial membrane line-crossings and l is the total length of lines in the Merz grid. In Paper I, a total number of 21813 mitochondrial points and 16135 line-crossings were counted with the Merz grid, corresponding numbers for Paper II were 34629 and 44310. In Paper II, the six micrographs from 15 randomly selected biopsies were individually coded and reanalyzed by the first observer, then recoded and analyzed by a second observer. The intra- and interobserver Intraclass Correlation Coefficient and Coefficient of Variation for morphological variables in 15 biopsies were calculated.

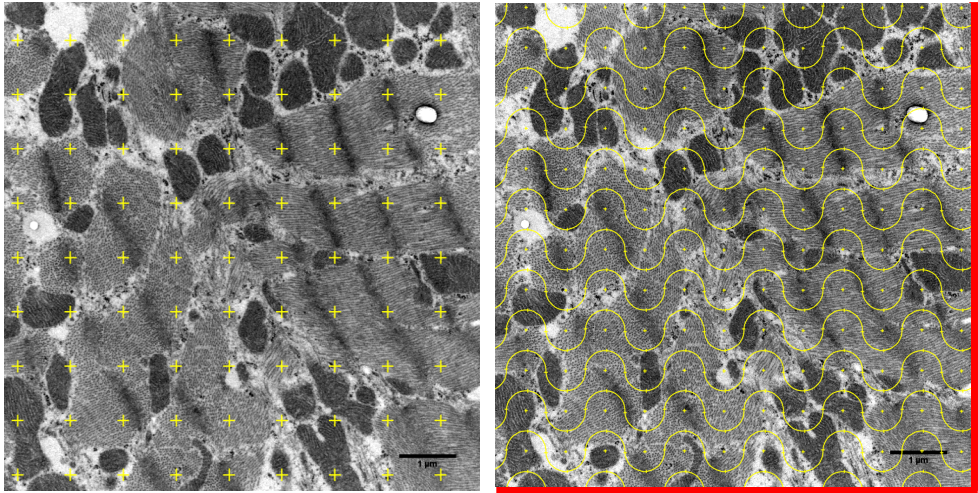


Figure 14. Evaluation of myocardial volume fraction of mitochondria, myofibrils and cytosol by a grid of 81 points (left). Merz grid for evaluation of mitochondrial surface-to-volume ratio and surface density (right). Mitochondria crossing beyond the lower horizontal and the right vertical edges (red) of the micrographs were not included.

8.7.6 Regional tissue blood flow and water content

Fluorescent microspheres (15 µm), with four different colors administered in a randomized sequence, were used for evaluation of regional tissue blood flow in Paper I and III. At each time point, 6 million microspheres were injected into the left atrium for distribution in the systematic circulation. Simultaneously, an arterial blood sample was extracted for 2 min using a constant rate pump (Sage Instruments, Cambridge, MA) as an artificial reference organ. Tissue- and reference samples were weighed, hydrolyzed, microspheres isolated by filtration, colors dissolved and quantified by fluorospectrophotometry. Regional tissue blood flow was subsequently calculated according to the distribution of embolized microspheres by using the formula:

$$Q_{sample} = \frac{I_{sample} * Q_{reference}}{I_{reference}}$$

where Q = flow and I = intensity measure from the fluorospectrophotometer.

For the evaluation of tissue water content, samples were dried for three weeks at 60°C before reweighing and water content calculated by the formula:

$$\text{Water content (\%)} = \frac{\text{wet weight} - \text{dry weight}}{\text{wet weight}} * 100$$

8.8 Left ventricular mechanical efficiency

An indirect way of evaluating MVO₂ is to use pressure-volume loops to define the pressure-volume area (PVA), which is the sum of stroke work and potential energy (Figure 8). PVA has been demonstrated to linearly correlate with LV oxygen consumption per beat independent of loading conditions, mode of contraction and contractile state.¹¹⁹ If myocardial blood flow is evaluated by the technique of fluorescent microspheres (Ch. 8.7.6), the relation between total mechanical work (PVA) and tissue blood flow rate in the left ventricle can be calculated as an index for mechanical efficiency.¹²⁰ In Paper III, the mechanical efficiency (Joule/mL/g myocardium) was calculated as the sum of mechanical and potential energy performed by the left ventricle per min related to blood flow rate by the formula:

$$\text{Mechanical Efficiency} = (PE + SW) * HR / BFR$$

where PE and SW are pressure-volume areas for the left ventricular potential energy and stroke work in Joule, HR is heart rate and BFR is left ventricular blood flow rate per g myocardium.

8.9 Blood chemistry

Blood samples were obtained from the arterial line in the groin, serum prepared and analyses of serum troponin-T (Troponin-T hs®, Roche Diagnostics, GmbH, Mannheim, Germany) were subsequently performed at the Laboratory for Clinical Biochemistry, Haukeland University Hospital. Blood for measuring arterial blood gases were sampled from the arterial line in the groin or directly from the heart-lung machine during CPB and momentarily analyzed at the Vivarium (ABL80 FLEX

COOX, Radiometer Medical ApS, Brønshøj, Denmark or OPTI CCA-TS2, OPTI Medical Systems, Atlanta, GA).

8.10 Experimental protocols

8.10.1 Paper I

Animal preparation and surgical instrumentation were performed as previously described (Ch. 8.2). Following baseline assessments, tepid (34°C) CPB was initiated before 60 min of CA with STH-POL or STH-2 administered every 20 min. Cardiac and hemodynamic variables were continuously recorded. Global and regional cardiac function and tissue blood flow rate at Baseline and 60, 120 and 180 min after declamping and weaning from CPB, were evaluated with pressure–conductance catheter, epicardial echocardiography and microsphere injections. After the final registration, the animal was euthanized with intracardiac injection of high-dose potassium chloride, the heart was explanted and myocardial samples were obtained for later analysis.

8.10.2 Paper II

Left ventricular and general hemodynamic variables were continuously recorded in Paper II. At Baseline, myocardial biopsies from the anterior left ventricular wall were sampled. CPB was established followed by 60 min of CA as described in Paper I. After 58 min of arrest, myocardial biopsies were repeated. The animals were weaned from CPB after 10 min of myocardial reperfusion. At 20 and 180 min after declamping, myocardial biopsies were repeated (Figure 13). Finally, the animal was euthanized with intracardiac injection of high-dose potassium chloride, the heart was removed, and myocardial samples obtained for complementary analysis.

8.10.3 Paper III

The protocol in Paper III was a modification of the protocol in Paper I. Following Baseline assessments using pressure–conductance catheter, epicardial echocardiography and microspheres, tepid CPB was initiated before 120 min of CA with STH-POL or STH-2 administered every 20 min. Ten min after declamping, the animals were weaned from CPB. Corresponding measurements as for Baseline were performed at 60, 150 and 240 min after myocardial reperfusion. After the final registration, the animal was euthanized with intracardiac injection of high-dose potassium chloride, the heart was explanted and myocardial samples were obtained for later analysis.

8.11 Statistical analysis

Data were analyzed by using the commercial software Statistical Package for Social Science (IBM Corp., Armonk, NY) with SPSS version 22 (Paper I) and SPSS version 23 (Paper II + III). Values were given as mean \pm SEM or median (25% quartile; 75% quartile) unless otherwise notified. In all studies, $P < 0.05$ was considered statistically significant except for the interaction effect in the two-way analysis of variance for repeated measurements, RM-ANOVA ($P_i < 0.10 =$ significant). Baseline variables were analyzed for normal distribution and equal variance using the Kolmogorov-Smirnov and Levene tests. After testing for normality, the baseline data were compared by two-sample Student's *t*-test or Wilcoxon–Mann–Whitney U-test on ranks. Both hemodynamic variables obtained during and after CPB and tissue contents of high-energy phosphates (Paper II) were analyzed by RM-ANOVA with time as within factor (P_w) and cardioplegia with STH-POL or STH-2 as grouping factor (P_g) and post hoc Bonferroni contrasts between individual group means.¹²¹ The Greenhouse-Geisser adjustment of the degrees of freedom was used for the evaluation of main effects when Mauchly's test of sphericity was significant ($P < 0.05$). If a significant interaction ($P_i < 0.10$) was found between the within and the grouping factor, new ANOVAs for simple main effect were performed with adjustment of the

degrees of freedom. Cell means were finally compared with Neumann-Keuls multiple contrast tests when justified by the preceding ANOVA. For estimation of caspase-3 activity (Paper I + III), GRK2 (Paper I) and MDA (Paper III), myocardial wall layers were set as related variables. The morphometric variables in Paper II were analyzed with a nested RM-ANOVA using 6 micrographs from each biopsy and 4 different biopsies (time) from each animal. Additionally, in Paper II the Intraclass Correlation Coefficient (ICC) and Coefficient of Variation (CV%) for inter- and intraobserver variability were calculated for morphometric data. In Paper III, the interobserver ICC for 20 randomly TDI and STE recordings were calculated. The Chi-square test was used for calculating group differences for nominal data.

9. SUMMARY OF RESULTS

9.1 Paper I

In the first paper, 20 animals were assigned for 60 min of cardioplegic arrest followed by 180 min of reperfusion after weaning from CPB. Asystole was rapidly induced and maintained throughout the ischemic period. During reperfusion, the heart rate was increased and left ventricular end-systolic and end-diastolic pressures decreased in both groups compared to Baseline. Cardiac index (CI), systolic pressure and radial peak systolic strain did not differ between groups. Contractility, evaluated as dP/dt_{max} gradually increased from 120 to 180 min after declamping in the STH-POL group, and was significantly higher compared to the STH-2 group after 180 min of reperfusion (1871 ± 160 (SEM) mmHg/s vs. 1351 ± 70 mmHg/s, $P = 0.008$). Furthermore, the load-independent contractility variable Preload Recrutable Stroke Work was increased with polarizing cardioplegia (64 ± 3 vs. 54 ± 2 mmHg, $P = 0.018$) 180 min after declamping and weaning. Likewise, radial peak ejection strain rate decreased in the STH-2 group at 180 min only, indicating better preserved left ventricular contractility with polarizing cardioplegia. At 180 min after aortic declamping, phosphorylation of GRK2 in myocardial tissue did not differ between groups. Fractional cytoplasmic volume in myocytes was reduced in hearts following polarizing

cardioplegia, indicating reduction of cytoplasmic edema. However, myocardial tissue water content did not differ between treatment groups.

In summary: In this study of myocardial function, polarizing oxygenated blood cardioplegia with esmolol, adenosine and Mg^{2+} , offered comparable myocardial protection and improved contractility compared to the standard potassium-based depolarizing blood cardioplegia. Contractility was increased three hours after reperfusion following polarizing cardioplegia.

9.2 Paper II

In Paper II, results were presented for 10 animals in each group. The protocol was 60 min of cardioplegic arrest followed by 180 min of observation after weaning from CPB. With STH-POL cardioplegia, myocardial creatine phosphate was increased compared to STH-2 at 58 min of aortic cross-clamping (59.9 ± 6.4 (SEM) vs. 44.5 ± 7.4 nmol/mg protein; $P < 0.025$), and at 20 min after reperfusion (61.0 ± 6.7 vs. 49.0 ± 5.5 nmol/mg protein; $P < 0.05$), ATP levels were increased at 20 min of reperfusion with STH-POL (35.4 ± 1.1 vs. 32.4 ± 1.2 nmol/mg protein; $P < 0.05$). Mitochondrial surface-to-volume ratio was decreased with polarizing compared to depolarizing cardioplegia 20 min after reperfusion (6.74 ± 0.14 vs. 7.46 ± 0.13 $\mu m^2/\mu m^3$; $P = 0.047$). None of these differences were present at 180 min of reperfusion. From 150 min of reperfusion and onwards, cardiac index was increased with STH-POL; 4.8 ± 0.2 compared to 4.0 ± 0.2 L/min/m² ($P = 0.011$) for STH-2 at 180 min.

In summary: In this study of myocardial energy metabolism and ultrastructure, polarizing cardioplegia (STH-POL) improved energy status compared to standard depolarizing (STH-2) blood cardioplegia during cardioplegic arrest and early after reperfusion.

9.3 Paper III

In Paper III, 20 animals (10 in each group) were randomized to cardioplegic arrest for 120 min followed by 240 min of reperfusion after weaning from CPB. Mean arterial pressure (MAP) was significantly decreased in the STH-POL compared to the STH-2 group at 60, 80 and 100 min of aortic cross-clamping, but equal at declamping after 120 min. Serum potassium gradually increased over time in both groups during CPB but more pronounced with STH-2 cardioplegia. At declamping, serum potassium averaged 4.4 ± 0.1 mmol/L in the STH-POL vs. 5.5 ± 0.2 mmol/L in the STH-2 group ($P < 0.001$). Electrical cardioversion of ventricular fibrillation before weaning from CPB was required in 2 out of 10 animals in the STH-POL vs. 8 out of 10 in the STH-2 group ($P = 0.025$). Preload Recrutable Stroke Work was significantly increased in the STH-POL compared to the STH-2 group 150 min after declamping (73.0 ± 3.2 vs. 64.3 ± 2.4 mmHg, $P = 0.047$), but did not differ after 240 min. Radial peak ejection strain rate decreased during reperfusion in both STH-POL and STH-2 with no significant differences between groups. Left ventricular wall blood flow rate decreased in the STH-POL group only ($P < 0.005$) from 60 min to 150 min after declamping and was essentially unchanged in the STH-2 group. At 240 min after declamping, left ventricular blood flow rate was significantly reduced in the STH-POL compared to the STH-2 group ($P < 0.05$). The left ventricular mechanical energy gain related to blood flow rate, was reduced by approximately 50% 60 min after aortic declamping compared to Baseline. Mechanical efficiency gradually decreased in the STH-2 group only and was significantly lower than in the STH-POL group at 150 and 240 min after declamping.

In summary: In this study of myocardial function following prolonged cardioplegic arrest, STH-POL in oxygenated blood alleviated the mismatch between myocardial function and perfusion after weaning from CPB compared to STH-2 blood cardioplegia. Left ventricular mechanical efficiency was better preserved after reperfusion following polarizing cardioplegia.

10. DISCUSSION

10.1 Polarizing cardioplegia

The mechanism of polarized cardioplegic arrest is previously described (Ch. 6.3.2). However, there is no clear definition of the concept of polarizing cardioplegia. The terminology is used to distinguish it from what was originally described by Cohen and colleagues in 1995, suggesting that the use of a Na⁺ channel blocker would induce hyperpolarized arrest.¹²² The initial studies of Chambers and Hearst measuring the resting membrane potential during arrest with tetrodotoxin (TTX), demonstrated that cardioplegic arrest was obtained with a membrane potential around – 70 mV, which is clearly not a hyperpolarized state.^{56,123} Others, such as Cohen and Dobson, used the Nernst equation to calculate what would occur with the myocyte membrane potential, but when actually measuring it with sharp electrodes it does not occur as calculated.^{45,46,122} There is, in fact, a depolarization but it is less than what occurs with potassium arrest (classically defined as depolarized arrest). The use of the phrase STH-polarized arrest is to distinguish the new solution from the original STH-2 cardioplegia. However, it cannot be stated that the resting membrane potential is – 70 mV during esmolol/adenosine/Mg²⁺ arrest. It is only assumed that there is a polarized arrest by the fact that esmolol also acts to inhibit the Na⁺ channel in the same way as TTX.¹²⁴

10.2 Esmolol and adenosine for myocardial protection

10.2.1 Esmolol

The short acting β_1 -blocker esmolol is the main component in the St. Thomas Hospital polarizing cardioplegic solution. The use of continuous infusion of esmolol solely to obtain cardiac arrest or minimal myocardial contraction, have previously been studied in translational large animal models and in clinical studies.¹²⁵⁻¹²⁷ Continuous coronary perfusion with normothermic esmolol-enriched blood without aortic cross-clamping avoids myocardial ischemia and minimize myocardial edema, thus completely

preserving cardiac performance in dogs.¹²⁸ In patients, a similar cardioplegic protocol with aortic cross-clamping during elective CABG is associated with slightly better functional recovery and less structural myocardial alterations compared to intermittent cold blood cardioplegia.¹²⁹ However, improved clinical outcome has not been reported.^{130,131}

Esmolol given prior to 80 min of cardioplegic arrest with cold oxygenated blood cardioplegia, alleviates left ventricular dysfunction in the early hours after weaning from CPB in a porcine model.¹³² Esmolol given immediately before CPB and as an additive in Custodiol® crystalloid cardioplegia in elective patients, reduced peak postoperative troponin levels but without differences in clinical outcome.¹³³ Esmolol supplementation in cardioplegia administered to patients with unstable angina operated with urgent CABG, did not increase the efficacy of cardioprotection.¹³⁴ In a porcine model, esmolol as additive in STH-2 cold blood cardioplegia preserved left ventricular systolic function during the first 3 hours after reperfusion following 100 min of cardioplegic arrest.⁵³ If esmolol was added to STH-2 crystalloid cardioplegia administered as a single-dose in pediatric patients operated for congenital heart defects, less inotropic support was required postoperatively with increased ejection fraction and cardiac output one week postoperatively.¹³⁵ In general, β -blockers significantly reduced the incidence of postoperative supraventricular and ventricular arrhythmias and the length of hospital stay, but with no reduction of all-cause mortality, acute myocardial ischaemia/infarction and cerebrovascular events.¹³⁶

The studies sited above are not contradictory to the results in Paper I - III, but somewhat confirm and support the main findings (Ch. 9) in this thesis. A potential protective mechanism of esmolol during and after cardioplegic arrest, is the inhibition of desensitization of β -adrenergic receptors (β -AR). Impaired signaling and desensitization of β -AR contribute to myocardial dysfunction and is demonstrated in both chronic heart failure as well as in patients undergoing cardiac surgery due to the acutely increased catecholamine and norepinephrine release following CPB and CA.¹¹² Furthermore, β -AR desensitization is associated with increased GRK2 activity (Ch. 8.7.2). Paper I demonstrated no differences in myocardial levels of phosphorylated GRK2 activity after STH-POL compared to STH-2 cardioplegia. However, neither

adenylate cyclase activity nor GRK2 activity were measured directly, thus the inhibition of β -AR desensitization cannot be entirely excluded as an explanation for the improved contractile function observed in animals with polarizing cardioplegia. Whether the time of CPB and CA in Paper I were too limited for detecting potential group differences of β -AR desensitization, remains unclear.

10.2.2 Adenosine

Adenosine administered before onset of ischemia (pharmacological preconditioning), during ischemia or at reperfusion (postconditioning), has been extensively investigated with clear evidence of protection of the myocardium through activation of various adenosine receptor subtypes (A_1 , A_{2a} , A_{2b} , A_3).¹³⁷⁻¹⁴⁰ Adenosine as a sole cardioplegic agent has been investigated in isolated rat hearts and induces rapid cardiac arrest and improved postischemic recovery compared to potassium cardioplegia.¹⁴¹ Also, adenosine as an adjunct to hyperkalemic cardioplegia has been investigated with similar results regarding arresting time and myocardial recovery.^{55,142} Adenosine instead of hyperkalemic cold crystalloid cardioplegia, has demonstrated improved postcardioplegic left ventricular systolic function and efficiency in addition to less myocardial cell damage in an *in-vivo* large animal model.⁵⁰ Also, adenosine as key agent in cold crystalloid cardioplegia increases postcardioplegic myocardial blood flow and preserves the endothelium-derived hyperpolarization dependent vasodilatation, compared to high potassium cardioplegia.¹⁴³ Other experimental studies have investigated adenosine as an adjunct to standard cardioplegia and demonstrate adenosine-supplemented cardioplegia to attenuate postoperative dysfunction in severely injured hearts.^{144,145} Adenosine in combination with lidocaine, has demonstrated better functional recovery compared to hyperkalemic cardioplegia both experimentally and clinically.^{46, 52,146}

Other clinical studies with adenosine instead of hyperkalemic cardioplegia, demonstrated a more rapid CA and lower incidence of postoperative atrial fibrillation, but without proof of differences regarding cardioprotection or preservation of hemodynamic parameters.¹⁴⁷ Moreover, treatment benefits from adenosine

supplementation have not been demonstrated regarding risk of myocardial infarction, low output syndrome, inotropic support, intra-aortic balloon pump (IABP) requirement or postoperative mortality.¹⁴⁸

Pharmacological preconditioning with adenosine has been investigated in patients with reduced left ventricular function ($EF < 30\%$) undergoing CABG, demonstrating better preserved CI and less creatine phosphokinase release in the adenosine group.¹⁴⁹ Adenosine pretreatment has also been investigated in pediatric patients undergoing congenital heart surgery. Main findings in this study were postoperative increased levels of serum troponin I and more use of inotropic agents in the control group, with the conclusion that adenosine pretreatment protects the myocardium during open heart surgery in pediatric patients.¹⁵⁰ During heart valve replacement in adults, the effect of adenosine given as a bolus injection immediately after aortic declamping, demonstrated less troponin I release, less inotropic drug use, and shorter stay in the intensive care unit.¹⁵¹

10.3 Polarized vs. depolarized cardioplegic arrest

In this clinically relevant porcine model, both STH-POL and STH-2 cardioplegic solutions trigger and maintain cardiac arrest when administered as repeated, cold, oxygenated blood. The STH-POL cardioplegia must be freshly mixed with the blood by a dual-head HLM pump at the time of infusion to prevent rapid degradation of both the esmolol and adenosine components.

The time from aortic cross-clamping to left ventricular mechanical arrest was comparable between groups in Paper I. However, the time to isoelectric ECG was significantly prolonged with STH-POL compared to STH-2 cardioplegia (Table 2). This was also confirmed in Paper III, demonstrating a similar difference, 121 s (105; 150) for STH-POL vs. 47 s (30; 61) for STH-2 ($P = 0.001$) until isoelectric ECG.

During the 60 min period of cardioplegic arrest, there were no differences between treatment groups regarding MAP during CPB in Paper I and II. This was also observed for the first 40 min of CA in Paper III. However, STH-POL cardioplegia significantly

reduced MAP at 60, 80 and 100 min after aortic cross-clamping. The increased amounts of esmolol and adenosine administered in Paper III compared to Paper I and II together with prolonged general hypothermia, may have resulted in accumulation of both esmolol and adenosine, due to prolonged half-lives at 34°C compared to 37°C. After rewarming and at the time of declamping, there were no differences between groups regarding MAP in Paper III (Figure 15). At this point of time, MAP was comparable to the levels observed in Paper I and II.

Table 2. Effects of polarizing (STH-POL) and depolarizing (STH-2) cardioplegia delivered as repeated oxygenated blood in pigs from Paper I. Mean \pm SEM or Median (25%; 75%).

	STH-POL (n = 10)	STH-2 (n = 10)	Statistics
X-clamp:			
Time to LV asystole (s):	28 (11; 43)	22 (18; 27)	$P = 0.79$
Time to isoelectric ECG (s):	86 (80; 134)	41 (32; 43)	$P = 0.002$
Declamp:			
Time to first LVP (s):	81 \pm 19	129 \pm 32	$P = 0.22$
Time to regular LVP (s):	108 (87; 122)	138 (112; 286)	$P = 0.13$

X-clamp = aortic cross-clamping; LV = left ventricle; LVP = left ventricular pressure, registered by the pressure-conductance catheter; s = time in seconds.

10.4 Energy metabolism

In Paper II, a transient improvement in energy status with STH-POL cardioplegia was demonstrated as an increase in the myocardial tissue content of creatine phosphate (CrP) after 58 min of CA and at 20 min after reperfusion and weaning from CPB compared to STH-2 cardioplegia. In addition, tissue ATP content was increased in the early period of reperfusion. In the metabolic pathway of high-energy phosphate degradation and synthesis, creatine kinases present in the mitochondrial inner membrane space and in cytosol, regenerates CrP from creatine imported from the cytosol and surplus mitochondrial ATP.

Cytosolic CrP serves as an energy reservoir for the rapid buffering and regeneration of ATP in situ. Myocardial creatine kinase thus facilitates intracellular energy transport by the phosphocreatine shuttle or circuit (Figure 1).

The reduced consumption of CrP demonstrated in Paper II during the 60 min of cardioplegic arrest and early after reperfusion in the STH-POL group, can be interpreted as a result of a reduced energy consumption with polarizing cardioplegia needed for maintaining intracellular ion balance.

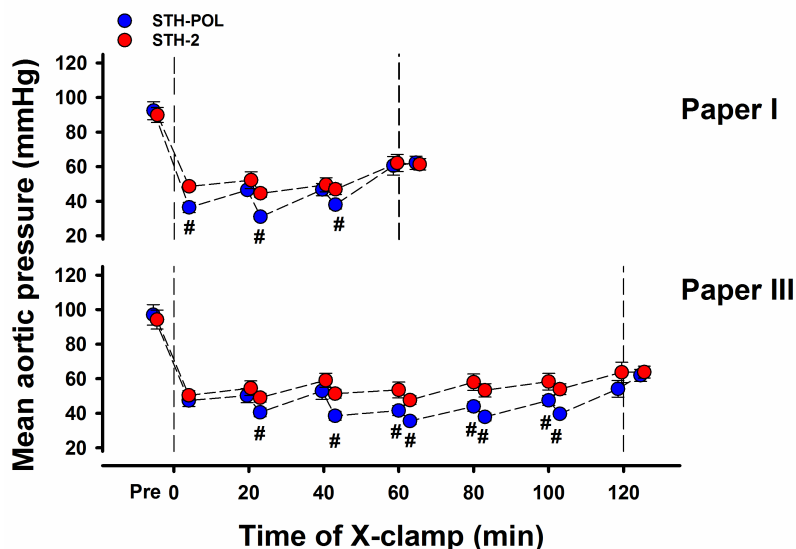


Figure 15. Mean aortic pressure (MAP) in Paper I and III during the period of aortic cross-clamping (X-clamp) and administration of cardioplegia, repeated every 20 min. Assessment of MAP was just before and one min after cardioplegic administrations. Pre = point in time just before X-clamp (0); # = significant difference ($P < 0.05$) between STH-POL (blue) and STH-2 (red) at corresponding point in time.

Also, the resulting abundance of CrP facilitates stabilizing of the myocyte membrane phospholipid bilayer by binding to the polar heads and decreasing membrane fluidity. As a consequence, this attenuates some of the damage caused by the transient ischemia and hypoxia and thus alleviates cytoplasmic leakage.^{124,152} Following 180 min of reperfusion, the levels of high-energy phosphates and degradation products regained baseline levels and did not differ between the treatment groups.

The adenosine component of STH-POL cardioplegia resulted in high tissue levels of the degradation product hypoxanthine both during the period of arrest and early after declamping (Paper II). This increase could represent a potential disadvantage due to further degradation to xanthine and uric acid by xanthine oxidase and subsequent production of detrimental reactive oxygen species in the endothelial cells.¹⁵² However, the levels of xanthine oxidase has been demonstrated to be low in the porcine heart and therefore the surplus myocardial hypoxanthine in the STH-POL group is more likely to be washed out during reperfusion.¹⁵³ This feasible explanation is further strengthened in Paper III where oxidative stress was evaluated by assessment of levels of MDA (Ch. 8.7.3), which did not differ between the two cardioplegic solutions in different regions of the left and in the right ventricle 240 min after aortic declamping.

10.5 Ultrastructure

Following 60 min of cardiac arrest with STH-POL cardioplegia and 180 min of reperfusion, a decrease in myocyte cytosolic volume fraction and mitochondrial surface-to-volume ratio was demonstrated compared to STH-2 arrested hearts (Paper I). This could be explained by a shift of intracellular volume from cytosol to mitochondria. Reduced tissue edema and improved left ventricular function after declamping have been linked to continuous esmolol perfusion compared to warm blood cardioplegia.¹²⁸ However, except for a temporary mitochondrial swelling with STH-POL cardioplegia 20 min after reperfusion, no ultrastructural differences were demonstrated between polarizing and depolarizing cardioplegia 180 min after declamping in Paper II.

10.6 Weaning from cardiopulmonary bypass

Following aortic declamping and reperfusion, ventricular fibrillation was a regular event in relation to declamping. In a total of 40 animals with 60 min of cardioplegic arrest (Paper I and II), electrical cardioversion was needed in eight out of 20 animals with STH-POL cardioplegia compared to 12 out of 20 animals with STH-2

cardioplegia ($P = 0.34$). The time to the first left ventricular contraction and the time needed to establish a regular ventricular rhythm did not differ between hearts arrested with STH-POL or STH-2 cardioplegia (Table 2).

The frequency of necessary electrical cardioversion is likely related to serum potassium levels at the time of reperfusion.¹⁵⁴ After 60 min of cardiac arrest, s-K⁺ averaged 4.3 ± 0.1 mmol/L for STH-POL and 4.8 ± 0.1 mmol/L for STH-2 cardioplegia at aortic declamping. Following 120 min of cardioplegic arrest, corresponding potassium levels were 4.4 ± 0.1 mmol/L in the STH-POL vs. 5.5 ± 0.2 mmol/L in the STH-2 group. Two out of 10 animals in the STH-POL and eight out of 10 in the STH-2 group needed electrical cardioversion following declamping (Paper III).

10.7 General hemodynamics

In all three studies, heart rate gradually increased following CPB and CA in both experimental groups over time. The left ventricular systolic pressure (LVSP) decreased in Paper I and III whereas was essentially unchanged in Paper II. End-diastolic pressure (LVEDP) decreased gradually in both groups in Paper I and II and was unchanged in Paper III after weaning from CPB. Venous filling, evaluated by central venous pressure (CVP), increased over time in Paper I and II but was unchanged in Paper III. These hemodynamic changes are not fully consistent, probably reflecting the experimental protocol differences between the studies. An increase in heart rate result in less left ventricular filling with reduced contribution of the Frank-Starling effect and reduction of LVSP after weaning from CPB. These changes are comparable between the different studies.

Cardiac index (CI) was increased in the period of reperfusion in the STH-POL compared to the STH-2 group in Paper II, whereas no differences between groups were observed in Paper I and III.

In Paper I – III, the mean pulmonary artery pressure (PAP_{mean}) had the similar tendency of increasing in the early period after CPB and CA but without significant

differences between groups. In Paper III, PAP_{mean} tended to decrease in the late period of observation. The duration of CPB has been identified as a factor of postoperative pulmonary hypertension, but this effect was not observed in our studies when the time of aortic cross-clamping was increased from 60 min (Paper I + II) to 120 min (Paper III).¹⁵⁵

In general, within each study, variables describing the pre- and afterload conditions after aortic declamping were comparable between treatment groups. Furthermore, variables like heart rate, mean aortic pressure, left ventricular end-diastolic pressures and volumes after declamping were reproducible between studies.

10.8 Systolic and diastolic function

Both left (LV-EF) and right (RV-EF) ventricular ejection fraction remained normal in all protocols and did not differ between groups. In Paper I, $LV-dP/dt_{\text{max}}$ was significantly higher compared to the STH-2 group after 165 and 180 min of reperfusion. A similar, but not significant difference was also observed in Paper II. In Paper III, $LV-dP/dt_{\text{max}}$ decreased from 90 min and onwards but without differences between treatment groups. Indexed stroke work (SW_i) was better maintained in the STH-POL group at 180 min after declamping in Paper I while this difference was not observed in Paper III.

The load-independent contractility variable PRSW was better maintained at 180 min of reperfusion in the STH-POL compared to the STH-2 group in Paper I. In Paper III, PRSW was significantly increased in the STH-POL compared to the STH-2 group 150 min after declamping but did not differ after 240 min. At the end of the experiment, peak ejection strain rate was significantly increased in the STH-POL compared to the STH-POL group in Paper I. As for PRSW, this difference was not observed after the prolonged cardioplegic arrest and observation period after aortic declamping in Paper III.

The left ventricular relaxation properties in diastole (lusitropy) were evaluated by the isovolumic relaxation time constant Tau (τ) and end-diastolic pressure-volume relation

β , which did not differ over time between groups or protocol (Paper I and III). Furthermore, $LV-dP/dt_{min}$ was more negative in the STH-POL compared to the STH-2 group at the end of reperfusion in Paper I.

With comparable loading conditions, the load-dependent systolic variables SW_i and dP/dt_{max} and the load-independent PRSW were better preserved at the end of reperfusion after STH-POL compared to STH-2 cardioplegia following 60 min of cardioplegic arrest (Paper I and II). These differences were not observed in Paper III when the time of CPB and CA were extended to 120 min following 240 min of reperfusion.

Data of general hemodynamics and functional variables, both from PV-loops and TDI/STE, have previously been reported from studies conducted in our laboratory using a similar porcine model with 60, 80 or 100 min of STH-2 cardioplegic arrest as control groups.^{52, 128, 151-153} Overall, data from these studies supports and verifies the results from the different STH-2 control groups in this thesis.

Despite strict standardized protocols where only time of CPB, CA and postoperative observation were different (Paper I and III), there will always be variations and compensatory mechanisms that will influence the complex hemodynamic interactions. However, our hemodynamic and functional data indicates that normokalemic polarized cardioplegic arrest is non-inferior to hyperkalemic depolarized arrest.

10.9 Myocardial injury

In this model of cardioplegic arrest, evaluation of myocardial injury due to the mechanism of ischemia/reperfusion (I/R) was implemented in Paper I and III. In both studies, serum troponin-T accumulated over time but did not differ between groups. At 180 min (Paper I), median values were 504 (328; 886) vs. 580 (401; 717) ng/L, compared to 802 ± 114 vs. 907 ± 169 ng/L at 240 min in Paper III. It is not clear if the observed higher level of troponin-T in Paper III was caused by the extended time of CA or longer time of observation compared to Paper I. In theory, a potential difference between groups was not revealed since myocardial troponins peaks later in the

postoperative period. Increased troponin levels following CA is set and ascribed to a number of causes, but in the context of this model, may be due to cell death from insufficient myocardial protection during the ischemic period. The serum levels of postoperative myocardial enzymes are independently associated with both increased intermediate- and long-term risk of mortality.¹⁵⁶

Myocardial apoptotic activation evaluated by caspase-3 activity, did not differ between groups neither in Paper I nor in Paper III. In both studies, cleaved caspase-3 activity was increased in the subepicardial layer compared to the mid- and subendocardial wall layers. This observation is contradictory if cardioplegia delivery and protection is favorable in the outer epicardium compared to the inner endocardium layer due to low coronary perfusion.¹⁵⁷ However, additional topical cooling of the heart was not integrated in either of the experimental protocols. Consequently, a gradual rewarming of the outer surface of the heart will occur between the administrations of cold cardioplegia and is likely to impair the subepicardial protection in this open chest model. Furthermore, in Paper III apoptotic activation was more pronounced in the right ventricular wall. Non-uniform distribution of the cardioplegic solution in hearts even without the presence of coronary artery disease, is acknowledged when using retrograde administration.¹⁵⁸ This is also reported during antegrade cardioplegia delivery and thus the right ventricle is especially vulnerable.¹⁵⁹ Also, in our porcine model, atrial P-waves at the ECG were observed frequently during cardioplegic arrest and were sometimes associated with right ventricular mechanical activity.

Oxidative stress was evaluated in Paper III only, where the assessment of MDA did not indicate any differences between treatment groups. To our knowledge, esmolol has no antioxidative effect, dissimilar from the combined α - and β -adrenergic blocker carvedilol.¹⁶⁰ Adenosine has antioxidative properties during reperfusion in both animal models and in clinical trials (Ch. 10.2.2). In our model, the final dose of adenosine was administered 20 min prior to reperfusion. Due to the dosage and short half-time in blood ($T_{1/2} < 10$ s), we did not expect to observe less oxidative stress in the STH-POL group caused by the effect of adenosine. In this thesis, there were no evidence for a relationship between loss of function and verified myocardial injury. Increased apoptotic activation during prolonged ischemia in Paper III compared to Paper I, could

be expected but was not demonstrated in our studies. This observation could be a consequence of adequate myocardial protection in both protocols. As a summary, there were no indications of better protection from I/R-injury in the esmolol/adenosine treated group, evaluated by the markers of apoptosis or oxidative stress used in this thesis.

Ischemia/reperfusion due to cardioplegic arrest may lead to injury demonstrated as myocardial inflammation and apoptosis, which clinically can be presented as arrhythmias, transient contractile dysfunction (stunning) or irreversible myocardial infarction.¹⁶¹ The pathophysiology and mediators of I/R-injury in correlation to hyperkalemic cardioplegic solutions, have been extensively investigated for over four decades.^{33,47,70} Prolonged depolarized myocyte membrane (Ch. 6.3.1) results in increased intracellular Na^+ and Ca^{2+} due to ion current across inactivated Na^+ and Ca^{2+} channels.¹⁶² The global ischemia results in compromised ATP production following ineffective ATP dependent pumps (sarcolemmal Na^+/K^+ ATPase, Ca^{2+} ATPase, sarcoplasmic reticulum Ca^{2+} ATPase), which also increases intracellular Na^+ and Ca^{2+} concentrations. Because of increased intracellular sodium, the reversal of the $\text{Na}^+/\text{Ca}^{2+}$ exchanger causes a net influx of Ca^{2+} (1 Na^+ out, 3 Ca^{2+} in) into to the myocardial cell.¹⁶³ Furthermore, metabolic acidosis due to proton accumulation activates the compensating Na^+/H^+ exchanger with the effect of additional augmented Na^+ concentrations. In addition, hypothermia has been demonstrated to exacerbate the adverse effect of Ca^{2+} loading during ischemia.¹⁶⁴

10.10 Myocardial dysfunction

Hyperkalemic depolarizing cardioplegic solutions have been demonstrated to both contribute and aggravate myocardial stunning/dysfunction due to continual metabolic requirements and detrimental transmembrane ionic fluxes as previously described (Ch. 10.9). The term stunning in this context is reversible postcardioplegic contractile dysfunction, which may last for hours or days. Myocardial stunning can also be defined as a temporary mismatch between myocardial function and oxygen consumption, hence also myocardial blood flow.^{165,166} With 120 min of cardioplegic

arrest (Paper III), the relationship between pressure-volume loop area of the left ventricle and blood flow rate in the left ventricular myocardium was clearly reduced 60 min after aortic declamping compared to Baseline. The mismatch between function and blood flow deteriorated further in the STH-2 group, only. However, the observation time of 240 min after declamping is too short to interpret this finding as alleviated stunning in the STH-POL group.

10.11 Methodological considerations

10.11.1 Animal model

The use of domestic pigs in *in-vivo* cardiovascular experiments is common.¹⁶⁷ The intact porcine model allows analysis of interventions on the heart, with the humoral, neural, adrenergic and anesthetic influence also seen in clinical practice. In general, the anatomy and physiology resemble human conditions and the porcine heart is applicable due to its similarity to the human heart regarding hemodynamic function and coronary circulation.¹⁶⁸ By operating on young pigs, advanced instrumentation is technically achievable, and medical devices and equipment developed for human healthcare can be used. Still, the possibility of species differences is a limitation. Furthermore, the use of healthy young hearts does not represent the common clinical practice.

The porcine heart is particularly predisposed for various tachyarrhythmias.¹⁶⁹ Additionally, patent foramen ovale (PFO) or other atrial septal defects (ASD) are often present.¹⁷⁰ Ventricular septal defect (VSD) and patent ductus arteriosus (PDA) are also more common compared to the human heart.¹⁷¹ After weaning from cardiopulmonary bypass, pulmonary arterial hypertension (PAH) is a frequent and a major problem in the porcine model. PAH followed by acute right heart failure in combination with PFO or ASD, result in right-to-left atrial shunting. This leads to a severe arterial hypoxia and may terminate in left ventricular failure. In general, porcine blood vessels are more fragile than in humans, hence with occasionally intimal dissection or other technical difficulties causing failure during instrumentation and cannulations.

Table 3. Baseline variables before cardioplegic arrest in three experimental studies. Values are mean (95% confidence interval).

Variable	Paper I (n = 20)	Paper II (n = 20)	Paper III (n = 20)
BW	42 (1)	42 (1)	42 (1)
HR (beats/min)	87 (3)	96 (7)	91 (5)
LV-SP _{max} (mmHg)	111 (6)	95 (5)	114 (7)
LV-EDP (mmHg)	11.2 (1.4)	7.5 (1.3)	9.3 (1.2)
LV-dP/dt _{max} (mmHg/s)	1577 (124)	1303 (128)	1506 (133)
LV-dP/dt _{min} (mmHg/s)	-2625 (216)	-1782 (116)	-2248 (280)
LV-Tau (ms)	32.1 (1.8)	31.6 (1.7)	36.6 (2.9)
LV-EDV _i (mL/m ²)	81 (7)	-	80 (5)
LV-ESV _i (mL/m ²)	38 (6)	-	36 (4)
LV-SV _i (mL/m ²)	50 (4)	-	44 (3)
LV-EF (%)	58 (4)	-	54 (2)
LV-SW _i (mmHg*mL/m ²)	4060 (354)	-	4310 (539)
CI (L/min/m ²)	4.0 (0.3)	3.8 (0.2)	4.0 (0.2)
RV-EDV _i (mL/m ²)	142 (9)	132 [#] (8)	135 (11)
RV-EF (%)	25 (2)	33 [#] (2)	26 (3)
AOP _{mean} (mmHg)	96 (5)	84 (7)	97 (7)
CVP _{mean} (mmHg)	6.0 (0.7)	7.0 (1.0)	7.0 (1.0)
PAP _{mean} (mmHg)	20 (2)	17 (1)	19 (2)
Tissue blood flow (mL/min per g)			
LV-Epi	0.98 (0.08)	-	0.84 (0.07)
LV-Mid	0.94 (0.09)	-	0.97 (0.07)
LV-Endo	1.02 (0.11)	-	1.02 (0.08)
RV	0.75 (0.11)	-	0.65 (0.08)

BW = bodyweight; *HR* = heart rate; *LV* and *RV* = left and right ventricle; *i* = value indexed for body surface area; *SP* = systolic pressure; *EDP* = end-diastolic pressure; *dP/dt* = pressure-volume relationship; *EDV* = end-diastolic volume; *ESV* = end-systolic volume; *SV* = stroke volume; *EF* = ejection fraction; *SW* = stroke work; *CI* = cardiac index; *AOP* = aortic pressure; *CVP* = central venous pressure; *PAP* = pulmonary artery pressure; *Epi*-, *Mid*- and *Endo*- = Subepi-, midmyo- and subendocardium; # = *n* = 19.

Our porcine model of cardiopulmonary bypass and cardioplegic arrest, requires open chest access in order to achieve an extensive preparation and instrumentation. The time from start of anesthesia to Baseline ranges from two to three hours in all studies

included in this project. After a period of stabilization, baseline variables were obtained. The stability and reproducibility of the model at Baseline is illustrated in Table 3. The experiments lasted up to 10 hours. The anesthetic protocol has been evaluated to be reliable and demonstrated to be hemodynamic consistent.⁸⁹

In Paper I - III, 60 animals (42 kg \pm SD 3) were included. In addition, a total of 14 animals were excluded due to non-technical failure. The causes were various situations of tachyarrhythmia, pulmonary arterial hypertension, acute right heart failure, arterial hypoxia, systemic hypotension and myocardial ischemia. The majority of these events occurred shortly after weaning from CPB, especially after prolonged cardioplegic arrest in Paper III.

10.11.2 Study design

This project is designed as an intervention study with comparison of a novel method to an established routine as control group. Acute experiments were performed using a translation large animal model. By using a strict protocol together with especially sensitive and reproducible methods for evaluation, minor, yet significant differences can be identified even if the sample size is relatively small. Furthermore, by using repeated measurements analyzes as a statistical tool, the probability of type II error is reduced. Thus, the sample size of 20 animals in each study is reasonable to satisfy statistical, ethical and economic considerations. Block randomization (four animals in five blocks) is used to achieve balance between the intervention and control groups by equally distribution with time. In complex experimental protocols with extensive surgery and instrumentation, the learning curve of the research team may influence the results. An unintended, but skewed distribution in time between intervention groups is avoided by using block randomization.

The time of cardioplegic arrest was 60 min in Paper I and II, which is an ischemic time typical for a single procedure in heart surgery like aortic valve replacement (AVR) or multiple coronary artery bypass grafting (CABG). The study protocol in Paper III was 120 min of cardioplegic arrest, simulating a combined procedure like AVR and

concomitant CABG, or other more complex and time-consuming procedures. In this study, also the observation period was extended from 180 to 240 min of reperfusion with the aim of further verifying and clarifying results from the previous studies.

The rate of unsuccessful weaning from CPB was high in Paper III (8 animals vs. 4 and 2 in Paper I and II), which is a limitation for the experimental study design. Furthermore, no additional surgery or intervention except for CPB and CA were implemented, and the period of postoperative observation was relatively short. Consequently, the relevance of this model for clinical cardiac surgery may be limited. In our experience, 120 min of aortic cross-clamping following weaning from the heart-lung machine and 240 min of reperfusion, is close to the limit of what is feasible and reproducible for a translational animal study design in pigs.

10.11.3 Conductance catheter

Pressure-volume loops acquired from the conductance catheter method is considered the be the gold standard in evaluating cardiac performance in translational animal models.¹⁷² The use of a correct catheter is essential due to the importance of appropriate electrode spacing to get a substantial number of segments into the ventricle for covering the entire ventricular long axis. Furthermore, the catheter must be placed as straight as possible and stabilized with the pigtail just above the aortic valve when the apical approach is used. While measuring real time pressure is straight forward after calibration of the catheter, calculation of exact volumes is more demanding. Several factors may influence the accuracy and hypothetically represents a limitation of the method, as demonstrated in the Baan equation:

$$V(t) = 1/\alpha * \rho * L^2 * (G(t) - G_p)$$

as previously described (Ch. 8.5.1).

The acquired total conductance (G(t)) also includes conductance of the surrounding cardiac tissue. Because of dissimilarity of electrical resistivity of the intraventricular blood (~140 Ω*cm) and adjacent myocardium (~750 Ω*cm), estimation of this parallel conductance (G_p) can be used to derive the actual intraventricular volume.¹⁷³

By rapid bolus injection of 5 mL hypertonic (10%) saline in the pulmonary artery during registration of the PV-loops, the conductivity (ρ) of blood in the left ventricle will increase temporarily, while both the volume and parallel conductance can be considered unaffected. The minimum (G_{\min}) and maximum (G_{\max}) conductance are plotted in a x-y diagram from the consecutive cardiac cycles during the saline bolus injection. By extrapolating the linear regression line for these points to the crossing for the line of unity, parallel conductance is found, where $G_{\max} = G_{\min}$. Both assessments of the conductance and the estimation by extrapolation are factors in the equation that may represent some degree of inaccuracy. For this reason, hypertonic saline injections were repeated three times at each occasion, averaged and used in the equation. The saline method has been used in Paper I and III. This routine is an indirect method that provides reliable estimates of parallel conductance.^{92,174} However, other studies have questioned whether G_p remains constant during preload reduction by IVC occlusion.^{175,176}

The alpha factor (α) in the Baan equation represents another variable that may represent an inaccuracy. This calibration factor adjusts for actual ventricular volumes (i.e. near apex and distal outflow tract) not assessed by the conductance catheter. Consequently, the estimated stroke volume by conductance is calibrated against a reference stroke volume. The alpha factor is calculated as the ratio between stroke volume from the conductance catheter and the actual stroke volume estimated by thermodilution. Stroke volume derived from thermodilution has also some limitations due to a potential $\pm 15\%$ margin of error for absolute values.¹⁷⁷ Some of these inaccuracies, related to catheter placement and injection technique, are reduced by using the continuous cardiac output technique (Figure 5).

In addition to the challenges in the acquisition from the conductance catheter, evaluation and interpretation of the results derived from the PV-loops may also have some limitations. In Paper I and III, left ventricular systolic- and diastolic function are evaluated by the PV-loops and are founded on the slope of end-systolic (ESPVR) and end-diastolic (EDPVR) pressure-volume relations as previously illustrated (Figure 9). The calculation of ESPVR is based on a presumption of a linear relationship between

the end-systolic volume and pressure during preload reductions. However, increased contractility enhances a convex tendency of curvilinearity, whereas a decrease in contractility changes the pressure-volume relationship to a more concave shape.⁹⁶ The linear relationship represents an empirical and not a mathematical model, purposed to fit the actual variance that occurs secondary to load alteration. Likewise, this is applicable to the linear model of PRSW (Figure 9 right). Preload Recrutable Stroke Work is considered the most reliable load-independent variable describing contractility. The slope of the end-diastolic pressure-volume relationship is curvilinear (Figure 9). Therefore, the logarithmic end-diastolic pressure-volume relationship (β) is presented in Paper I and III.

The acquired data from the pressure-volume catheter, electron microscopy (Ch. 8.7.5) and epicardial echocardiography (Ch. 8.6.5) necessitate post-processing by the investigator to calculate the relevant variables, which involves a possibility for observer bias. Thus, randomly selected situations/images were grouped, coded, post-processed and analyzed as independent entities by two independent observers (Table 4). Evaluations of the reliability of these analyses were done by using both the inter- and intraobserver Intraclass Correlation Coefficient (ICC). According to Altman, an ICC below 0.2 demonstrates poor agreement, 0.21 - 0.40 fair agreement, 0.41 - 0.60 moderate agreement, 0.61 - 0.80 good agreement, and 0.81 - 1.00 a very good agreement.¹⁷⁸

The ICC for interobserver variance demonstrated a high intertester reliability for both values from selected cardiac cycles obtained from the dynamic runs (Figure 9) and volume estimates. Also, values obtained from the morphometric evaluation and TDI recordings demonstrated good or very good reproducibility. The interobserver variance of the STE short-axis values were defined as moderate, while ICC for the long-axis recordings were good (Ch. 10.11.4).

It should be emphasized that the use of ICC in this thesis is not an evaluation of the quality of the methods and the data collected, but a validation of the post-processing complementary analyses for various variables used in Paper I – III. The ICC values for interobserver variability are presented in Table 4.

Table 4. Interobserver variability between two independent observers evaluated by the intraclass correlation coefficient (ICC) for key variables requiring post-analysis of data acquired during experiments from Paper I - III.

Study	Variable	ICC
Paper I (n = 34)	ESPVR (mmHg/mL)	0.951
	PRSW (mmHg)	0.734
	β (unitless)	0.621
	SW (mmHg*mL)	0.997
	EDV (mL)	0.786
	ESV (mL)	0.657
	SV (mL)	0.999
	EF (%)	0.743
	τ	0.990
Paper II (n = 15 x 6)	V_{Vmit} (%)	0.897
	V_{Vmyo} (%)	0.741
	V_{Vcyt} (%)	0.780
	$S_{Vratio_{mit}}$	0.790
	S_{Vmit}	0.871
Paper III (n = 20)	TDI_{Rad} Strain (%)	0.783
	TDI_{Rad} Strain Rate (s^{-1})	0.874
	STE_{Circ} Strain AntSept (%)	0.486
	STE_{Rad} Strain AntSept (%)	0.512
	STE_{Long} Strain AntSept (%)	0.794

ESPVR = End-systolic pressure-volume relation; PRSW = Preload Recrutable Stroke Work; β = the logarithmic regression coefficient of LV compliance; SW = Stroke Work; EDV = end-diastolic volume; ESV = end-systolic volume; SV = stroke volume; EF = ejection fraction; τ = Tau, time constant of isovolumic relaxation; V_{Vmit} = myocyte volume fraction of mitochondria; V_{Vmyo} = myocyte volume fraction of myofibrils; V_{Vcyt} = myocyte volume fraction of cytosol; $S_{Vratio_{mit}}$ = mitochondrial surface-to-volume ratio; S_{Vmit} = mitochondrial surface density; TDI = Tissue Doppler Imaging; STE = Speckle Tracking Echocardiography; Rad, Circ, Long = radial, circumferential or longitudinal direction; AntSept = antero-septal segment of the left ventricle.

10.11.4 Epicardial echocardiography

An important advantage of using echocardiography in an open chest model, is the use of a high frequency transducer directly on the epicardium. By using a soft silicon pad as offset for optimal sector and acoustic transmission, image acquisition at high frequency (6.5 MHz in this project) produces B-mode images with high spatial

resolution. In theory, epicardial echocardiography may affect the assessed regional function if the probe influences the deformation of the myocardium. By applying pressure with the probe, alterations in ventricular configuration may occur, especially in the diastolic phase with low interventricular pressure. However, in the present model of continuously monitoring of hemodynamic variables (e.g. HR, MAP), a distortion will be noticed immediately and a new assessment performed after a short period of stabilization. In the systolic phase, this potential error is less relevant because of high intraventricular pressures. In addition, the soft silicon pad used as offset reduces the applied pressure on the epicardium. Using a conductance-catheter through the LV apex (Figure 5) may interfere with the correct position of the probe for obtaining longitudinal strain recordings from the apical long-axis four-chamber view. In an open chest model, both sternotomy and pericardiotomy influence on hemodynamic and respiratory variables, but a significant effect on strain measurements has not been demonstrated.^{179,180}

The angular dependency of TDI is a limitation due to the principle of decreased Doppler shift as the angle of the ultrasound beam increases.¹⁰⁰ However, in this open chest porcine model, obtaining TDI SAX recordings perpendicular to the anterior wall of the left ventricle is feasible due to a rotation of the pig heart to the right side compared to the human heart. Conversely, simultaneous SAX assessment of the posterior wall is less accurate, since radial deformation of the myocardial wall will not be perpendicular to the ultrasound beam due to the asymmetrical geometry of the porcine heart. Therefore, TDI strain and strain rate are reported in the radial directions of the left ventricular anterior wall, only (Paper I and Paper III). Moreover, one-layer analysis of deformation was performed since healthy hearts without coronary pathology have an almost uniform myocardial blood flow distribution. Likewise, the induced ischemia (cardioplegic arrest) was global, and one-layer analysis in this setting has shown to be reliable compared to multi-layer analysis.¹⁸¹

Another potential inaccuracy of TDI is the influence of deformation by adjacent myocardium (tethering effect) or cardiac translation.¹⁰⁴ The TDI strain curves obtained from epicardial echocardiography will not necessarily return to baseline because of the

beat to beat variation. This was taken into consideration by the default software setting of drift compensation.

For reliable measurement of the ejection strain rate, a clear definition of the ejection phase is mandatory. For this reason, timing from the PWD recordings in the aortic orifice were used and ejection phase was defined as aortic valve opening (AVO) to closure (AVC) in addition to the definition of end-diastole by ECG.

The algorithm for deformation calculation used in STE is different compared to TDI.¹⁸² Angle dependency is not a limitation and quantification of strain and strain rate in two directions within 2D imaging is feasible. Furthermore, STE derived deformation parameters only reflects active contraction and is not influenced by tethering effects.¹⁰² Despite the accuracy, validity and clinical applications of STE, image quality is still a limitation, especially for recordings obtained at high heart rates.¹⁰⁹ Occasionally, some of the six myocardial segments cannot be analyzed and result in an inaccurate estimation of global deformation parameters. For this reason, global STE strain was not evaluated in Paper III.

Both TDI and B-mode recordings by epicardial echocardiography generate images of high quality. Nevertheless, there is always a tradeoff between the spatial and the temporal resolution in echocardiography. This is especially challenging in this project due to the variable heart rates, especially at the end of the experiments. The mean frame rate for the TDI recordings in Paper I and Paper III were 544 (range 249-696) and 619 (range 327-749) frames/s, respectively. The mean frame rate for the STE recordings in Paper III was 74 (range 63-88) in the short-axis view and 74 (range 63-93) frames/s in the four-chamber view. Likewise, the averaged heart rates in these two studies were 115 beats/min. Adequate myocardial tracking is demanding and may be unreliable if the ratio frame rate (fps) to heart rate (bpm) is too low. This is not a problem in TDI due to the high frame rate but represents a limitation in STE where the frame rates are substantially lower. As a rule of thumb, this ratio should be more than 0.7 fps/bpm if acceptable tracking for both strain and strain rate should be achieved.¹⁸³ In Paper III, frame rate to heart rate ratio was approximately 0.64 fps/bpm.

The methodologies of TDI and STE are fundamentally different, therefore direct comparison is difficult to interpret.¹⁰⁴ Factors like different image resolution, frame rate, TDI parameters (ROI size, SL) and STE parameters (ROI width, default spatial and temporal smoothing) make the results intricate to interpret. Occasionally, inadequate tracking occurred, and consequently, data were not accepted by the software algorithm during the blinded analyzes. These recordings were discussed by the two investigators performing the analyses together with a third impartial investigator, and consensus was made within the group. The same examiner performed all echocardiographic recordings in this thesis, while two investigators performed all analyses. The interobserver variability using epicardial echocardiography in Paper I and Paper III, are previously presented (Ch. 10.11.3). As Table 4 illustrates, the interobserver variability diverge from good to very good for the TDI and STE for longitudinal strain, in the same order of range as the variables from the conductance catheter. However, the interobserver agreement for the STE short-axis measurements in Paper III are moderate. This is caused by in and out of plane motion in the short-axis recordings, which depends on the especially high frame rate for STE. The increased variability in short-axis parameters with STE has previously been demonstrated by others.^{184,185} Also, the geometry of the recorded images tends to produce ultrasound artifacts (reverberations) in epicardial echocardiography.

10.11.5 Myocardial oxygen consumption and mechanical efficiency

In principle, there are three energy-consuming processes in the myocardium; basal metabolism, excitation-contraction coupling and generation of mechanical work (Figure 2). Due to the aerobic cardiac metabolism, myocardial oxygen consumption (MVO_2) is an index of total energy consumption. The reference method for assessment of MVO_2 is the use of coronary flow probes and measurement of arteriovenous pO_2 difference, simultaneously obtained from coronary sinus and the proximal aorta. Cardiac output can be obtained by flow probe to the main pulmonary artery, Swan Ganz catheter or by conductance catheter.

In Paper III, an alternative method has been used for evaluation of mechanical efficiency based on the concept previously described by others.¹²⁰ There is a strong correlation between the total left ventricular work (PVA) defined from pressure-volume loops and myocardial blood flow rate. Furthermore, there is a strong correlation between the pressure-volume area and MVO_2 in the left ventricle.¹¹⁹ It must be emphasized that PVA is not an indirect estimate of MVO_2 . Neither oxygen consumption due to mechanical work in the atria, the right ventricle nor oxygen used for sustaining basic metabolism and the excitation-contraction coupling are included. The total pressure-volume loop area of the left ventricle included in the formula (Ch. 8.8) defines only the potential (PE) and the mechanical energy (SW) generated by the left ventricle. If the arterial and coronary sinus oxygen saturations are not altered, tissue blood flow rate in the left ventricular myocardium is an indirect estimate of oxygen consumption in the left ventricle. Coronary sinus pO_2 was not measured in Paper III. Hemoglobin levels and the arterial pO_2 values did not differ significantly between groups (Supplemental Material, Paper III).

10.11.6 Metabolism

Evaluation of myocardial metabolism became relevant and of interest when the linkage between chemical cardioplegic arrest, bioenergetics and contractile consequences were revealed in the early 1970s.^{16,186} The awareness of the rare but fatal ischemic contracture of the left ventricle (“stone heart”) following cardiac surgery, initiated a focus on pathophysiologic research and new methods for myocardial protection.¹⁸⁷ Shortage of ATP energy reserves was an essential etiology and these findings resulted in a focus on optimizing cardioplegic arrest and hypothermia, hence to delay ATP depletion and to provide anaerobic production of a minor but essential amount of ATP.¹⁸⁸ In isolated working rat hearts, an almost linear correlation between myocardial ATP levels and function was demonstrated.¹⁸⁹ A corresponding relationship between energy status and functional recovery is predicted as an essential factor for rapid and uncomplicated weaning from CPB.

10.11.7 Ultrastructure

Myocyte alterations during ischemia following different methods of cardioplegic arrest, can be evaluated by various morphological or morphometrical parameters.^{190,191} Evaluation of myocyte volume is a morphometric quantification of myocyte swelling. In the context of ischemic injury caused by calcium entering the mitochondria, water will follow and lead to mitochondrial swelling.¹⁹² The myofibril is the organelle most resistant to hypoxia, while the mitochondrion is the most susceptible.¹⁹³ Furthermore, the surface-to-volume ratio of mitochondria ($S_{Vratio_{mit}}$) has been demonstrated to be an independent parameter of mitochondrial swelling, serving as an indicator of the state of structural preservation of mitochondria during ischemia. Increasing volume of the myocyte (swelling) also increases the reference space, and with simultaneously ischemic swelling of the mitochondria, the consequence will be a relative decrease of the free sarcoplasm. For this reason, volume densities of mitochondria (V_{Vmit}) and sarcoplasm (V_{Vsarc}) are not considered as reliable indicators of the degree of edema.¹⁹¹

Myocardial tissue requires extensive preparation prior to TEM, including chemical fixation, cryofixation, dehydration, embedding, sectioning, staining, freeze fracturing and finally mounting. The structure of the sample can be altered in all these steps of preparation. The electron beam can also damage biological material. Another possible limitation is that the region being analyzed is not representative for the whole sample due to the extensive magnification.

In Paper I and II, a total of six randomly selected micrographs from each biopsy were coded and independently evaluated with random offset of the grids. The mean values for the six micrographs represent the result from one single animal at one point in time. Both the inter- and the intraobserver Intraclass Correlation Coefficients were high. It should be emphasized that ICC in Paper II is calculated based on the mean values for a given biopsy. When using the recommended random offset for grids, an ICC based on a number of single micrographs is futile. To increase reliability, the number of micrographs analyzed from each biopsy and several biopsies from each heart at the same point in time, should be sampled.

11. FUTURE PERSPECTIVES

This translational experimental porcine model of cardiopulmonary bypass and cardioplegic arrest simulates a clinical setting involving myocardial ischemia and reperfusion. The results demonstrate that the polarizing cardioplegia with esmolol, adenosine and magnesium, has several advantages compared to standard depolarizing, potassium-based repeated, oxygenated blood cardioplegia. Based on the results presented in this PhD-thesis, clinical research protocols may safely be initiated. Validation of adverse effects and comparable results should be obtained in clinical trials before implementation into a new clinical routine. Due to the increasing life expectancy of the population in general, together with a considerable number of patients with previous cardiac surgery and interventional cardiology, future patients in need of CPB and CA are likely to be increasing in numbers.^{194,195} The use of STH-POL could be beneficial especially in patients with enhanced co-morbidity and/or in patients requiring a prolonged period of cardioplegic arrest due to complex procedures. Furthermore, modifications of the current procedure in term of increasing time intervals between cardioplegic administrations may be a forthcoming advantage with non-depolarizing cardioplegic solutions.¹⁹⁶⁻¹⁹⁸ Optimal protection of the arrested heart during cardiac surgery is essential, not only regarding the choice of cardioplegic solution but also in terms of administration strategies.¹⁹⁹ Furthermore, the translation of knowledge from animal experiments into new clinical routines and subsequently patient outcome studies is challenging.²⁰⁰ In this perspective, the results from the experimental studies presented in this thesis, may contribute to establishing improved myocardial protection routines in future cardiac surgery.

12. CONCLUSION

From the results of the experimental studies presented in this thesis, the following conclusions are:

- The administration of STH-POL blood cardioplegia is feasible, induces rapid diastolic arrest and the heart remains quiescent during the ischemic period.
- STH-POL minimizes potassium accumulation compared to STH-2 blood cardioplegia.
- STH-POL protects against ventricular fibrillation at onset of reperfusion.
- STH-POL offers comparable myocardial protection and improves contractility compared to STH-2 blood cardioplegia.
- STH-POL blood cardioplegia results in advantageous energy status during cardioplegic arrest and early after reperfusion.
- STH-POL blood cardioplegia alleviates mismatch between myocardial function and perfusion during reperfusion following prolonged cardioplegic arrest.

13. ERRATUM

In Paper I, s-troponin-T is given in $\mu\text{mol/L}$, which should be read ng/L .

In Paper II (Table 5), V_{vsarc} should be read V_{vcyt} .

In Figure 9 (right) X-axis, spelling error is corrected to Left ventricular EDV (mL).

Some minor typing errors are corrected.

14. REFERENCES

1. Yamamoto H, Yamamoto F. *Myocardial protection in cardiac surgery: a historical review from the beginning to the current topics*. Gen Thorac Cardiovasc Surg. 2013;61:485-496.
2. Diegeler A, Falk V, Matin M, Battellini R, Walther T, Autschbach R, Mohr FW. *Minimally invasive coronary artery bypass grafting without cardiopulmonary bypass: early experience and follow-up*. Ann Thorac Surg. 1998;66:1022-1025.
3. Bainbridge D, Cheng D, Martin J, Novick R. *Does off-pump or minimally invasive coronary artery bypass reduce mortality, morbidity, and resource utilization when compared with percutaneous coronary intervention? A meta-analysis of randomized trials*. J Thorac Cardiovasc Surg. 2007;133:623-631.
4. Panchal HB, Ladia V, Desai S, Shah T, Ramu V. *A meta-analysis of mortality and major adverse cardiovascular and cerebrovascular events following transcatheter aortic valve implantation versus surgical aortic valve replacement for severe aortic stenosis*. Am J Cardiol. 2013;112:850-860.
5. Arnaoutakis GJ, Szeto WY. *The future is now: An endovascular option for type A aortic dissection*. J Thorac Cardiovasc Surg. 2017;153:S12-S13.
6. Mentias A, Raza MQ, Barakat AF, Youssef D, Raymond R, Menon V, Simpfendorfer C, Franco I, Ellis S, Tuzcu EM, Kapadia SR. *Effect of Shorter Door-to-Balloon Times Over 20 Years on Outcomes of Patients With Anterior ST-Elevation Myocardial Infarction Undergoing Primary Percutaneous Coronary Intervention*. Am J Cardiol. 2017;120:1254-1259.
7. Weir HK, Anderson RN, Coleman King SM, Soman A, Thompson TD, Hong Y, Moller B, Leadbetter S. *Heart Disease and Cancer Deaths - Trends and Projections in the United States, 1969-2020*. Prev Chronic Dis. 2016;13:E157.
8. Mortality GBD, Causes of Death C. *Global, regional, and national life expectancy, all-cause mortality, and cause-specific mortality for 249 causes of death, 1980-2015: a systematic analysis for the Global Burden of Disease Study 2015*. Lancet. 2016;388:1459-1544.
9. Murray CJ, Lopez AD. *Alternative projections of mortality and disability by cause 1990-2020: Global Burden of Disease Study*. Lancet. 1997;349:1498-1504.
10. Neubauer S. *The failing heart--an engine out of fuel*. N Engl J Med. 2007;356:1140-1151.
11. Doenst T, Nguyen TD, Abel ED. *Cardiac metabolism in heart failure: implications beyond ATP production*. Circ Res. 2013;113:709-724.
12. Wallimann T, Dolder M, Schlattner U, Eder M, Hornemann T, O'Gorman E, Ruck A, Brdiczka D. *Some new aspects of creatine kinase (CK): compartmentation, structure, function and regulation for cellular and mitochondrial bioenergetics and physiology*. Biofactors. 1998;8:229-234.

13. Buckberg GD, Brazier JR, Nelson RL, Goldstein SM, McConnell DH, Cooper N. *Studies of the effects of hypothermia on regional myocardial blood flow and metabolism during cardiopulmonary bypass. I. The adequately perfused beating, fibrillating, and arrested heart.* J Thorac Cardiovasc Surg. 1977;73:87-94.
14. Gerbode F, Melrose D. *The use of potassium arrest in open cardiac surgery.* Am J Surg. 1958;96:221-227.
15. Ali JM, Miles LF, Abu-Omar Y, Galhardo C, Falter F. *Global Cardioplegia Practices: Results from the Global Cardiopulmonary Bypass Survey.* J Extra Corpor Technol. 2018;50:83-93.
16. Hearse DJ, Stewart DA, Braimbridge MV. *Hypothermic arrest and potassium arrest: metabolic and myocardial protection during elective cardiac arrest.* Circ Res. 1975;36:481-489.
17. Vinten-Johansen J, Thourani VH. *Myocardial protection: an overview.* J Extra Corpor Technol. 2000;32:38-48.
18. Zeng J, He W, Qu Z, Tang Y, Zhou Q, Zhang B. *Cold blood versus crystalloid cardioplegia for myocardial protection in adult cardiac surgery: a meta-analysis of randomized controlled studies.* J Cardiothorac Vasc Anesth. 2014;28:674-681.
19. Jacob S, Kallikourdis A, Sellke F, Dunning J. *Is blood cardioplegia superior to crystalloid cardioplegia?* Interact Cardiovasc Thorac Surg. 2008;7:491-498.
20. Munch F, Purbojo A, Kellermann S, Janssen C, Cesnjevar RA, Ruffer A. *Improved contractility with tepid modified full blood cardioplegia compared with cold crystalloid cardioplegia in a piglet model.* Eur J Cardiothorac Surg. 2015;48:236-243.
21. Anselmi A, Abbate A, Girola F, Nasso G, Biondi-Zoccai GG, Possati G, Gaudino M. *Myocardial ischemia, stunning, inflammation, and apoptosis during cardiac surgery: a review of evidence.* Eur J Cardiothorac Surg. 2004;25:304-311.
22. Bolli R, Marban E. *Molecular and cellular mechanisms of myocardial stunning.* Physiol Rev. 1999;79:609-634.
23. Schaper J, Schaper W. *Time course of myocardial necrosis.* Cardiovasc Drugs Ther. 1988;2:17-25.
24. Hausenloy DJ, Barrabes JA, Botker HE, Davidson SM, Di Lisa F, et al. *Ischaemic conditioning and targeting reperfusion injury: a 30 year voyage of discovery.* Basic Res Cardiol. 2016;111:70.
25. Liakopoulos OJ, Kuhn EW, Choi YH, Chang W, Wittwer T, Madershahian N, Wassmer G, Wahlers T. *Myocardial protection in cardiac surgery patients requiring prolonged aortic cross-clamp times: a single-center evaluation of clinical outcomes comparing two blood cardioplegic strategies.* J Cardiovasc Surg (Torino). 2010;51:895-905.

26. Stahle E, Bergstrom R, Holmberg L, Nystrom SO, Hansson HE. *Risk factors for operative mortality and morbidity in patients undergoing coronary artery bypass surgery for stable angina pectoris*. Eur Heart J. 1991;12:162-168.
27. Jennings RB. *Historical perspective on the pathology of myocardial ischemia/reperfusion injury*. Circ Res. 2013;113:428-438.
28. Freude B, Masters TN, Robicsek F, Fokin A, Kostin S, Zimmermann R, Ullmann C, Lorenz-Meyer S, Schaper J. *Apoptosis is initiated by myocardial ischemia and executed during reperfusion*. J Mol Cell Cardiol. 2000;32:197-208.
29. Gottlieb RA, Bursleson KO, Kloner RA, Babior BM, Engler RL. *Reperfusion injury induces apoptosis in rabbit cardiomyocytes*. J Clin Invest. 1994;94:1621-1628.
30. Rousou JH, Engelman RM, Dobbs WA, Meeran MK. *The effect of acute coronary artery occlusion during cardioplegic arrest and reperfusion on myocardial preservation*. Ann Thorac Surg. 1982;33:385-390.
31. Brunvand H, Kvitting PM, Rynning SE, Berge RK, Grong K. *Carvedilol protects against lethal reperfusion injury through antiadrenergic mechanisms*. J Cardiovasc Pharmacol. 1996;28:409-417.
32. Kleber AG. *Resting membrane potential, extracellular potassium activity, and intracellular sodium activity during acute global ischemia in isolated perfused guinea pig hearts*. Circ Res. 1983;52:442-450.
33. Chambers DJ, Fallouh HB. *Cardioplegia and cardiac surgery: pharmacological arrest and cardioprotection during global ischemia and reperfusion*. Pharmacol Ther. 2010;127:41-52.
34. Chapman RA. *Calcium channels, the sodium-calcium exchange and intracellular sodium in the predisposition of the heart to the calcium paradox*. Biomed Biochim Acta. 1987;46:S512-516.
35. Jynge P. *Protection of the ischemic myocardium: cold chemical cardioplegia, coronary infustates and the importance of cellular calcium control*. Thorac Cardiovasc Surg. 1980;28:310-321.
36. Chambers DJ, Sakai A, Braimbridge MV, Kosker S, Manzanera G, Kind PR, Jupp RA, Smith LD, Slavin B. *Clinical validation of St. Thomas' Hospital cardioplegic solution No. 2 (Plegisol)*. Eur J Cardiothorac Surg. 1989;3:346-352.
37. Sternbergh WC, Brunsting LA, Abd-Elfattah AS, Wechsler AS. *Basal metabolic energy requirements of polarized and depolarized arrest in rat heart*. Am J Physiol. 1989;256:H846-851.
38. Opie LH. *Heart physiology : from cell to circulation*. 4th edition. Philadelphia, PA: Lippincott Williams & Wilkins; 2004.
39. Hiraoka M. *Metabolic pathways for ion homeostasis and persistent Na⁽⁺⁾ current*. J Cardiovasc Electrophysiol. 2006;17 Suppl 1:S124-S126.

-
40. Podesser BK, Chambers DJ. *New Solutions for the Heart. An Update in Advanced Perioperative Protection*: Springer Verlag/Wien; 2001.
 41. Saint DA. *The role of the persistent Na^{+} current during cardiac ischemia and hypoxia*. J Cardiovasc Electrophysiol. 2006;17 Suppl 1:S96-S103.
 42. Saint DA. *Persistent (current) in the face of adversity ... a new class of cardiac anti-ischaemic compounds on the horizon?* Br J Pharmacol. 2009;156:211-213.
 43. Sperelakis N, Sunagawa M, Yokoshiki H, Seki T, Nakamura M. *Regulation of ion channels in myocardial cells and protection of ischemic myocardium*. Heart Fail Rev. 2000;5:139-166.
 44. Habertheuer A, Kocher A, Laufer G, Andreas M, Szeto WY, Petzelbauer P, Ehrlich M, Wiedemann D. *Cardioprotection: a review of current practice in global ischemia and future translational perspective*. Biomed Res Int. 2014;2014:325725.
 45. Snabaitis AK, Shattock MJ, Chambers DJ. *Comparison of polarized and depolarized arrest in the isolated rat heart for long-term preservation*. Circulation. 1997;96:3148-3156.
 46. Dobson GP, Jones MW. *Adenosine and lidocaine: a new concept in nondepolarizing surgical myocardial arrest, protection, and preservation*. J Thorac Cardiovasc Surg. 2004;127:794-805.
 47. Ferguson ZG, Yarborough DE, Jarvis BL, Sistino JJ. *Evidence-based medicine and myocardial protection - where is the evidence?* Perfusion. 2015;30:415-422.
 48. Lin R, Zhang ZW, Xiong QX, Cao CM, Shu Q, Bruce IC, Xia Q. *Pinacidil improves contractile function and intracellular calcium handling in isolated cardiac myocytes exposed to simulated cardioplegic arrest*. Ann Thorac Surg. 2004;78:970-975.
 49. Steensrud T, Nordhaug D, Husnes KV, Aghajani E, Sorlie DG. *Replacing potassium with nicorandil in cold St. Thomas' Hospital cardioplegia improves preservation of energetics and function in pig hearts*. Ann Thorac Surg. 2004;77:1391-1397.
 50. Jakobsen O, Muller S, Aarsaether E, Steensrud T, Sorlie DG. *Adenosine instead of supranormal potassium in cardioplegic solution improves cardioprotection*. Eur J Cardiothorac Surg. 2007;32:493-500.
 51. Vinten-Johansen J, Dobson GP. *Adenosine-procaine cardioplegia and adenosine-lidocaine cardioplegia: Two sides of the same coin?* J Thorac Cardiovasc Surg. 2013;145:1684-1685.
 52. Onorati F, Dobson GP, San Biagio L, Abbasciano R, Fanti D, Covajes C, Menon T, Gottin L, Biancari F, Mazzucco A, Faggian G. *Superior Myocardial Protection Using "Polarizing" Adenosine, Lidocaine, and Mg^{2+} Cardioplegia in Humans*. J Am Coll Cardiol. 2016;67:1751-1753.

53. Dahle GO, Salminen PR, Moen CA, Eliassen F, Jonassen AK, Haaverstad R, Matre K, Grong K. *Esmolol added in repeated, cold, oxygenated blood cardioplegia improves myocardial function after cardiopulmonary bypass*. J Cardiothorac Vasc Anesth. 2015;29:684-693.
54. Bessho R, Chambers DJ. *Myocardial protection with oxygenated esmolol cardioplegia during prolonged normothermic ischemia in the rat*. J Thorac Cardiovasc Surg. 2002;124:340-351.
55. Boehm DH, Human PA, von Oppell U, Owen P, Reichenspurner H, Opie LH, Rose AG, Reichart B. *Adenosine cardioplegia: reducing reperfusion injury of the ischaemic myocardium?* Eur J Cardiothorac Surg. 1991;5:542-545.
56. Chambers DJ, Hearse DJ. *Developments in cardioprotection: "polarized" arrest as an alternative to "depolarized" arrest*. Ann Thorac Surg. 1999;68:1960-1966.
57. Fallouh HB, Bardswell SC, McLatchie LM, Shattock MJ, Chambers DJ, Kentish JC. *Esmolol cardioplegia: the cellular mechanism of diastolic arrest*. Cardiovasc Res. 2010;87:552-560.
58. Deng CY, Lin SG, Zhang WC, Kuang SJ, Qian WM, Wu SL, Shan ZX, Yang M, Yu XY. *Esmolol inhibits Na⁺ current in rat ventricular myocytes*. Methods Find Exp Clin Pharmacol. 2006;28:697-702.
59. Sum CY, Yacobi A, Kartzinel R, Stampfli H, Davis CS, Lai CM. *Kinetics of esmolol, an ultra-short-acting beta blocker, and of its major metabolite*. Clin Pharmacol Ther. 1983;34:427-434.
60. Quon CY, Stampfli HF. *Biochemical properties of blood esmolol esterase*. Drug Metab Dispos. 1985;13:420-424.
61. Zaroslinski J, Borgman RJ, O'Donnell JP, Anderson WG, Erhardt PW, Kam ST, Reynolds RD, Lee RJ, Gorczynski RJ. *Ultra-short acting beta-blockers: a proposal for the treatment of the critically ill patient*. Life Sci. 1982;31:899-907.
62. Arlock P, Wohlfart B, Sjoberg T, Steen S. *The negative inotropic effect of esmolol on isolated cardiac muscle*. Scand Cardiovasc J. 2005;39:250-254.
63. Cork RC, Kramer TH, Dreischmeier B, Behr S, DiNardo JA. *The effect of esmolol given during cardiopulmonary bypass*. Anesth Analg. 1995;80:28-40.
64. Barbier GH, Shettigar UR, Appunn DO. *Clinical rationale for the use of an ultra-short acting beta-blocker: esmolol*. Int J Clin Pharmacol Ther. 1995;33:212-218.
65. Shibata S, Okamoto Y, Endo S, Ono K. *Direct effects of esmolol and landiolol on cardiac function, coronary vasoactivity, and ventricular electrophysiology in guinea-pig hearts*. J Pharmacol Sci. 2012;118:255-265.
66. Belardinelli L, Shryock JC, Song Y, Wang D, Srinivas M. *Ionic basis of the electrophysiological actions of adenosine on cardiomyocytes*. FASEB J. 1995;9:359-365.

-
67. Belardinelli L, Giles WR, West A. *Ionic mechanisms of adenosine actions in pacemaker cells from rabbit heart.* J Physiol. 1988;405:615-633.
 68. Jovanovic A, Alekseev AE, Lopez JR, Shen WK, Terzic A. *Adenosine prevents hyperkalemia-induced calcium loading in cardiac cells: relevance for cardioplegia.* Ann Thorac Surg. 1997;63:153-161.
 69. Mustafa SJ, Morrison RR, Teng B, Pelleg A. *Adenosine receptors and the heart: role in regulation of coronary blood flow and cardiac electrophysiology.* Handb Exp Pharmacol. 2009;161-188.
 70. Dobson GP, Faggian G, Onorati F, Vinten-Johansen J. *Hyperkalemic cardioplegia for adult and pediatric surgery: end of an era?* Front Physiol. 2013;4:228.
 71. Chambers A, Fallouh H, Kentish JC, Chambers DJ. *Cardioplegia by polarised arrest: experimental studies with potential for clinical application.* Eur J Heart Fail Suppl. 2009;8(2):abstract 256.
 72. Iseri LT, French JH. *Magnesium: nature's physiologic calcium blocker.* Am Heart J. 1984;108:188-193.
 73. Hearse DJ, Stewart DA, Braimbridge MV. *Myocardial protection during ischemic cardiac arrest. The importance of magnesium in cardioplegic infusates.* J Thorac Cardiovasc Surg. 1978;75:877-885.
 74. Ichiba T, Matsuda N, Takemoto N, Ishiguro S, Kuroda H, Mori T. *Regulation of intracellular calcium concentrations by calcium and magnesium in cardioplegic solutions protects rat neonatal myocytes from simulated ischemia.* J Mol Cell Cardiol. 1998;30:1105-1114.
 75. Tsukube T, McCully JD, Faulk EA, Federman M, LoCicero J, 3rd, Krukenkamp IB, Levitsky S. *Magnesium cardioplegia reduces cytosolic and nuclear calcium and DNA fragmentation in the senescent myocardium.* Ann Thorac Surg. 1994;58:1005-1011.
 76. McLean RM. *Magnesium and its therapeutic uses: a review.* Am J Med. 1994;96:63-76.
 77. Yeatman M, Caputo M, Narayan P, Lotto AA, Ascione R, Bryan AJ, Angelini GD. *Magnesium-supplemented warm blood cardioplegia in patients undergoing coronary artery revascularization.* Ann Thorac Surg. 2002;73:112-118.
 78. Guay J. *Adverse events associated with intravenous regional anesthesia (Bier block): a systematic review of complications.* J Clin Anesth. 2009;21:585-594.
 79. Hearse DJ, O'Brien K, Braimbridge MV. *Protection of the myocardium during ischemic arrest. Dose-response curves for procaine and lignocaine in cardioplegic solutions.* J Thorac Cardiovasc Surg. 1981;81:873-879.
 80. Sellevold OF, Berg EM, Levang OW. *Procaine is effective for minimizing postischemic ventricular fibrillation in cardiac surgery.* Anesth Analg. 1995;81:932-938.

81. Guru V, Omura J, Alghamdi AA, Weisel R, Fremes SE. *Is blood superior to crystalloid cardioplegia? A meta-analysis of randomized clinical trials.* Circulation. 2006;114:331-338.
82. Scrascia G, Guida P, Rotunno C, De Palo M, Mastro F, Pignatelli A, de Luca Tupputi Schinosa L, Paparella D. *Myocardial protection during aortic surgery: comparison between Bretschneider-HTK and cold blood cardioplegia.* Perfusion. 2011;26:427-433.
83. Buckberg GD. *Update on current techniques of myocardial protection.* Ann Thorac Surg. 1995;60:805-814.
84. Buckberg GD. *Oxygenated cardioplegia: blood is a many splendored thing.* Ann Thorac Surg. 1990;50:175-177.
85. Mehlhorn U, Allen SJ, Davis KL, Geissler HJ, Warters RD, Rainer de Vivie E. *Increasing the colloid osmotic pressure of cardiopulmonary bypass prime and normothermic blood cardioplegia minimizes myocardial oedema and prevents cardiac dysfunction.* Cardiovasc Surg. 1998;6:274-281.
86. Gunday M, Bingol H. *Is crystalloid cardioplegia a strong predictor of intra-operative hemodilution?* J Cardiothorac Surg. 2014;9:23.
87. Korvald C, Elvenes OP, Myrmel T, Sorlie DG. *Cardiac dysfunction and inefficiency after substrate-enriched warm blood cardioplegia.* Eur J Cardiothorac Surg. 2001;20:555-562.
88. Salerno TA. *Warm heart surgery: reflections on the history of its development.* J Card Surg. 2007;22:257-259.
89. Fannelop T, Dahle GO, Matre K, Segadal L, Grong K. *An anaesthetic protocol in the young domestic pig allowing neuromuscular blockade for studies of cardiac function following cardioplegic arrest and cardiopulmonary bypass.* Acta Anaesthesiol Scand. 2004;48:1144-1154.
90. Baan J, van der Velde ET, de Bruin HG, Smeenk GJ, Koops J, van Dijk AD, Temmerman D, Senden J, Buis B. *Continuous measurement of left ventricular volume in animals and humans by conductance catheter.* Circulation. 1984;70:812-823.
91. Steendijk P, van der Velde ET, Baan J. *Single and dual excitation of the conductance-volume catheter analysed in a spheroidal mathematical model of the canine left ventricle.* Eur Heart J. 1992;13 Suppl E:28-34.
92. Steendijk P, Staal E, Jukema JW, Baan J. *Hypertonic saline method accurately determines parallel conductance for dual-field conductance catheter.* Am J Physiol Heart Circ Physiol. 2001;281:H755-763.
93. Baan J, van der Velde ET, Steendijk P. *Ventricular pressure-volume relations in vivo.* Eur Heart J. 1992;13 Suppl E:2-6.
94. Sagawa K. *The ventricular pressure-volume diagram revisited.* Circ Res. 1978;43:677-687.

-
95. Carabello BA. *Evolution of the study of left ventricular function: everything old is new again*. *Circulation*. 2002;105:2701-2703.
 96. Burkhoff D, Mirsky I, Suga H. *Assessment of systolic and diastolic ventricular properties via pressure-volume analysis: a guide for clinical, translational, and basic researchers*. *American Journal of Physiology-Heart and Circulatory Physiology*. 2005;289:H501-H512.
 97. Glower DD, Spratt JA, Snow ND, Kabas JS, Davis JW, Olsen CO, Tyson GS, Sabiston DC, Jr., Rankin JS. *Linearity of the Frank-Starling relationship in the intact heart: the concept of preload recruitable stroke work*. *Circulation*. 1985;71:994-1009.
 98. Raff GL, Glantz SA. *Volume loading slows left ventricular isovolumic relaxation rate. Evidence of load-dependent relaxation in the intact dog heart*. *Circ Res*. 1981;48:813-824.
 99. Hawk CT, Leary SL, Morris TH. *Formulary for laboratory animals*. 3rd edition. Ames: Blackwell Publishing Professional; 2005.
 100. Lang RM, Goldstein S, Kronzon I, Khaderia B, Mor-Avi V. *ASE's Comprehensive Echocardiography*. 2nd edition. Philadelphia PA: Elsevier Saunders; 2015.
 101. Heimdal A, Stoylen A, Torp H, Skjaerpe T. *Real-time strain rate imaging of the left ventricle by ultrasound*. *J Am Soc Echocardiogr*. 1998;11:1013-1019.
 102. Blessberger H, Binder T. *NON-invasive imaging: Two dimensional speckle tracking echocardiography: basic principles*. *Heart*. 2010;96:716-722.
 103. Hashimoto I, Li X, Hejmadi Bhat A, Jones M, Zetts AD, Sahn DJ. *Myocardial strain rate is a superior method for evaluation of left ventricular subendocardial function compared with tissue Doppler imaging*. *J Am Coll Cardiol*. 2003;42:1574-1583.
 104. Mor-Avi V, Lang RM, Badano LP, Belohlavek M, Cardim NM, et al. *Current and evolving echocardiographic techniques for the quantitative evaluation of cardiac mechanics: ASE/EAE consensus statement on methodology and indications endorsed by the Japanese Society of Echocardiography*. *J Am Soc Echocardiogr*. 2011;24:277-313.
 105. Sitia S, Tomasoni L, Turiel M. *Speckle tracking echocardiography: A new approach to myocardial function*. *World J Cardiol*. 2010;2:1-5.
 106. Uematsu M. *Speckle tracking echocardiography - Quo Vadis?* *Circ J*. 2015;79:735-741.
 107. Sebag IA, Handschumacher MD, Ichinose F, Morgan JG, Hataishi R, et al. *Quantitative assessment of regional myocardial function in mice by tissue Doppler imaging: comparison with hemodynamics and sonomicrometry*. *Circulation*. 2005;111:2611-2616.

108. Edvardsen T, Gerber BL, Garot J, Bluemke DA, Lima JA, Smiseth OA. *Quantitative assessment of intrinsic regional myocardial deformation by Doppler strain rate echocardiography in humans: validation against three-dimensional tagged magnetic resonance imaging*. *Circulation*. 2002;106:50-56.
109. Amundsen BH, Helle-Valle T, Edvardsen T, Torp H, Crosby J, Lyseggen E, Stoylen A, Ihlen H, Lima JA, Smiseth OA, Slordahl SA. *Noninvasive myocardial strain measurement by speckle tracking echocardiography: validation against sonomicrometry and tagged magnetic resonance imaging*. *J Am Coll Cardiol*. 2006;47:789-793.
110. Matre K, Fannelop T, Dahle GO, Heimdal A, Grong K. *Radial strain gradient across the normal myocardial wall in open-chest pigs measured with doppler strain rate imaging*. *J Am Soc Echocardiogr*. 2005;18:1066-1073.
111. Fischer UM, Klass O, Stock U, Easo J, Geissler HJ, Fischer JH, Bloch W, Mehlhorn U. *Cardioplegic arrest induces apoptosis signal-pathway in myocardial endothelial cells and cardiac myocytes*. *Eur J Cardiothorac Surg*. 2003;23:984-990.
112. Bulcao CF, Pandalai PK, D'Souza KM, Merrill WH, Akhter SA. *Uncoupling of myocardial beta-adrenergic receptor signaling during coronary artery bypass grafting: the role of GRK2*. *Ann Thorac Surg*. 2008;86:1189-1194.
113. Paparella D, Yau TM, Young E. *Cardiopulmonary bypass induced inflammation: pathophysiology and treatment. An update*. *Eur J Cardiothorac Surg*. 2002;21:232-244.
114. Schomig A, Haass M, Richardt G. *Catecholamine release and arrhythmias in acute myocardial ischaemia*. *Eur Heart J*. 1991;12 Suppl F:38-47.
115. Zakkar M, Guida G, Suleiman MS, Angelini GD. *Cardiopulmonary bypass and oxidative stress*. *Oxid Med Cell Longev*. 2015;2015:189863.
116. Froyland L, Madsen L, Eckhoff KM, Lie O, Berge RK. *Carnitine palmitoyltransferase I, carnitine palmitoyltransferase II, and acyl-CoA oxidase activities in Atlantic salmon (*Salmo salar*)*. *Lipids*. 1998;33:923-930.
117. Taegtmeier H, Young ME, Lopaschuk GD, Abel ED, Brunengraber H, et al. *Assessing Cardiac Metabolism A Scientific Statement From the American Heart Association*. *Circulation Research*. 2016;118:1659-U1485.
118. Heggtveit HA. *Contributions of electron microscopy to the study of myocardial ischaemia*. *Bull World Health Organ*. 1969;41:865-872.
119. Suga H. *Ventricular energetics*. *Physiol Rev*. 1990;70:247-277.
120. Knaapen P, Germans T, Knuuti J, Paulus WJ, Dijkmans PA, Allaart CP, Lammertsma AA, Visser FC. *Myocardial energetics and efficiency: current status of the noninvasive approach*. *Circulation*. 2007;115:918-927.
121. Tybout A, Sternthal B, Keppel G, Verducci J, Meyers-Levy J, Barnes J, Maxwell S, Allenby G, Gupta S, Steenkamp J-B, Maxwell S. *Analysis of Variance*. *J Consum Psychol*. 2001;10:5-35.

-
122. Cohen NM, Damiano RJ, Jr., Wechsler AS. *Is there an alternative to potassium arrest?* Ann Thorac Surg. 1995;60:858-863.
 123. Chambers DJ. *Polarization and myocardial protection.* Curr Opin Cardiol. 1999;14:495-500.
 124. Fallouh HB, Kentish JC, Chambers DJ. *Targeting for cardioplegia: arresting agents and their safety.* Curr Opin Pharmacol. 2009;9:220-226.
 125. Ede M, Ye J, Gregorash L, Summers R, Pargaonkar S, LeHouerou D, Lessana A, Salerno TA, Deslauriers R. *Beyond hyperkalemia: beta-blocker-induced cardiac arrest for normothermic cardiac operations.* Ann Thorac Surg. 1997;63:721-727.
 126. Warters RD, Allen SJ, Davis KL, Geissler HJ, Bischoff I, Mutschler E, Mehlhorn U. *Beta-blockade as an alternative to cardioplegic arrest during cardiopulmonary bypass.* Ann Thorac Surg. 1998;65:961-966.
 127. Geissler HJ, Davis KL, Laine GA, Ostrin EJ, Mehlhorn U, Hekmat K, Warters RD, Allen SJ. *Myocardial protection with high-dose beta-blockade in acute myocardial ischemia.* Eur J Cardiothorac Surg. 2000;17:63-70.
 128. Mehlhorn U, Allen SJ, Adams DL, Davis KL, Gogola GR, Warters RD. *Cardiac surgical conditions induced by beta-blockade: effect on myocardial fluid balance.* Ann Thorac Surg. 1996;62:143-150.
 129. Kuhn-Regnier F, Natour E, Dhein S, Dapunt O, Geissler HJ, LaRose K, Gorg C, Mehlhorn U. *Beta-blockade versus Buckberg blood-cardioplegia in coronary bypass operation.* Eur J Cardiothorac Surg. 1999;15:67-74.
 130. Mehlhorn U, Fattah M, Kuhn-Regnier F, Sudkamp M, Geissler HJ, Raji MR, Fischer UM, Rainer de Vivie E. *Impact of myocardial protection during coronary bypass surgery on patient outcome.* Cardiovasc Surg. 2001;9:482-486.
 131. Scorsin M, Mebazaa A, Al Attar N, Medini B, Callebort J, Raffoul R, Ramadan R, Maillet JM, Ruffenach A, Simoneau F, Nataf P, Payen D, Lessana A. *Efficacy of esmolol as a myocardial protective agent during continuous retrograde blood cardioplegia.* J Thorac Cardiovasc Surg. 2003;125:1022-1029.
 132. Fannelop T, Dahle GO, Matre K, Moen CA, Mongstad A, Eliassen F, Segadal L, Grong K. *Esmolol before 80 min of cardiac arrest with oxygenated cold blood cardioplegia alleviates systolic dysfunction. An experimental study in pigs.* Eur J Cardiothorac Surg. 2008;33:9-17.
 133. Bignami E, Guarnieri M, Franco A, Gerli C, De Luca M, Monaco F, Landoni G, Zangrillo A. *Esmolol before cardioplegia and as cardioplegia adjuvant reduces cardiac troponin release after cardiac surgery. A randomized trial.* Perfusion. 2017;32:313-320.
 134. Rinne T, Harmoinen A, Kaukinen S. *Esmolol cardioplegia in unstable coronary revascularisation patients. A randomised clinical trial.* Acta Anaesthesiol Scand. 2000;44:727-732.

135. Fazelifar S, Bigdelian H. *Effect of esmolol on myocardial protection in pediatrics congenital heart defects*. Adv Biomed Res. 2015;4:246.
136. Blessberger H, Kammler J, Domanovits H, Schlager O, Wildner B, Azar D, Schillinger M, Wiesbauer F, Steinwender C. *Perioperative beta-blockers for preventing surgery-related mortality and morbidity*. Cochrane Database Syst Rev. 2014:CD004476.
137. Randhawa MP, Jr., Lasley RD, Mentzer RM, Jr. *Adenosine and the stunned heart*. J Card Surg. 1993;8:332-337.
138. Vinten-Johansen J, Thourani VH, Ronson RS, Jordan JE, Zhao ZQ, Nakamura M, Velez D, Guyton RA. *Broad-spectrum cardioprotection with adenosine*. Ann Thorac Surg. 1999;68:1942-1948.
139. Cohen MV, Downey JM. *Adenosine: trigger and mediator of cardioprotection*. Basic Res Cardiol. 2008;103:203-215.
140. Kassimis G, Davlouros P, Patel N, De Maria G, Kallistratos MS, Kharbanda RK, Manolis AJ, Alexopoulos D, Banning AP. *Adenosine as an Adjunct Therapy in ST Elevation Myocardial Infarction Patients: Myth or Truth?* Cardiovasc Drugs Ther. 2015;29:481-493.
141. Schubert T, Vetter H, Owen P, Reichart B, Opie LH. *Adenosine cardioplegia. Adenosine versus potassium cardioplegia: effects on cardiac arrest and postischemic recovery in the isolated rat heart*. J Thorac Cardiovasc Surg. 1989;98:1057-1065.
142. de Jong JW, van der Meer P, van Loon H, Owen P, Opie LH. *Adenosine as adjunct to potassium cardioplegia: effect on function, energy metabolism, and electrophysiology*. J Thorac Cardiovasc Surg. 1990;100:445-454.
143. Jakobsen O, Stenberg TA, Losvik O, Ekse S, Sorlie DG, Ytrebo LM. *Adenosine instead of supranormal potassium in cardioplegic solution preserves endothelium-derived hyperpolarization factor-dependent vasodilation*. Eur J Cardiothorac Surg. 2008;33:18-24.
144. Hudspeth DA, Nakanishi K, Vinten-Johansen J, Zhao ZQ, McGee DS, Williams MW, Hammon JW, Jr. *Adenosine in blood cardioplegia prevents postischemic dysfunction in ischemically injured hearts*. Ann Thorac Surg. 1994;58:1637-1644.
145. Thourani VH, Ronson RS, Van Wylen DG, Shearer ST, Katzmark SL, Zhao ZQ, Han DC, Guyton RA, Vinten-Johansen J. *Adenosine-supplemented blood cardioplegia attenuates postischemic dysfunction after severe regional ischemia*. Circulation. 1999;100:376-383.
146. Jin ZX, Zhang SL, Wang XM, Bi SH, Xin M, Zhou JJ, Cui Q, Duan WX, Wang HB, Yi DH. *The myocardial protective effects of a moderate-potassium adenosine-lidocaine cardioplegia in pediatric cardiac surgery*. J Thorac Cardiovasc Surg. 2008;136:1450-1455.

147. Jakobsen O, Naesheim T, Aas KN, Sorlie D, Steensrud T. *Adenosine instead of supranormal potassium in cardioplegia: it is safe, efficient, and reduces the incidence of postoperative atrial fibrillation. A randomized clinical trial.* J Thorac Cardiovasc Surg. 2013;145:812-818.
148. Cohen G, Feder-Elituv R, Iazetta J, Bunting P, Mallidi H, et al. *Phase 2 studies of adenosine cardioplegia.* Circulation. 1998;98:II225-233.
149. Lee HT, LaFaro RJ, Reed GE. *Pretreatment of human myocardium with adenosine during open heart surgery.* J Card Surg. 1995;10:665-676.
150. Jin Z, Duan W, Chen M, Yu S, Zhang H, Feng G, Xiong L, Yi D. *The myocardial protective effects of adenosine pretreatment in children undergoing cardiac surgery: a randomized controlled clinical trial.* Eur J Cardiothorac Surg. 2011;39:90-96.
151. Jin ZX, Zhou JJ, Xin M, Peng DR, Wang XM, Bi SH, Wei XF, Yi DH. *Postconditioning the human heart with adenosine in heart valve replacement surgery.* Ann Thorac Surg. 2007;83:2066-2072.
152. Wallimann T, Wyss M, Brdiczka D, Nicolay K, Eppenberger HM. *Intracellular compartmentation, structure and function of creatine kinase isoenzymes in tissues with high and fluctuating energy demands: the 'phosphocreatine circuit' for cellular energy homeostasis.* Biochem J. 1992;281 (Pt 1):21-40.
153. Muxfeldt M, Schaper W. *The activity of xanthine oxidase in heart of pigs, guinea pigs, rabbits, rats, and humans.* Basic Res Cardiol. 1987;82:486-492.
154. Evans KJ, Greenberg A. *Hyperkalemia: a review.* J Intensive Care Med. 2005;20:272-290.
155. Winterhalter M, Antoniou T, Loukanov T. *Management of adult patients with perioperative pulmonary hypertension: technical aspects and therapeutic options.* Cardiology. 2010;116:3-9.
156. Domanski MJ, Mahaffey K, Hasselblad V, Brener SJ, Smith PK, et al. *Association of myocardial enzyme elevation and survival following coronary artery bypass graft surgery.* JAMA. 2011;305:585-591.
157. Hoffman JJ. *Transmural myocardial perfusion.* Prog Cardiovasc Dis. 1987;29:429-464.
158. Allen BS, Winkelmann JW, Hanafy H, Hartz RS, Bolling KS, Ham J, Feinstein S. *Retrograde cardioplegia does not adequately perfuse the right ventricle.* J Thorac Cardiovasc Surg. 1995;109:1116-1124.
159. Han JS, Soh DM, Joh CW, Choi BI, Lee YS, Lee CJ, Park CH. *Heterogeneous distribution of cardioplegic solution in pigs.* Br J Anaesth. 2001;86:427-430.
160. Dahle GO, Salminen PR, Moen CA, Eliassen F, Nygreen E, Kyto V, Saukko P, Haaverstad R, Matre K, Grong K. *Carvedilol-Enriched Cold Oxygenated Blood Cardioplegia Improves Left Ventricular Diastolic Function After Weaning From Cardiopulmonary Bypass.* J Cardiothorac Vasc Anesth. 2016;30:859-868.

161. Vaage J, Valen G. *Pathophysiology and mediators of ischemia-reperfusion injury with special reference to cardiac surgery. A review.* Scand J Thorac Cardiovasc Surg Suppl. 1993;41:1-18.
162. Shattock MJ, Ottolia M, Bers DM, Blaustein MP, Boguslavskiy A, et al. *Na⁺/Ca²⁺ exchange and Na⁺/K⁺-ATPase in the heart.* J Physiol. 2015;593:1361-1382.
163. Bers DM, Despa S. *Cardiac myocytes Ca²⁺ and Na⁺ regulation in normal and failing hearts.* J Pharmacol Sci. 2006;100:315-322.
164. Gaillard D, Bical O, Paumier D, Trivin F. *A review of myocardial normothermia: its theoretical basis and the potential clinical benefits in cardiac surgery.* Cardiovasc Surg. 2000;8:198-203.
165. Heusch G, Schulz R. *Perfusion-contraction match and mismatch.* Basic Res Cardiol. 2001;96:1-10.
166. Guaricci AI, Bulzis G, Pontone G, Scicchitano P, Carbonara R, Rabbat M, De Santis D, Ciccone MM. *Current interpretation of myocardial stunning.* Trends Cardiovasc Med. 2018;28:263-271.
167. Swindle MM, Makin A, Herron AJ, Clubb FJ, Jr., Frazier KS. *Swine as models in biomedical research and toxicology testing.* Vet Pathol. 2012;49:344-356.
168. Hughes HC. *Swine in cardiovascular research.* Lab Anim Sci. 1986;36:348-350.
169. Janse MJ, Opthof T, Kleber AG. *Animal models of cardiac arrhythmias.* Cardiovasc Res. 1998;39:165-177.
170. Hara H, Virmani R, Ladich E, Mackey-Bojack S, Titus JL, Karnicki K, Stewart M, Pelzel JM, Schwartz RS. *Patent foramen ovale: standards for a preclinical model of prevalence, structure, and histopathologic comparability to human hearts.* Catheter Cardiovasc Interv. 2007;69:266-273.
171. Hsu FS, Du SJ. *Congenital heart diseases in swine.* Vet Pathol. 1982;19:676-686.
172. Baan J, Vandervelde ET, Debruin HG, Smeenk GJ, Koops J, Vandijk AD, Temmerman D, Senden J, Buis B. *Continuous Measurement of Left-Ventricular Volume in Animals and Humans by Conductance Catheter.* Circulation. 1984;70:812-823.
173. Geddes LA, Baker LE. *The specific resistance of biological material - a compendium of data for the biomedical engineer and physiologist.* Med Biol Eng. 1967;5:271-293.
174. Szwarc RS, Laurent D, Allegrini PR, Ball HA. *Conductance catheter measurement of left ventricular volume: evidence for nonlinearity within cardiac cycle.* Am J Physiol. 1995;268:H1490-1498.
175. Szwarc RS, Mickleborough LL, Mizuno S, Wilson GJ, Liu P, Mohamed S. *Conductance catheter measurements of left ventricular volume in the intact dog: parallel conductance is independent of left ventricular size.* Cardiovasc Res. 1994;28:252-258.

-
176. Applegate RJ, Cheng CP, Little WC. *Simultaneous conductance catheter and dimension assessment of left ventricle volume in the intact animal*. *Circulation*. 1990;81:638-648.
 177. Marik PE. *Obituary: pulmonary artery catheter 1970 to 2013*. *Ann Intensive Care*. 2013;3:38.
 178. Altman DG. *Practical Statistics for Medical Research*. London: Taylor & Francis Ltd Chapman & Hall/CRC; 1991.
 179. Skulstad H, Andersen K, Edvardsen T, Rein KA, Tonnessen TI, Hol PK, Fosse E, Ihlen H. *Detection of ischemia and new insight into left ventricular physiology by strain Doppler and tissue velocity imaging: assessment during coronary bypass operation of the beating heart*. *J Am Soc Echocardiogr*. 2004;17:1225-1233.
 180. Hjertaas JJ, Fannelop T, Grong K, Moen CA, Matre K. *Tissue Doppler Imaging in open-chest pigs before and after pericardiotomy*. Abstract; Scandinavian Society for Research in Cardiothoracic Surgery (SSRCTS) Annual Meeting; 2011.
 181. Moen CA, Salminen PR, Dahle GO, Hjertaas JJ, Grong K, Matre K. *Multi-layer radial systolic strain vs. one-layer strain for confirming reperfusion from a significant non-occlusive coronary stenosis*. *Eur Heart J Cardiovasc Imaging*. 2013;14:24-37.
 182. Urheim S, Edvardsen T, Torp H, Angelsen B, Smiseth OA. *Myocardial strain by Doppler echocardiography. Validation of a new method to quantify regional myocardial function*. *Circulation*. 2000;102:1158-1164.
 183. Rosner A, Barbosa D, Aarsaether E, Kjonas D, Schirmer H, D'Hooge J. *The influence of frame rate on two-dimensional speckle-tracking strain measurements: a study on silico-simulated models and images recorded in patients*. *Eur Heart J Cardiovasc Imaging*. 2015;16:1137-1147.
 184. Reant P, Labrousse L, Lafitte S, Bordachar P, Pillois X, Tariosse L, Bonoron-Adele S, Padois P, Deville C, Roudaut R, Dos Santos P. *Experimental validation of circumferential, longitudinal, and radial 2-dimensional strain during dobutamine stress echocardiography in ischemic conditions*. *J Am Coll Cardiol*. 2008;51:149-157.
 185. Leischik R, Dworrak B, Hensel K. *Intraobserver and interobserver reproducibility for radial, circumferential and longitudinal strain echocardiography*. *Open Cardiovasc Med J*. 2014;8:102-109.
 186. Bretschneider HJ, Hubner G, Knoll D, Lohr B, Nordbeck H, Spieckermann PG. *Myocardial resistance and tolerance to ischemia: physiological and biochemical basis*. *J Cardiovasc Surg (Torino)*. 1975;16:241-260.
 187. Cooley DA, Reul GJ, Wukasch DC. *Ischemic contracture of the heart: "stone heart"*. *Am J Cardiol*. 1972;29:575-577.
 188. Hearse DJ, Garlick PB, Humphrey SM. *Ischemic contracture of the myocardium: mechanisms and prevention*. *Am J Cardiol*. 1977;39:986-993.

189. Hearse DJ, Stewart DA, Chain EB. *Recovery from cardiac bypass and elective cardiac arrest. The metabolic consequences of various cardioplegic procedures in the isolated rat heart.* Circ Res. 1974;35:448-457.
190. Balibrea JL, Bullon A, de la Fuente A, de la Alarcon A, Farinas J, Collantes P, Gil M, Gombau M, Morales R, Sanchez F. *Myocardial ultrastructural changes during extracorporeal circulation with anoxic cardiac arrest and its prevention by coronary perfusion. Experimental study.* Thorax. 1975;30:371-381.
191. Schmiedl A, Schnabel PA, Mall G, Gebhard MM, Hunneman DH, Richter J, Bretschneider HJ. *The surface to volume ratio of mitochondria, a suitable parameter for evaluating mitochondrial swelling. Correlations during the course of myocardial global ischaemia.* Virchows Arch A Pathol Anat Histopathol. 1990;416:305-315.
192. McCully JD, Tsukube T, Ataka K, Krukenkamp IB, Feinberg H, Levitsky S. *Myocardial cytosolic calcium accumulation during ischemia/reperfusion: the effects of aging and cardioplegia.* J Card Surg. 1994;9:449-452.
193. Schaper J, Schwarz F, Kittstein H, Stammeler G, Winkler B, Scheld H, Hehrlein F. *The effects of global ischemia and reperfusion on human myocardium: quantitative evaluation by electron microscopic morphometry.* Ann Thorac Surg. 1982;33:116-122.
194. Luckraz H, Nagarajan K, Chnaris A, Jayia PK, Muhammed I, Mahboob S, Nevill A. *Preserved Quality of Life in Octogenarians at Early, Mid, and Late Follow-Up Intervals Irrespective of Cardiac Procedure.* Semin Thorac Cardiovasc Surg. 2016;28:48-53.
195. Yaffee DW, Williams MR. *Cardiovascular Surgery in the Elderly.* Semin Thorac Cardiovasc Surg. 2016;28:741-747.
196. Durandy YD. *Is there a rationale for short cardioplegia re-dosing intervals?* World J Cardiol. 2015;7:658-664.
197. Nishina D, Chambers DJ. *Efficacy of esmolol cardioplegia during hypothermic ischaemia.* Eur J Cardiothorac Surg. 2017.
198. Malhotra A, Wadhawa V, Ramani J, Garg P, Sharma P, Pandya H, Rodricks D, Tavar R. *Normokalemic nondepolarizing long-acting blood cardioplegia.* Asian Cardiovasc Thorac Ann. 2017;25:495-501.
199. Buckberg GD, Athanasuleas CL. *Cardioplegia: solutions or strategies?* Eur J Cardiothorac Surg. 2016;50:787-791.
200. Heusch G. *Critical Issues for the Translation of Cardioprotection.* Circ Res. 2017;120:1477-1486.

15. PAPERS I - III

PAPER I

with Supplemental Material

Cite this article as: Aass T, Stangeland L, Moen CA, Salminen P-R, Dahle GO, Chambers DJ *et al.* Myocardial function after polarizing versus depolarizing cardiac arrest with blood cardioplegia in a porcine model of cardiopulmonary bypass. *Eur J Cardiothorac Surg* 2016;50:130–9.

Myocardial function after polarizing versus depolarizing cardiac arrest with blood cardioplegia in a porcine model of cardiopulmonary bypass[†]

Terje Aass^{a,b,*}, Lodve Stangeland^b, Christian Arvei Moen^a, Pirjo-Riitta Salminen^{a,b}, Geir Olav Dahle^{a,b}, David J. Chambers^c, Thomais Markou^c, Finn Eliassen^a, Malte Urban^a, Rune Haaverstad^{a,b}, Knut Matre^b and Ketil Grong^b

^a Department of Heart Disease, Haukeland University Hospital, Bergen, Norway

^b Faculty of Medicine and Dentistry, Department of Clinical Science, University of Bergen, Bergen, Norway

^c Cardiac Surgical Research, The Rayne Institute (King's College London), Guy's and St Thomas' NHS Foundation Trust, St Thomas' Hospital, London, UK

* Corresponding author. Section of Cardiothoracic Surgery, Department of Heart Disease, Haukeland University Hospital, Jonas Lies vei 65, 5021 Bergen, Norway. Tel: +47-55975000; fax: +47-55975150; e-mail: terje.aass@helse-bergen.no (T. Aass).

Received 30 October 2015; received in revised form 7 December 2015; accepted 11 December 2015

Abstract

OBJECTIVES: Potassium-based depolarizing St Thomas' Hospital cardioplegic solution No 2 administered as intermittent, oxygenated blood is considered as a gold standard for myocardial protection during cardiac surgery. However, the alternative concept of polarizing arrest may have beneficial protective effects. We hypothesize that polarized arrest with esmolol/adenosine/magnesium (St Thomas' Hospital Polarizing cardioplegic solution) in cold, intermittent oxygenated blood offers comparable myocardial protection in a clinically relevant animal model.

METHODS: Twenty anaesthetized young pigs, 42 ± 2 (standard deviation) kg on standardized tepid cardiopulmonary bypass (CPB) were randomized (10 per group) to depolarizing or polarizing cardiac arrest for 60 min with cardioplegia administered in the aortic root every 20 min as freshly mixed cold, intermittent, oxygenated blood. Global and local baseline and postoperative cardiac function 60, 120 and 180 min after myocardial reperfusion was evaluated with pressure–conductance catheter and strain by Tissue Doppler Imaging. Regional tissue blood flow, cleaved caspase-3 activity, GRK2 phosphorylation and mitochondrial function and ultrastructure were evaluated in myocardial tissue samples.

RESULTS: Left ventricular function and general haemodynamics did not differ between groups before CPB. Cardiac asystole was obtained and maintained during aortic cross-clamping. Compared with baseline, heart rate was increased and left ventricular end-systolic and end-diastolic pressures decreased in both groups after weaning. Cardiac index, systolic pressure and radial peak systolic strain did not differ between groups. Contractility, evaluated as dP/dt_{max} , gradually increased from 120 to 180 min after declamping in animals with polarizing cardioplegia and was significantly higher, 1871 ± 160 (standard error) mmHg/s, compared with standard potassium-based cardioplegic arrest, 1351 ± 70 mmHg/s, after 180 min of reperfusion ($P = 0.008$). Radial peak ejection strain rate increased and the load-independent variable preload recruitable stroke work was increased with polarizing cardioplegia after 180 min, 64 ± 3 vs 54 ± 2 mmHg ($P = 0.018$), indicating better preserved left ventricular contractility with polarizing cardioplegia. Phosphorylation of GRK2 in myocardial tissue did not differ between groups. Fractional cytoplasmic volume in myocytes was reduced in hearts arrested with polarizing cardioplegia, indicating reduction of cytoplasmic oedema.

CONCLUSIONS: Polarizing oxygenated blood cardioplegia with esmolol/adenosine/magnesium offers comparable myocardial protection and improves contractility compared with the standard potassium-based depolarizing blood cardioplegia.

Keywords: Cardioplegia • Myocardial protection • Cardiac function • Animal model

INTRODUCTION

Over the past two decades, surgical treatment for cardiac disease has occurred in patients that are more elderly and have more

complex disease. As a consequence, there is an increasing demand for new perfusion strategies associated with prolonged duration of cardiopulmonary bypass (CPB) and cardiac arrest that will provide improved myocardial protection. Potassium-based depolarizing cardioplegia, delivered as oxygenated cold blood, is a dominant routine used worldwide [1]. A number of different techniques for optimizing myocardial protection have been studied, both

[†]Presented at the 95th Annual Meeting of the American Association for Thoracic Surgery, Seattle, WA, USA 25–29 April 2015.

experimentally and clinically. Polarizing cardioplegic protocols have also been extensively studied [2]; the concept of polarized arrest has shown that enhanced protection can be achieved [3]. A new polarizing cardioplegic solution, the St Thomas' Hospital Polarizing cardioplegic solution (STH-POL), containing a mixture of the short-acting β -adrenergic receptor blocker esmolol, adenosine and Mg^{2+} , has recently been suggested. The solution combines the inhibition of fast Na^+ - and L-type Ca^{2+} -channels of esmolol, the K_{ATP} -channel opener effect of adenosine and the reduced myocardial Ca^{2+} load caused by magnesium [3, 4]. Before implementation of a new technique for myocardial protection in clinical studies and practice, it must be compared and found to be non-inferior or superior to the current technique in a translational large animal *in vivo* model.

In a standardized clinically relevant porcine model involving CPB, we have investigated whether cardioplegic arrest with STH-POL offers myocardial protection comparable with a standard depolarizing potassium-based cardioplegic solution; both delivered as repeated, cold, oxygenated blood cardioplegia. The main focus for the evaluation was to compare the left ventricular global and local function up to 3 h after aortic declamping, weaning and decannulation.

MATERIALS AND METHODS

Animals and anaesthesia

The experimental protocol was approved by the Norwegian State Commission for Laboratory Animals (Project 20135835), and conducted in accordance with the European Communities Council Directive of 2010 (63/EU). The animals were brought to the animal facility about 1 week in advance for acclimatization. Twenty-four young pigs (Norwegian land race) of either gender, weighing 42 ± 2 [standard deviation (SD)] kg were used. After premedication with intramuscular injection of a mixture of ketamine (20 mg/kg), diazepam (10 mg) and atropine (1 mg), the pigs were ventilated spontaneously on mask for a short period with oxygen and 3% isoflurane (Rhodia, Bristol, UK) allowing intravenous access through two ear veins. Before tracheotomy and intubation, loading doses of intravenous fentanyl (0.02 mg/kg), midazolam (0.3 mg/kg), pancuronium (0.063 mg/kg) and pentobarbital (15 mg/kg) were given, and continuous infusions of fentanyl (0.02 mg/kg per h), midazolam (0.3 mg/kg per h), pancuronium (0.2 mg/kg per h) and pentobarbital (4 mg/kg per h) were initialized. The animals were ventilated (Julian, Drägerwerk, Lübeck, Germany) with a mixture of nitrous oxide (56–58%) and oxygen. Prophylactic antibiotic therapy with cefalotin 1 g (in 50 ml 0.9% NaCl) was given IV initially, followed by 0.5 g during CPB and 1.0 g after weaning. Fluid substitution, Ringer's acetate 15 ml/kg per h with 20 mmol/l KCl added, was given throughout the experiment. In addition, Ringer's acetate 5 ml/kg per h was provided after weaning from CPB. The anaesthetic protocol has been thoroughly evaluated, allowing the use of neuro-muscular blocking agents in young pigs [5].

Surgical protocol and instrumentation

The right femoral artery and vein were cannulated for blood sampling and infusion by surgical cut-down in the groin. An early arterial blood gas analysis determined the need for ventilator adjustments. An open suprapubic cystostomy with insertion of a catheter drained the urine bladder. Rectal temperature was monitored. Midline sternotomy and pericardiectomy was performed and heparin (125 IU/

kg) given IV to prevent clotting of catheters. A continuous cardiac output catheter (CCO/EDV 177HF 75, Edwards Lifesciences, Inc., Irvine, CA, USA) was advanced from the left internal mammary vein into the pulmonary artery for monitoring cardiac output, right ventricular end-diastolic volume, central venous pressure (CVP) and pulmonary artery pressure (PAP) (Vigilance II® and TruWave® transducers, Edwards Lifescience, Inc.). The aorta was cannulated proximally with a Millar microtip pressure catheter (Millar MPC-500, Houston, TX, USA) through the left internal mammary artery. The haemodynamic parameters were sampled in real time by a 16-channel Ponemah (ACQ-7700; Data Sciences International, St Paul, MN, USA), digitized and later analysed (Ponemah Physiology Platform v. 5.2, Data Sciences International). A dual-field conductance-pressure catheter (CA71083-PL, CDLeycom, Hengelo, Netherlands) was inserted through the apex and into the left ventricle with the distal part in position just above the aortic valve, verified by epicardial echocardiography (Vivid E9, GE Vingmed Ultrasound, Horten, Norway). The catheter was connected to a Sigma-M signal conditioner (CDLeycom). The left atrium was cannulated by an infant feeding tube for microsphere injections and a tape placed around the inferior vena cava for brief intermittent dynamic preload reductions.

Cardiopulmonary bypass

CPB (Stöckert SIII, Munich, Germany) was set up with 1200 ml Ringer's acetate as prime in the circuit. After anticoagulation with heparin 500 IU/kg, the brachiocephalic artery (EOPA 18 Fr, Medtronic, Inc., Minneapolis, MN, USA) and right atrial appendage (MC2 28/36 Fr, Medtronic Inc.) were cannulated, and CPB was established with a flow of 90 ml/min per kg and water temperature of 32°C in the heat exchanger. Aortic cross-clamp time was 60 min and a left heart vent catheter (E061 17 Fr, Edwards Lifesciences, Inc.) was placed through the left atrial appendage into the ventricle. The body temperature was allowed to drift towards 34°C and the CPB flow was reduced to 72 ml/min per kg when the rectal temperature reached 35°C or after 20 min. Rewarming was commenced after 40 min of cross-clamping with reset of CPB flow to 90 ml/min per kg and water temperature at 40°C. Arterial blood gases were obtained before cross-clamping, after 30 min and just before declamping after 60 min. If ventricular fibrillation occurred after declamping, defibrillation was the only allowed antiarrhythmic intervention. All animals were weaned from CPB at 10 min after declamping followed by decannulation. The residual blood in the circuit was returned and protamine sulphate 1 mg/kg was given for heparin reversal.

Cardioplegia

The animals were block-randomized to receive either hyperkalaemic cardioplegia based on a modification of St Thomas' Hospital cardioplegic solution No. 2 (STH-2), or cardioplegia containing the short-acting β -adrenergic blocking agent esmolol, adenosine and magnesium; St Thomas' Hospital polarizing solution (STH-POL) (Table 1). Both solutions were pre-prepared as concentrate and administered as cold (12°C), oxygenated, blood cardioplegia, freshly mixed and delivered by a dual-pump with separate cooling. The cardioplegia was delivered into the aortic root with a flow set to 7% of CPB flow, following a standardized protocol with an initial 'high-dose' (1:4 concentrate/blood) for 3 min and 2 min of 'low-dose' (1:8 concentrate/blood) given at 20 and 40 min after

Table 1: Final molar concentrations in oxygenated blood cardioplegia

	STH-POL		STH-2	
	High-dose (3 min)	Low-dose (2 min)	High-dose (3 min)	Low-dose (2 min)
Esmolol (mM)	1.35	0.68	–	–
Adenosine (mM)	0.50	0.25	–	–
Mg ²⁺ (mM)	20	10	16	9
K ⁺ (mM)	4.3	4.3	22	14
Cl ⁻ (mM)	106	106	134	120
Procaine HCl (mM)	0.8	0.4	0.8	0.4

STH-POL: St Thomas' Hospital Polarizing cardioplegic solution;
STH-2: Modified St Thomas' Hospital cardioplegic solution No. 2.

cross-clamping. The final concentrations of key components in the two cardioplegic solutions are presented in Table 1.

Experimental protocol

After 10 min of stabilization, baseline variables were obtained; arterial blood gases (ABL80 FLEX COOX, Radiometer Medical ApS, Brønshøj, Denmark), s-troponin-T (Troponin-T hs®, Roche Diagnostics, GmbH, Mannheim, Germany), haemodynamic variables and the first injection of 15-µm microspheres (Dye-Trak 'F'; Triton Technology, Inc., San Diego, CA, USA). After a short period of ventilation with 100% oxygen, left ventricular pressure-volume loops were registered with respirator shut-off in end-expirium before and during a brief period of inferior vena cava occlusion. A bolus of 5 ml hypertonic saline (10%) was injected into the pulmonary artery and pressure volume loops were recorded in a stable situation three times for estimation of parallel conductance [6, 7]. Epicardial echocardiography was performed with a soft silicone pad placed between the probe (6 MHz sector probe, GE Vingmed Ultrasound) and the epicardium. During brief periods of respiratory shut-off, pulsed wave Doppler (PWD) velocity spectrum recordings in the left aortic outflow tract were noted for timing of end-systole and end-diastole. Tissue Doppler images (TDIs) of the anterior left ventricular wall in short axis view were recorded for radial strain and strain rate measurements.

At full CPB flow, an arterial blood gas was sampled followed by aortic cross-clamping and cardioplegic arrest with STH-POL or STH-2 given as cold blood cardioplegia. During CPB, the ventilator volume was reduced to 50% and with passive drainage of the heart. Additional heparin (250 IU/kg) was given at 30 min of cross-clamping. After 60 min of cardioplegic arrest, the aortic clamp was removed. The animals were weaned from CPB after 10 min of myocardial reperfusion. General haemodynamics were continuously recorded for 180 min. As for baseline, measurements of left ventricular pressures, volumes, contractility, systolic and diastolic function, regional tissue blood flow and echocardiographic recordings were repeated at 60, 120 and 180 min after aortic declamping. Finally, the animal was euthanized with intracardiac injection of high-dose potassium chloride, the heart removed and samples were obtained for regional tissue blood flow measurements, analysis of mitochondrial ultrastructure and mitochondrial fatty acid oxidation capacity, phosphorylated GRK2, Caspase-3 activity and tissue water content.

Pressure-conductance catheter

Data from the pressure-conductance catheter were analysed with a custom-made programme. The mean of 5–8 cardiac cycles during the stable condition and load-independent variables obtained during the dynamic preload reduction were calculated. Absolute volumes were estimated by correcting for parallel conductance and cardiac output. Volumes were indexed by body surface area (BSA) calculated as $BSA (m^2) = (BW^{2/3} \times k)/100$ where BW is body weight in kg and k for pigs is $9 m^2/kg^{-2/3}$ [8].

Epicardial echocardiography

Local myocardial function (TDI strain and strain rate) in the anterior wall was recorded. Peak systolic strain and peak ejection strain rate were measured with commercial software (EchoPack BT12, GE Vingmed Ultrasound). The size of the region of interest (ROI) was set to 6×6 mm and the strain length (SL) to 6 mm. Care was taken not to place the ROIs within a distance of $\frac{1}{2}$ SL from the epicardium and $\frac{1}{2}$ SL from the endocardium [9]. End-diastole was defined as the first deflection in the QRS complex in the ECG, and start of ejection was defined at the aortic valve opening and end-systole was defined as the time of aortic valve closure from the PWD recording. The mean frame rate for the TDI recordings was 544 ± 78 (SD) frames/s (range 249–696).

Myocardial tissue samples and analyses

Multiple biopsies were obtained from the LV endo-, mid- and epicardium, snap-frozen in liquid nitrogen and stored at -80°C for later analysis. Caspase-3 activity was determined using the Caspase-3 Colorimetric Assay Kit (BioVision, Inc., Milpitas, CA, USA). Tissue was homogenized and lysis performed according to the manufacturer's instructions, and triplet samples containing 400 µg total protein, measured by the Quick Start™ Bradford Protein Assay (Bio-Rad Laboratories, Inc., Hercules, CA, USA), were incubated for 2 h before fluorometric readings. The activation of G-protein-coupled receptor kinase 2 (GRK2) in the myocardium was assessed with immunoblotting using antibodies against phosphorylated GRK2 (LS-C199027, LifeSpan BioSciences Inc., Seattle, WA, USA) and total GRK2 (CST3982, Cell Signaling, Boston, MA, USA) according to manufacturer's instructions. The blots were quantified using scanning densitometry. Mitochondrial carnitine palmitoyltransferase I and II (CPT-I, CPT-II) activity in the outer and inner mitochondrial membranes were measured in frozen myocardial tissue samples. Each sample was homogenized after adding 500 µl of ice-cold sucrose (0.25 M sucrose, 5 mM HEPES-buffer, 0.2 mM ethylene glycol tetraacetic acid, pH 7.4) and centrifuged at 4°C , 600 g for 12 min. The protein concentration in the supernatant (post-nuclear fraction) was measured (Bio-Rad Protein Assay, Bio-Rad Laboratories, Inc.). In 150 µg of protein, CPT-I and CPT-II were measured as earlier described [10]. In addition, corresponding biopsies were obtained and fixed overnight in 0.1 M Na-cacodylate buffer with 2.5% glutaraldehyde, washed, post-fixed with 1% OsO₄, dehydrated and stored in 70% ethanol, sectioned and stained with uranyl acetate for the analysis of myocardial ultrastructure with electron microscopy. From six randomly selected sections, images ($\times 15\,000$) were obtained from the mid-myocardium, myocyte volume fractions of mitochondria, myofibrils and sarco-plasma were calculated by point counting. The mitochondrial

surface density and surface-to-volume ratio were calculated by a Merz grid using the ImageJ freeware [11, 12]. Tissues obtained from the left and the right ventricle were weighed, hydrolysed, microspheres isolated by filtration, colours dissolved and quantified by fluorospectrophotometry together with the reference blood samples. Blood flow rate was calculated as earlier described [13]. Myocardial tissue water content was calculated as a fraction of wet weight after drying samples for 3 weeks at 60°C.

Statistical analysis

Data were analysed by using SPSS v. 22 (SPSS, Inc., Chicago, IL, USA) and values given as mean \pm (SE) or median (25% quartile; 75% quartile) unless otherwise noted. Baseline variables were compared by two-sample Student's *t*-test on data with normal distribution and with Wilcoxon–Mann–Whitney *U*-test on ranks if the Kolmogorov–Smirnov test or the Levene equal variance tests were significant. Variables obtained during and after CPB were analysed separately by two-way analysis of variance (ANOVA) for repeated measurement (RM-ANOVA) with time as within factor (P_w) and cardioplegia with STH-POL or STH-2 as grouping factor (P_g) and *post hoc* Bonferroni contrasts between individual group means. If Mauchly's test of sphericity was significant ($P < 0.05$), the Greenhouse–Geisser adjustment of degrees of freedom was selected for the evaluation of main effects. For Caspase-3 activity and estimation of GRK2, wall layers were set as related variables. If a significant interaction ($P_i < 0.10$) effect was found, new ANOVAs for simple main effect were performed with adjustment of degrees of freedom. Cell means were finally compared with Neumann–Keuls multiple contrast tests when justified by the preceding ANOVA. The morphological variables were analysed with a nested ANOVA. $P < 0.05$ was considered statistically significant.

RESULTS

Group characteristics at baseline and during cardiopulmonary bypass

Four animals were excluded due to reasons other than technical failure: two in the STH-POL group developed severe pulmonary hypertension and arterial hypoxia with heart failure during baseline measurements before allocation to treatment groups; two in the STH-2 group, one due to severe pulmonary hypertension during instrumentation before CPB and one due to persistent ventricular fibrillation after declamping. Excluded animals were replaced by consecutive experiments and the results are given for 10 animals in each group. Baseline variables describing left and right ventricular function, general haemodynamics, tissue blood flow rate, arterial blood gases and serum troponin-T did not differ between groups (Table 2, Figs 1–3).

The myocardial contraction rapidly ceased after aortic cross-clamping and start of the cardioplegic infusion, with the median time being 28 (11; 43) s for STH-POL and 22 (18; 27) s for STH-2 group ($P = 0.79$). During CPB, haemoglobin levels and serum-potassium were moderately, but significantly increased in the STH-2 group compared with the STH-POL group at 30 and 60 min (see [Supplementary Material](#)). There were no differences between the groups regarding mean arterial pressure, temperature and arterial blood gases during CPB.

Table 2: Baseline variables before cardiac arrest with polarizing (STH-POL) and depolarizing (STH-2) cardioplegia

Variable	STH-POL	STH-2	Statistics
LV-EDV _i (ml/m ²)	83 \pm 5	78 \pm 4	$P = 0.50$
LV-ESV _i (ml/m ²)	41 \pm 4	35 \pm 4	$P = 0.28$
LV-SV _i (ml/m ²)	50 \pm 3	51 \pm 2	$P = 0.72$
RV-EDV _i (ml/m ²)	136 \pm 4	148 \pm 7	$P = 0.16$
RV-EF (%)	24 \pm 1	26 \pm 1	$P = 0.28$
MAP (mmHg)	95 \pm 4	96 \pm 3	$P = 0.77$
CVP _{mean} (mmHg)	5.8 \pm 0.5	6.2 \pm 0.5	$P = 0.58$
PAP _{mean} (mmHg)	18.8 (15.5; 21.8)	19.6 (18.3; 20.4)	$P = 0.47$
LV blood flow (ml/min per g)	0.92 \pm 0.05	1.04 \pm 0.06	$P = 0.16$
RV blood flow (ml/min per g)	0.68 \pm 0.07	0.83 \pm 0.05	$P = 0.14$
Arterial blood gases			
pH	7.51 (7.49; 7.52)	7.52 (7.51; 7.53)	$P = 0.25$
pCO ₂ (kPa)	5.2 \pm 0.1	5.02 \pm 0.1	$P = 0.24$
HCO ₃ ⁻ (mmol/l)	31.2 \pm 0.2	31.2 \pm 0.4	$P = 0.95$
BE (mmol/l)	7.3 \pm 0.2	7.2 \pm 0.4	$P = 0.89$
pO ₂ (kPa)	25.8 \pm 0.8	25.6 \pm 0.5	$P = 0.88$
Hb (g/dl)	8.2 \pm 0.2	8.1 \pm 0.2	$P = 0.64$
Hct (%)	25.6 \pm 0.5	25.2 \pm 0.6	$P = 0.64$
s-Na ⁺ (mmol/l)	142 (140; 143)	142 (141; 143)	$P = 0.94$
s-K ⁺ (mmol/l)	3.7 \pm 0.1	3.7 \pm 0.1	$P = 0.59$
s-Cl ⁻ (mmol/l)	103.1 \pm 0.9	103.4 \pm 0.6	$P = 0.78$
s-Troponin-T (μmol/l)	47.6 \pm 4.7	53.4 \pm 6.5	$P = 0.48$

Values are mean \pm SE or median (25-percentile; 75-percentile), $n = 10$. LV and RV: left and right ventricle; *i*: value indexed for body surface area; EDV: end-diastolic volume; ESV: end-systolic volume; SV: stroke volume; MAP: mean arterial pressure; CVP_{mean}: mean central venous pressure; PAP_{mean}: mean pulmonary artery pressure; STH-POL: St Thomas' Hospital Polarizing cardioplegic solution; STH-2: St Thomas' Hospital cardioplegic solution No. 2; SE: standard error. *P*-values from two-sample *t*-tests or Mann–Whitney rank sum tests.

Cardiac and haemodynamic variables after declamping

Heart rate was increased and left ventricular systolic (LVSP) and diastolic (LVEDP) pressures decreased with time in both groups after weaning from CPB (Fig. 1). Cardiac index (CI) increased during the first hour after declamping in both groups, but then decreased slightly but staying above baseline levels during the remaining 120 min of reperfusion ($P_w = 0.024$). There were no significant differences between the groups. In the STH-POL group, the first derivative of the left ventricular pressure (LV-dP/dt_{max}) increased from 120 to 180 min of reperfusion, reaching values significantly higher than the STH-2 group after 165 and 180 min of reperfusion. LV-dP/dt_{min} was more negative in the STH-POL group after 180 min. There was a significant difference between groups for indexed stroke work (SW_i) and for the load-independent contractility variable preload recruitable stroke work (PRSW) at 180 min after declamping (Fig. 2). Ejection fraction and the slope of the end-systolic pressure–volume relationship (ESPVR_{slope}) did not differ between groups, neither did the isovolumic relaxation constant Tau nor the left ventricular compliance β . Whereas radial peak systolic strain in the anterior left ventricular wall decreased significantly over time in both groups ($P_w = 0.004$), radial peak ejection strain rate decreased in the STH-2 group to values significantly lower than in the STH-POL group at 180 min (Fig. 3). There was a significant decrease over time in indexed left ventricular stroke volume (LV-SV_i) and a decrease in

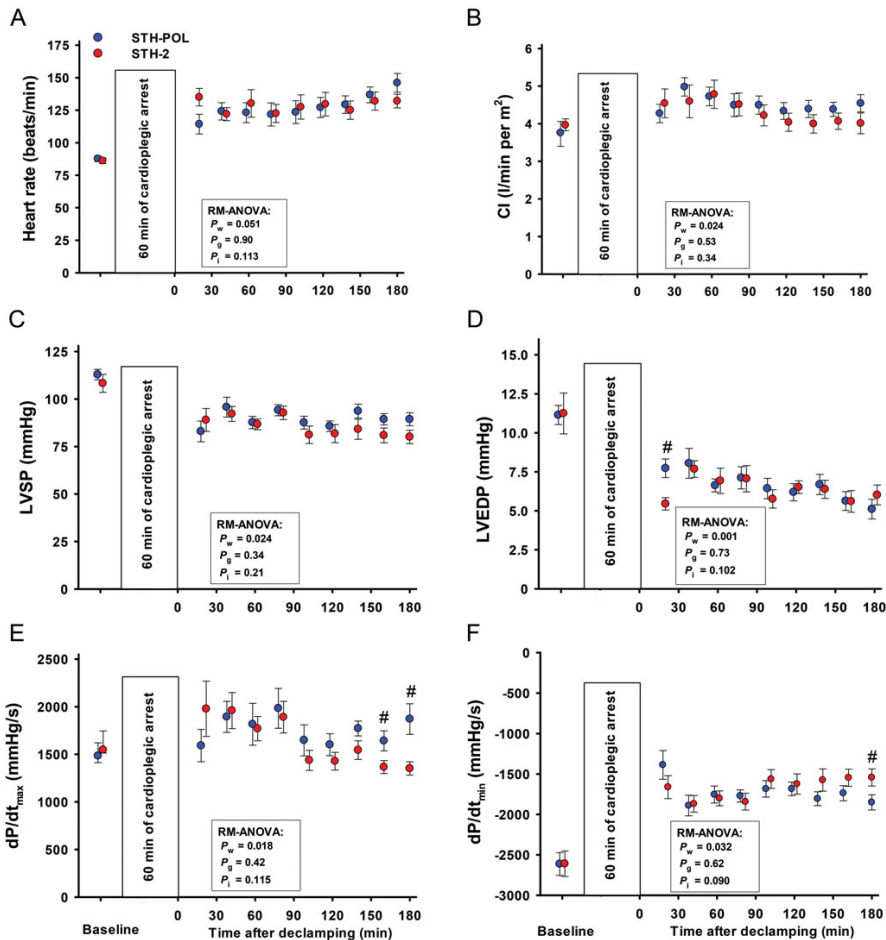


Figure 1: Baseline left ventricular haemodynamic variables mean (SE) or median (25%; 75%), and values obtained after CPB and 60 min of cardiac arrest with polarizing (STH-POL) and depolarizing (STH-2) cardioplegia. Bars represent SE. P_w , P_g , and P_t : P -values for within subjects, between groups and interaction from two-way RM-ANOVA, respectively; #Significantly different from STH-POL at 180 min of reperfusion with Bonferroni *post hoc* test. SE: standard error of the mean; CPB: cardiopulmonary bypass; RM-ANOVA: analysis of variance for repeated measurement; CI: Cardiac Index; LVSP: left ventricular peak systolic pressure; LVEDP: left ventricular peak end-diastolic pressures; dP/dt_{max} and dP/dt_{min} : peak positive and peak negative of the first derivative of left ventricular pressure.

right ventricular end-diastolic volume (RV-EDV) for both groups (Table 3). The mean aortic blood pressure (MAP) was unchanged in the STH-POL group and decreased over time in the STH-2 group with a significant difference between groups at 180 min of reperfusion. The mean PAP was unchanged and CVP slightly increased over time in both groups ($P_w = 0.003$). Regional tissue blood flow rate in the left and the right ventricular wall was unchanged from 60 to 180 min of reperfusion. Left ventricular tissue water content averaged $80.1 \pm 0.1\%$ ($n = 20$), with no group difference. Serum troponin-T levels did not differ between groups at 180 min after declamping; median values were 504 (328; 886) $\mu\text{mol/l}$ in the STH-POL group and 580 (401; 717) $\mu\text{mol/l}$ in the STH-2 group ($P = 0.73$).

Myocardial apoptosis and β -receptor activity

There was no difference between groups in myocardial apoptotic activation evaluated as cleaved caspase-3 activity ($P_g = 0.84$) (Fig. 4). In the subepicardium, cleaved caspase-3 activity was increased in both groups compared with that in the mid-myocardial and subendocardial wall layers ($P_{layer} = 0.024$). Phosphorylation of GRK2 (relative to tissue from control heart) in the mid-myocardial wall layers was increased in both groups compared with levels in the subendo- and subepicardial wall layers ($P_{layer} = 0.001$). The total GRK2 content did not differ between wall layers or between groups.

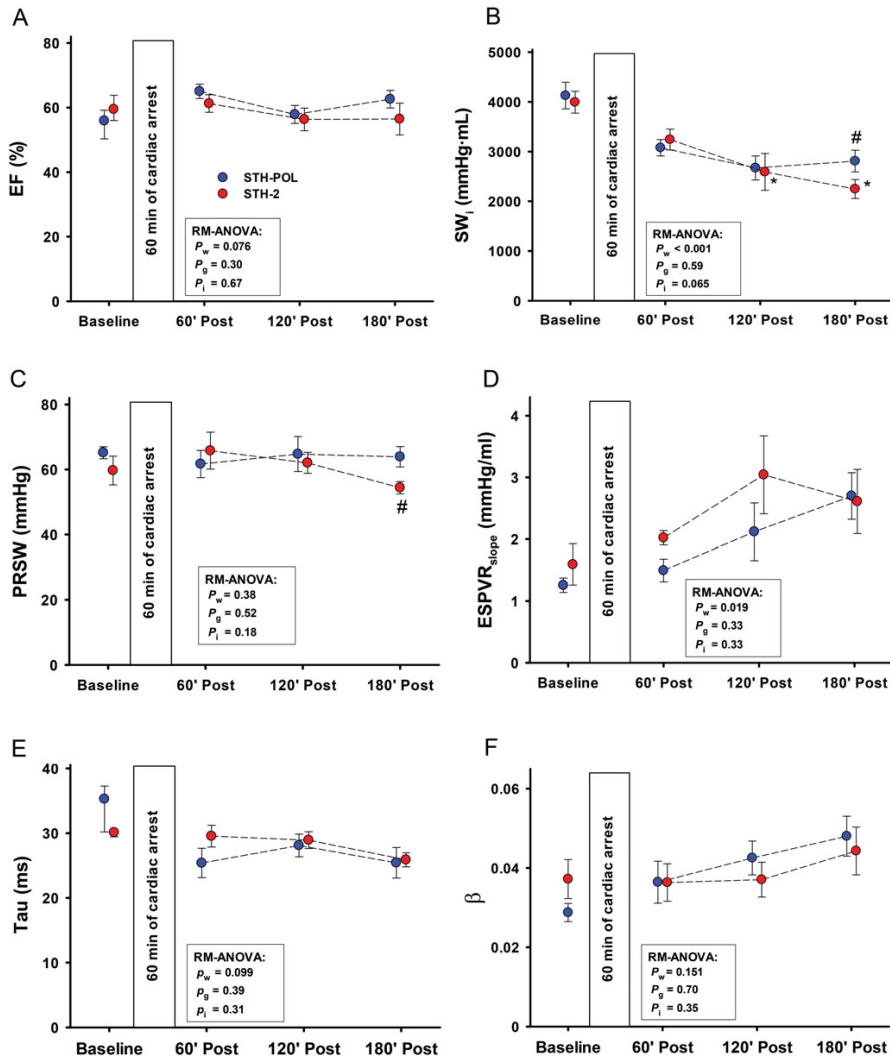


Figure 2: Left ventricle functional variables at baseline and 60, 120 and 180 min after CPB and aortic declamping following cardiac arrest with polarizing (STH-POL) and depolarizing (STH-2) cardioplegia. Mean or median values, bars are SE or 25 and 75 percentiles. Statistics as in Fig. 1. *Significantly different from STH-POL at 180 min of reperfusion, #Significantly different from 60 min of reperfusion within STH-2 group. EF: ejection fraction; SW₁: indexed stroke work; PRSW: slope of preload recruitable stroke work; ESPVR_{slope}: slope of the end-systolic pressure volume relationship; Tau: isovolumic relaxation constant; β: the logarithmic end-diastolic pressure volume relationship; RM-ANOVA: analysis of variance for repeated measurements.

Mitochondrial ultrastructure and metabolism

In the mid-myocardium, there was a significant increase in the volume fraction of the sarcoplasm resulting in a concomitant decrease in the volume fraction of myofibrils in the STH-2 group (Fig. 5). The volume fraction of mitochondria did not differ significantly. Furthermore, the surface density of the mitochondria did not differ between groups. The surface-to-volume ratio was slightly decreased for the STH-POL group, indicating mitochondrial swelling. The carnitine transport systems for long chain fatty acids,

evaluated as CPT-I and CPT-II activity, were not affected by the selection of the cardioplegic protocol.

DISCUSSION

This study provides evidence that 'polarised' arrest with a solution containing a mixture of esmolol, adenosine and magnesium in oxygenated blood offers myocardial protection that is comparable with standard potassium-based (depolarised) cold, intermittent

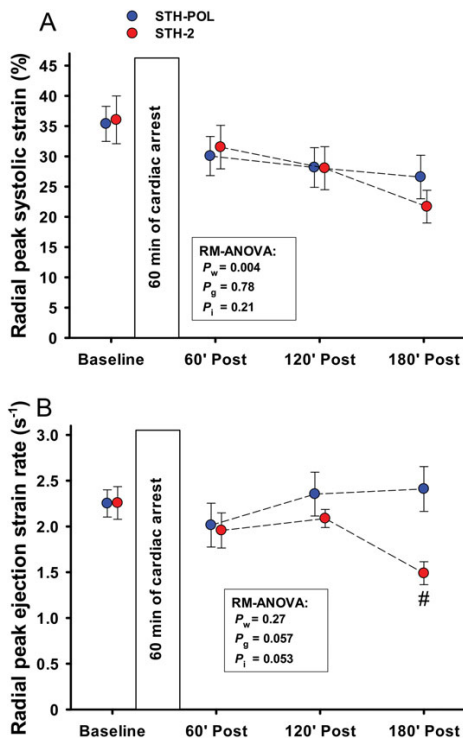


Figure 3: (A) Radial peak systolic TDI strain and (B) peak ejection strain rate at baseline and 60, 120 and 180 min after CPB and aortic declamping in the left ventricular anterior wall following cardiac arrest with polarizing (STH-POL) and depolarizing (STH-2) cardioplegia. Mean values, bars are SE. #Significantly different from STH-POL at 180 min of reperfusion. Statistics as in Fig. 1. SE: standard error; RM-ANOVA: analysis of variance for repeated measurements.

oxygenated blood cardioplegia in a clinically relevant porcine model. At 180 min after aortic declamping, left ventricular contractile function evaluated as $LV-dP/dt_{max}$, PRSW and peak ejection strain rate was better maintained in animals with polarizing compared with depolarizing cardioplegic arrest for 60 min. Furthermore, the hearts arrested with polarizing cardioplegia generate an increased systemic blood pressure (MAP) 180 min after declamping. This could be a result of reduced development of left ventricular myocardial stunning in the STH-POL group 3 h after declamping. Troponin-T release and the degree of apoptosis did not differ and contradict differences in irreversible myocardial damage between groups. The increase in variables describing contractility such as PRSW, $LV-dP/dt_{max}$ and strain rate in the STH-POL group 180 min after declamping is not a result of activation of the Frank-Starling mechanism in the left ventricle. The left ventricular end-diastolic volume was unchanged and did not differ between groups (Table 3). Similarly, the load-dependent variables of left ventricular EF (Fig. 2) and radial TDI strain (Fig. 3) were not different between groups during the 180 min of observation after declamping. Group differences in $LV-dP/dt_{max}$ and strain rate could be affected by the differences in heart rate. However, heart rate did not differ between groups after declamping (Fig. 1). The increased contractility did not improve cardiac

function evaluated by LV-EF and Cardiac Index. The increased indexed stroke works at 180 min in the STH-POL group, potentially resulting from slight, but non-significant increases in LVSP and CI, indicate that left ventricle performance was improved following polarizing cardioplegic arrest in the present study. This increase in left ventricular workload was not reflected in a substantial increase in left ventricular tissue blood flow rate. We interpret these results due to an improvement in myocardial protective efficacy with polarised cardioplegic arrest, possibly due to a reduced ionic inhomogeneity and consequently reduced energy utilization [3].

In chronic heart failure, increased catecholamine release with impaired signalling and desensitization of β -adrenergic receptors (β -AR) contributes to myocardial dysfunction [14]. During CPB and cardioplegic arrest, serum catecholamines increase and norepinephrine is released locally from the hypothermic and anoxic myocardium [15, 16]. This can lead to β -AR desensitization and is associated with increased GRK2 activity. Hence, β -AR desensitization and increased GRK2 activity may explain several aspects of the myocardial stunning observed after cardiac surgery [17]. The addition of esmolol systemically during CPB in dog hearts subsequently arrested with potassium-based crystalloid cardioplegia demonstrated enhanced β -adrenergic receptor signalling with improved postischaemic function [18]. Similarly, the addition of esmolol before CPB in pigs arrested with cold potassium-based blood cardioplegia improved late contractile function [19]. Interestingly, the addition of esmolol to cold potassium-based blood cardioplegia was also able to enhance late myocardial recovery of function in pigs subjected to CPB and 100 min of ischaemic arrest [20]. As indicated by the tissue levels of phosphorylated GRK2 in the present study, there is no evidence for altered GRK2 activity in either group (Fig. 4). Since neither adenylate cyclase activity nor GRK2 activity was measured directly, the prevention of β -receptor desensitization could not be completely ruled out as an explanation for the improved contractile function observed in animals with polarizing cardioplegia (Figs 1-3).

The administration of repeated oxygenated blood cardioplegia during cardiac surgery implies multiple episodes of ischaemia and re-oxygenation before the final declamping and reperfusion. Beta-receptor blockade during cardioplegic arrest is of potential interest for reducing both ischaemic- and lethal reperfusion injury. However, the unwanted negative inotropic effect during reperfusion and weaning could be potentially harmful, especially if the β -blocking agent has a prolonged half-life. Esmolol is rapidly metabolized by blood esterase and has a half-life of ~ 9 min [21]. Esmolol has been found beneficial as an alternative to cardioplegia by inducing 'minimal myocardial contraction' [22], or as a supplement to standard cardioplegic regimes [19, 20]. In the present study, there was a trend towards an early but transient reduction in heart rate as well as a significantly higher LVEDP at 20 min after declamping (Fig. 1), indicating a residual negative chronotropic and inotropic effect of esmolol early after declamping. However, by 30 min after declamping, these negative effects were abolished.

Myocardial ischaemic injury and lethal reperfusion injury are reduced by β -adrenergic blockers and the modulation of apoptotic cell death is also linked to β -receptor adrenergic signalling and GRK2 activation [23]. In the present study, neither release of troponin-T at 180 min after aortic declamping nor activation of apoptotic activity (judged by tissue cleaved caspase-3 activity) differed between treatment groups.

In research and in clinical practice, different forms of cardioplegic solutions delivered as crystalloid or as blood-based cardioplegia

Table 3: Cardiac and haemodynamic variables and tissue blood flow 60, 120 and 180 min after aortic declamping following 60 min of polarizing (STH-POL) or depolarizing (STH-2) cardioplegic arrest

Variable	60 min (A)	120 min (B)	180 min (C)	RM-ANOVA statistics
LV-EDV _i (ml/m ²)				
STH-POL	60 ± 3	59 ± 4	54 ± 2	<i>P</i> _w = 0.26, <i>P</i> _g = 0.55, <i>P</i> _i = 0.92
STH-2	64 ± 4	60 ± 6	58 ± 4	
LV-ESV _i (ml/m ²)				
STH-POL	23 ± 2	28 ± 4	22 ± 2	<i>P</i> _w = 0.54, <i>P</i> _g = 0.36, <i>P</i> _i = 0.53
STH-2	27 ± 3	29 ± 4	30 ± 7	
LV-SV _i (ml/m ²)				
STH-POL	42 ± 2	37 ± 2	37 ± 1	<i>P</i> _w < 0.001, <i>P</i> _g = 0.22, <i>P</i> _i = 0.51
STH-2	42 ± 3	37 ± 4	34 ± 3	
RV-EDV _i (ml/m ²)				
STH-POL	134 ± 5	128 ± 4	123 ± 3	<i>P</i> _w = 0.006, <i>P</i> _g = 0.55, <i>P</i> _i = 0.73
STH-2	142 ± 6	132 ± 4	130 ± 5	
RV-EF (%)				
STH-POL	30 ± 2	28 ± 1	31 ± 2	<i>P</i> _w = 0.162, <i>P</i> _g = 0.32, <i>P</i> _i = 0.35
STH-2	30 ± 2	26 ± 1	27 ± 2	
MAP (mmHg)				
STH-POL	72 ± 4	71 ± 4	74 ± 4	<i>P</i> _w = 0.127, <i>P</i> _g = 0.31, <i>P</i> _i = 0.046
STH-2	73 ± 3	67 ± 4	63 ± 3 ^{a#}	
CVP (mmHg)				
STH-POL	8.0 ± 0.7	8.1 ± 0.8	9.3 ± 0.9	<i>P</i> _w = 0.003, <i>P</i> _g = 0.57, <i>P</i> _i = 0.85
STH-2	8.4 ± 0.7	8.9 ± 0.8	10.1 ± 1.1	
PAP (mmHg)				
STH-POL	24 ± 1	24 ± 2	25 ± 1	<i>P</i> _w = 0.30, <i>P</i> _g = 0.12, <i>P</i> _i = 0.63
STH-2	26 ± 2	28 ± 2	28 ± 2	
LV blood flow (ml/min per g)				
STH-POL	1.39 ± 0.15	1.24 ± 0.10	1.36 ± 0.10	<i>P</i> _w = 0.16, <i>P</i> _g = 0.46, <i>P</i> _i = 0.69
STH-2	1.32 ± 0.08	1.19 ± 0.06	1.21 ± 0.09	
RV blood flow (ml/min per g)				
STH-POL	1.53 ± 0.21	1.27 ± 0.10	1.30 ± 0.09	<i>P</i> _w = 0.073, <i>P</i> _g = 0.58, <i>P</i> _i = 0.92
STH-2	1.60 ± 0.17	1.34 ± 0.08	1.42 ± 0.17	

Values are mean ± SE for 10 animals in each group.

LV and RV: left and right ventricle; i: value indexed for body surface area; EDV: end-diastolic volume; ESV: end-systolic volume; SV: stroke volume; MAP: mean arterial pressure; CVP: mean central venous pressure; PAP: mean pulmonary artery pressure; STH-POL: St Thomas' Hospital polarizing cardioplegic solution; STH-2: St Thomas' Hospital cardioplegic solution No. 2; RM-ANOVA: analysis of variance for repeated measurement.

*P*_w, *P*_g and *P*_i: *P*-values for within subjects, between groups and interaction from two-way RM-ANOVA, respectively.

^aSignificant difference within group means from value(s) in columns with corresponding capital letters.

[#]Significantly different from STH-POL at 180 min of reperfusion.

have been studied and are in use. Both intracellular solutions with amino acids as buffer and low levels of Na⁺ and Ca²⁺, and extracellular solutions with normal levels of Na⁺ and Ca²⁺ rely on moderately increased concentrations of potassium to obtain cardiac arrest [1]. Potassium-based depolarizing cardioplegia inactivates the fast Na⁺ channel in the myocyte membrane, by inducing re-equilibration of the membrane potential to a more positive level and thereby preventing the voltage-activated Na⁺ spike of the action potential and the triggering of contraction [3]. This, together with myocardial cooling, reduces energy consumption and oxygen demands during cardiac arrest. At this re-equilibrated membrane potential, the non-inactivating Na⁺ current leads to increases in intracellular Na⁺, with subsequent reversal of the Na⁺/Ca²⁺-exchanger; the resultant Na⁺ and Ca²⁺ overload is potentially harmful. Increased tissue oedema in hearts arrested with the hyperkalaemic STH-2 cardioplegia was found compared with the normokalaemic STH-POL cardioplegia, and this is consistent with previous findings [22]. In contrast, esmolol inhibits the fast Na⁺-channels and the L-type Ca²⁺-channels [4]; adenosine is a K_{ATP}-channel opener and magnesium is an endogenous Ca²⁺-channel blocker. These pharmacological effects will reduce the ionic heterogeneity that occurs during ischaemia and will concomitantly reduce high-energy phosphate utilization. Adenosine

induces hyperpolarized cardiac arrest in normokalaemic cardioplegic solutions, and also in a clinical setting [24]. Magnesium is a component of STH-2 cardioplegia, exerting an anti-ischaemic protective effect. However, the efficacy of magnesium as adjuvant to cardioplegic solutions has been questioned [25]. One could therefore speculate if esmolol and adenosine alone could be an alternative polarizing cardioplegic solution.

Limitations

In addition to the obvious possibility of species differences, the present study is performed in healthy young hearts without coronary pathology where the conditions for myocardial protection are optimized. In addition, the limited cross-clamp time and the total potassium load in the present study could obscure possible advantages with polarizing cardioplegic arrest. Furthermore, an increase in both ischaemic time connected to more complex surgical procedures and prolonged observation time after declamping could more precisely clarify such differences. Also, intermittent STH-POL cardioplegia should be compared with other routines, for instance with solutions designed for single-shot administration.

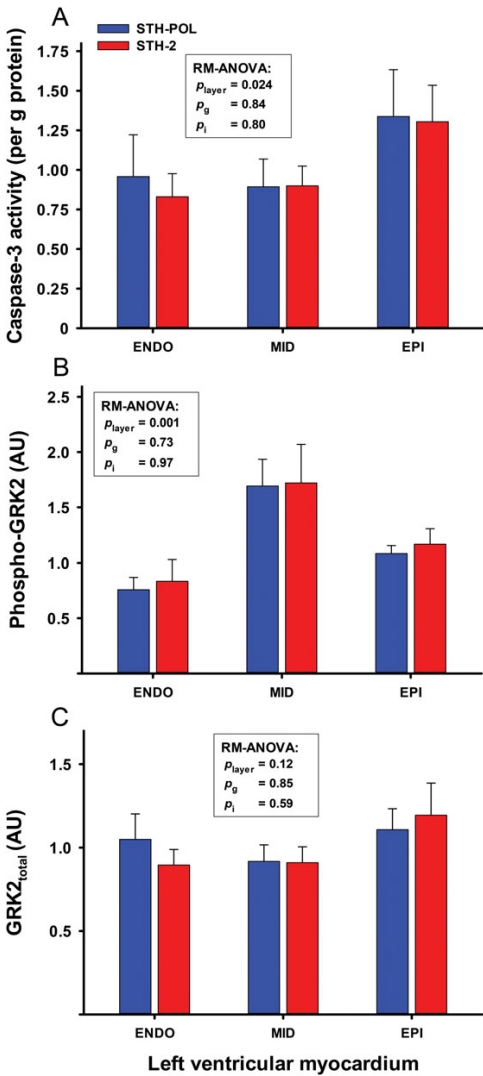


Figure 4: (A) Caspase-3 activity ($n = 10 + 9$), (B) phosphorylated (Phospho-GRK2) and (C) total (GRK2_{total}) G protein-coupled receptor kinase-2 ($n = 9 + 9$) in myocardial tissue samples obtained 180 min after reperfusion following CPB and 60 min of cardioplegic arrest with polarizing (STH-POL) and depolarizing (STH-2) cardioplegia. Bars are mean + SE. Statistics as in Fig. 1. SE: standard error; RM-ANOVA: analysis of variance for repeated measurements.

Clinical implications

On the basis of the present study, polarizing cardioplegia with esmolol, adenosine and magnesium seems non-inferior to standard depolarizing, potassium-based repeated, oxygenated blood cardioplegia. Clinical research protocols could be initiated, at least in patients requiring a short-to-medium time of cardiac arrest during heart surgery.

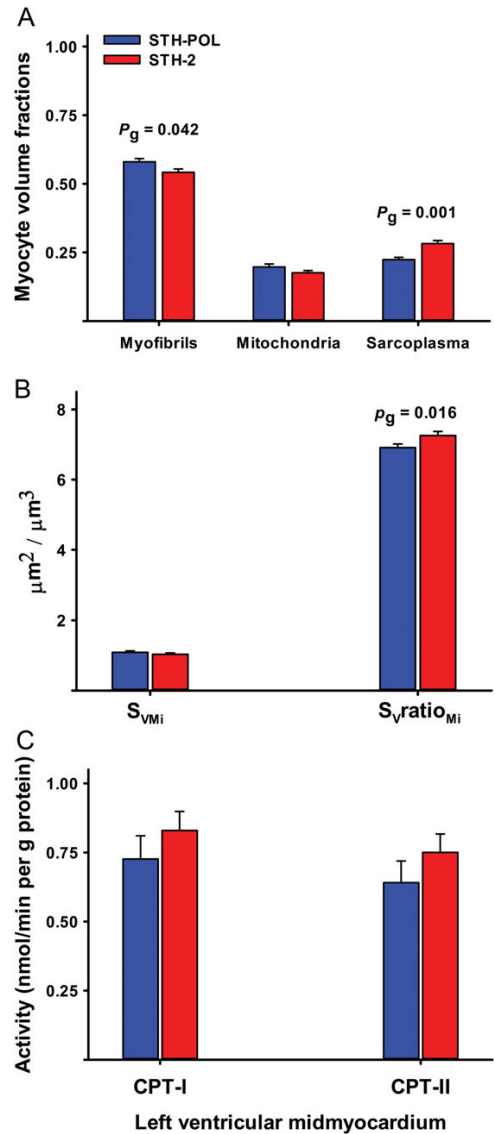


Figure 5: (A) Mid-myocardial myocyte volume fractions, (B) mitochondrial surface density (S_{VMi}), surface-to-volume ratio ($S_{Vratio_{Mi}}$) and (C) carnitine palmitoyltransferase activity in the outer (CPT-I) and inner (CPT-II) mitochondrial membrane. Bars are mean + SE. P_g is the probability by two-sample t-tests. SE: standard error.

CONCLUSIONS

This translational large animal study demonstrates that polarizing oxygenated blood cardioplegia with esmolol/adenosine/magnesium offers comparable myocardial protection and improves contractility

compared with the standard potassium-based depolarizing blood cardioplegia.

SUPPLEMENTARY MATERIAL

Supplementary material is available at [EJCTS online](#).

ACKNOWLEDGEMENTS

We acknowledge the supply of the Merz grid developed for the ImageJ and the kind advice by Aleksandr Mironov, University of Manchester. The technical assistance from Lill-Harriet Andreassen, Cato Johnsen, Kjersti Milde, Gry-Hilde Nilsen, Anne Aarsand, Randi Sandvik and the staff at the Vivarium, University of Bergen is greatly appreciated.

Funding

Pirjo-Riitta Salminen and Geir Olav Dahle were research fellows funded by the Western Norway Regional Health Authority. Financial support was received from the Western Norway Regional Health Authority, the Bergen University Heart Fund, Norwegian Health Association, the Norwegian Research School in Medical Imaging and the Grieg Foundation. Funding to pay the Open Access publication charges for this article was provided by the University of Bergen.

Conflict of interest: none declared.

REFERENCES

- [1] Habertheuer A, Kocher A, Laufer G, Andreas M, Szeto WY, Petzelbauer P *et al.* Cardioprotection: a review of current practice in global ischemia and future translational perspective. *Biomed Res Int* 2014;2014:325725.
- [2] Maruyama Y, Chambers DJ, Ochi M. Future perspective of cardioplegic protection in cardiac surgery. *J Nippon Med Sch* 2013;80:328–41.
- [3] Chambers DJ, Fallouh HB. Cardioplegia and cardiac surgery: pharmacological arrest and cardioprotection during global ischemia and reperfusion. *Pharmacol Ther* 2010;127:41–52.
- [4] Fallouh HB, Bardswell SC, McLatchie LM, Shattock MJ, Chambers DJ, Kentish JC. Esmolol cardioplegia: the cellular mechanism of diastolic arrest. *Cardiovasc Res* 2010;87:552–60.
- [5] Fannelop T, Dahle GO, Matre K, Segadal L, Grong K. An anaesthetic protocol in the young domestic pig allowing neuromuscular blockade for studies of cardiac function following cardioplegic arrest and cardiopulmonary bypass. *Acta Anaesthesiol Scand* 2004;48:1144–54.
- [6] Steendijk P, Staal E, Jukema JW, Baan J. Hypertonic saline method accurately determines parallel conductance for dual-field conductance catheter. *Am J Physiol Heart Circ Physiol* 2001;281:H755–63.
- [7] Swarc RS, Mickleborough LL, Mizuno S, Wilson GJ, Liu P, Mohamed S. Conductance catheter measurements of left ventricular volume in the intact dog: parallel conductance is independent of left ventricular size. *Cardiovasc Res* 1994;28:252–8.
- [8] Hawk C, Leary SL, Morris TH. *Formulary for Laboratory Animals*. 3rd edn. Ames: Blackwell Publishing Professional, 2005.
- [9] Matre K, Fannelop T, Dahle GO, Heimdal A, Grong K. Radial strain gradient across the normal myocardial wall in open-chest pigs measured with Doppler strain rate imaging. *J Am Soc Echocardiogr* 2005;18:1066–73.
- [10] Froyland L, Madsen L, Eckhoff KM, Lie O, Berge RK. Carnitine palmitoyltransferase I, carnitine palmitoyltransferase II, and acyl-CoA oxidase activities in Atlantic salmon (*Salmo salar*). *Lipids* 1998;33:923–30.
- [11] Howard C, Reed MG. *Unbiased Stereology*. 2nd edn. Oxford: QTP Publications, 2010.
- [12] Weibel ER, Kistler GS, Scherle WF. Practical stereological methods for morphometric cytology. *J Cell Biol* 1966;30:23–38.
- [13] Kowallik P, Schulz R, Guth BD, Schade A, Paffhausen W, Gross R *et al.* Measurement of regional myocardial blood flow with multiple colored microspheres. *Circulation* 1991;83:974–82.
- [14] Cannavo A, Liccardo D, Koch WJ. Targeting cardiac beta-adrenergic signaling via GRK2 inhibition for heart failure therapy. *Front Physiol* 2013;4:264.
- [15] Reves JG, Karp RB, Buttner EE, Tosone S, Smith LR, Samuelson PN *et al.* Neuronal and adrenomedullary catecholamine release in response to cardiopulmonary bypass in man. *Circulation* 1982;66:49–55.
- [16] Schomig A, Haass M, Richardt G. Catecholamine release and arrhythmias in acute myocardial ischemia. *Eur Heart J* 1991;12(Suppl F):38–47.
- [17] Bulcao CF, Pandalai PK, D'Souza KM, Merrill WH, Akhter SA. Uncoupling of myocardial beta-adrenergic receptor signaling during coronary artery bypass grafting: the role of GRK2. *Ann Thorac Surg* 2008;86:1189–94.
- [18] Booth JV, Spahn DR, McRae RL, Chesnut LC, El-Moalem H, Atwell DM *et al.* Esmolol improves left ventricular function via enhanced beta-adrenergic receptor signaling in a canine model of coronary revascularization. *Anesthesiology* 2002;97:162–9.
- [19] Fannelop T, Dahle GO, Matre K, Moen CA, Mongstad A, Eliassen F *et al.* Esmolol before 80 min of cardiac arrest with oxygenated cold blood cardioplegia alleviates systolic dysfunction. An experimental study in pigs. *Eur J Cardiothorac Surg* 2008;33:9–17.
- [20] Dahle GO, Salminen PR, Moen CA, Eliassen F, Jonassen AK, Haavestad R *et al.* Esmolol added in repeated, cold, oxygenated blood cardioplegia improves myocardial function after cardiopulmonary bypass. *J Cardiothorac Vasc Anesth* 2015;29:684–93.
- [21] Sum CY, Yacobi A, Kartzinel R, Stampfli H, Davis CS, Lai CM. Kinetics of esmolol, an ultra-short-acting beta blocker, and of its major metabolite. *Clin Pharmacol Ther* 1983;34:427–34.
- [22] Mehlhorn U, Sauer H, Kuhn-Regnier F, Sudkamp M, Dhein S, Eberhardt F *et al.* Myocardial beta-blockade as an alternative to cardioplegic arrest during coronary artery surgery. *Cardiovasc Surg* 1999;7:549–57.
- [23] Brinks H, Boucher M, Gao E, Chuprun JK, Pesant S, Raake PW *et al.* Level of G protein-coupled receptor kinase-2 determines myocardial ischemia/reperfusion injury via pro- and anti-apoptotic mechanisms. *Circ Res* 2010;107:1140–9.
- [24] Jakobsen O, Naesheim T, Aas KN, Sorlie D, Steensrud T. Adenosine instead of supranormal potassium in cardioplegia: it is safe, efficient, and reduces the incidence of postoperative atrial fibrillation. A randomized clinical trial. *J Thorac Cardiovasc Surg* 2013;145:812–8.
- [25] Duan L, Zhang CF, Luo WJ, Gao Y, Chen R, Hu GH. Does magnesium-supplemented cardioplegia reduce cardiac injury? A meta-analysis of randomized controlled trials. *J Card Surg* 2015;30:338–45.

Online Table 1.

Mean arterial pressure, temperature, haemoglobin, arterial blood gases and electrolytes during cardiopulmonary bypass in two groups of pigs with 60 min of polarising (STH-POL) or depolarising (STH-2) cardioplegic arrest. Values are mean \pm SE, n = 10.

Variable	1 min before X-clamp (A)	30 min X-clamp (B)	58 min X-clamp (C)	RM-ANOVA statistics
MAP (mmHg)				
STH-POL	61 \pm 6	44 \pm 3	62 \pm 6	$p_w = 0.012, p_g = 0.82, p_i = 0.26$
STH-2	63 \pm 5	52 \pm 5	56 \pm 4	
Temp_{rect} ($^{\circ}$C)				
STH-POL	38.1 \pm 0.2	34.4 \pm 0.1	37.4 \pm 0.3	$p_w < 0.001, p_g = 0.14, p_i = 0.59$
STH-2	38.6 \pm 0.1	34.5 \pm 0.2	37.7 \pm 0.3	
Hb (g/dl)				
STH-POL	6.0 \pm 0.2	6.6 \pm 0.2 ^a	7.4 \pm 0.3 ^{a,b}	$p_w < 0.001, p_g = 0.077, p_i = 0.008$
STH-2	5.9 \pm 0.1	7.6 \pm 0.3 ^{a,#}	8.1 \pm 0.3 ^{a,#}	
pH				
STH-POL	7.43 \pm 0.01	7.42 \pm 0.01	7.42 \pm 0.01	$p_w = 0.73, p_g = 0.73, p_i = 0.70$
STH-2	7.44 \pm 0.01	7.41 \pm 0.02	7.42 \pm 0.02	
pO₂ (kPa)				
STH-POL	12.9 \pm 1.4	19.1 \pm 1.5	18.3 \pm 1.4	$p_w = 0.002, p_g = 0.96, p_i = 0.26$
STH-2	15.2 \pm 1.9	17.8 \pm 1.5	17.1 \pm 1.1	
pCO₂ (kPa)				
STH-POL	5.4 \pm 0.1	6.1 \pm 0.2	6.0 \pm 0.2	$p_w < 0.001, p_g = 0.77, p_i = 0.74$
STH-2	5.4 \pm 0.2	6.1 \pm 0.3	5.8 \pm 0.2	
HCO₃⁻ (mmol/l)				
STH-POL	26.6 \pm 0.4	28.5 \pm 0.4	27.9 \pm 0.4	$p_w < 0.001, p_g = 0.90, p_i = 0.20$
STH-2	27.3 \pm 0.4	28.2 \pm 0.4	27.7 \pm 0.6	
s-K⁺ (mmol/l)				
STH-POL	4.4 \pm 0.1	3.9 \pm 0.1 ^a	4.5 \pm 0.1 ^b	$p_w < 0.001, p_g = 0.019, p_i < 0.001$
STH-2	4.4 \pm 0.1	4.6 \pm 0.1 ^{a,#}	4.8 \pm 0.1 ^{a,#}	
s-Na⁺ (mmol/l)				
STH-POL	141 \pm 1	142 \pm 1	142 \pm 1	$p_w = 0.20, p_g = 0.78, p_i = 0.64$
STH-2	142 \pm 1	142 \pm 1	142 \pm 1	

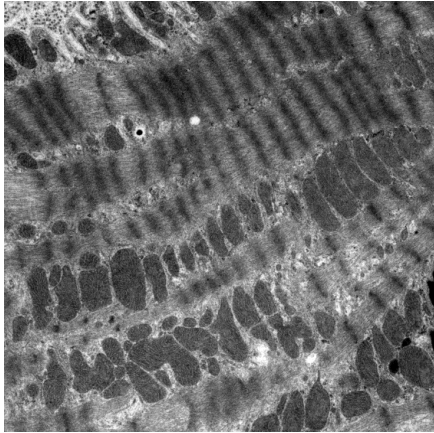
MAP = mean aortic pressure; Temp_{rect} = rectal temperature; s = serum levels; p_w, p_g, p_i = p-values for within subjects, between groups and for interaction from two-way RM-ANOVA, respectively. ^a and ^b: significant difference within group means from value(s) in columns with corresponding capital letters; # = significantly different from STH-POL at 58 min of X-clamp.

Online Table 2.

Diuresis, rectal temperature, haemoglobin, arterial blood gases and serum electrolytes at Baseline and 60, 120 and 180 min after cardioplegic arrest in two groups of pigs with 60 min of polarising (STH-POL) or depolarising (STH-2) cardioplegic arrest. Values are mean \pm SE, n = 10.

Variable	Time after aortic declamping and reperfusion			
	Baseline	60 min	120 min	180 min
Diuresis (ml/kg per h)				
STH-POL	2.5 \pm 0.3	6.3 \pm 1.4	3.8 \pm 0.8	3.8 \pm 2.0
STH-2	2.5 \pm 0.4	4.6 \pm 1.3	3.9 \pm 0.6	2.2 \pm 0.5
Temp_{rect} ($^{\circ}$C)				
STH-POL	38.1 \pm 0.2	38.1 \pm 0.1	38.3 \pm 0.1	38.5 \pm 0.1
STH-2	38.5 \pm 0.2	38.2 \pm 0.1	38.6 \pm 0.1	38.7 \pm 0.1
Hb (g/dl)				
STH-POL	8.2 \pm 0.2	7.4 \pm 0.4	7.2 \pm 0.4	7.5 \pm 0.4
STH-2	8.1 \pm 0.2	7.6 \pm 0.3	7.0 \pm 0.3	6.9 \pm 0.3
pH				
STH-POL	7.51 \pm 0.01	7.45 \pm 0.01	7.47 \pm 0.01	7.47 \pm 0.01
STH-2	7.50 \pm 0.3	7.43 \pm 0.02	7.48 \pm 0.01	7.47 \pm 0.02
pO₂ (kPa)				
STH-POL	25.8 \pm 0.9	20.4 \pm 2.3	21.8 \pm 1.3	21.9 \pm 1.3
STH-2	25.6 \pm 0.5	19.8 \pm 1.9	21.0 \pm 1.8	20.9 \pm 1.7
pCO₂ (kPa)				
STH-POL	5.2 \pm 0.1	5.3 \pm 0.2	5.2 \pm 0.1	5.2 \pm 0.1
STH-2	5.0 \pm 0.1	5.7 \pm 0.2	5.0 \pm 0.1	5.1 \pm 0.1
HCO₃⁻ (mmol/l)				
STH-POL	31.2 \pm 0.2	27.6 \pm 0.5	28.0 \pm 0.6	28.4 \pm 0.6
STH-2	31.2 \pm 0.4	27.4 \pm 0.8	27.9 \pm 0.6	28.1 \pm 0.7
s-K⁺ (mmol/l)				
STH-POL	3.7 \pm 0.1	3.9 \pm 0.1	4.1 \pm 0.1	4.6 \pm 0.1
STH-2	3.7 \pm 0.1	4.2 \pm 0.1	4.3 \pm 0.2	4.4 \pm 0.1
s-Na⁺ (mmol/l)				
STH-POL	142 \pm 1	143 \pm 1	143 \pm 1	144 \pm 1
STH-2	142 \pm 1	143 \pm 1	142 \pm 1	143 \pm 1

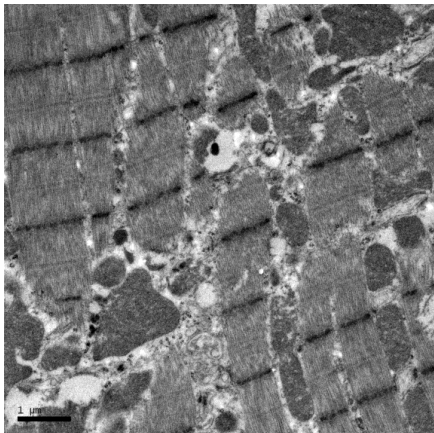
Control:



Volume fractions

Myofibrils: 0.58
Mitochondria: 0.25
Sarcoplasm: 0.17

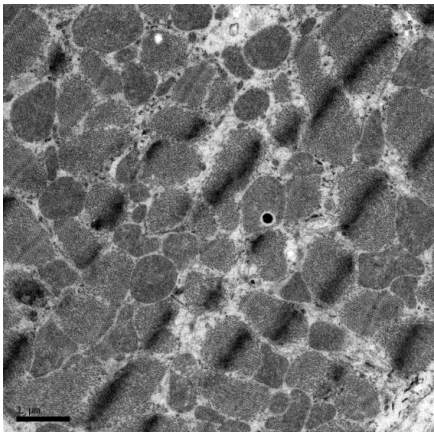
STH-POL cardioplegia:



Volume fractions

Myofibrils: 0.58
Mitochondria: 0.21
Sarcoplasm: 0.21

STH-2 cardioplegia:



Volume fractions

Myofibrils: 0.53
Mitochondria: 0.18
Sarcoplasm: 0.29

Representative micrographs (x15.000) from a Control heart not on CPB and cardioplegic arrest and from the STH-POL and the STH-2 group 180 min after aortic declamping, demonstrating volume fractions close to the mean values for the two groups (Figure 5 in the paper).

PAPER II

with Supplemental Material

Cite this article as: Aass T, Stangeland L, Chambers DJ, Hallström S, Rossmann C, Podesser BK *et al.* Myocardial energy metabolism and ultrastructure with polarizing and depolarizing cardioplegia in a porcine model. *Eur J Cardiothorac Surg* 2017;52:180–8.

Myocardial energy metabolism and ultrastructure with polarizing and depolarizing cardioplegia in a porcine model[†]

Terje Aass^{a,b,*}, Lodve Stangeland^b, David J. Chambers^c, Seth Hallström^d, Christine Rossmann^d,
Bruno K. Podesser^e, Malte Urban^a, Knut Nesheim^a, Rune Haaverstad^{a,b}, Knut Matre^b and Ketil Grong^b

^a Department of Heart Disease, Haukeland University Hospital, Bergen, Norway

^b Department of Clinical Science, University of Bergen, Bergen, Norway

^c Cardiac Surgical Research, The Rayne Institute (King's College London), Guy's and St Thomas' NHS Foundation Trust, St Thomas' Hospital, London, UK

^d Institute of Physiological Chemistry, Center of Physiological Medicine, Medical University Graz, Graz, Austria

^e Department of Biomedical Research, Ludwig Boltzmann Cluster for Cardiovascular Research, Medical University of Vienna, Vienna, Austria

* Corresponding author. Section of Cardiothoracic Surgery, Department of Heart Disease, Haukeland University Hospital, P.O Box 1400, 5021 Bergen, Norway. Tel: +47-559-75000; fax: +47-559-75150; e-mail: terje.aass@helse-bergen.no (T. Aass).

Received 17 October 2016; received in revised form 4 January 2017; accepted 18 January 2017

Abstract

OBJECTIVES: This study investigated whether the novel St. Thomas' Hospital polarizing cardioplegic solution (STH-POL) with esmolol/adenosine/magnesium offers improved myocardial protection by reducing demands for high-energy phosphates during cardiac arrest compared to the depolarizing St. Thomas' Hospital cardioplegic solution No 2 (STH-2).

METHODS: Twenty anaesthetised pigs on tepid cardiopulmonary bypass were randomized to cardiac arrest for 60 min with antegrade freshly mixed, repeated, cold, oxygenated STH-POL or STH-2 blood cardioplegia every 20 min. Haemodynamic variables were continuously recorded. Left ventricular biopsies, snap-frozen in liquid nitrogen or fixed in glutaraldehyde, were obtained at Baseline, 58 min after cross-clamp and 20 and 180 min after weaning from bypass. Adenine nucleotides were evaluated by high-performance liquid chromatography, myocardial ultrastructure with morphometry.

RESULTS: With STH-POL myocardial creatine phosphate was increased compared to STH-2 at 58 min of cross-clamp [59.9 ± 6.4 (SEM) vs 44.5 ± 7.4 nmol/mg protein; $P < 0.025$], and at 20 min after reperfusion (61.0 ± 6.7 vs 49.0 ± 5.5 nmol/mg protein; $P < 0.05$). ATP levels were increased at 20 min of reperfusion with STH-POL (35.4 ± 1.1 vs 32.4 ± 1.2 nmol/mg protein; $P < 0.05$). Mitochondrial surface-to-volume ratio was decreased with polarizing compared to depolarizing cardioplegia 20 min after reperfusion (6.74 ± 0.14 vs $7.46 \pm 0.13 \mu\text{m}^2/\mu\text{m}^3$; $P = 0.047$). None of these differences were present at 180 min of reperfusion. From 150 min of reperfusion and onwards, cardiac index was increased with STH-POL; 4.8 ± 0.2 compared to 4.0 ± 0.2 l/min/m² ($P = 0.011$) for STH-2 at 180 min.

CONCLUSIONS: Polarizing STH-POL cardioplegia improved energy status compared to standard STH-2 depolarizing blood cardioplegia during cardioplegic arrest and early after reperfusion.

Keywords: Cardioplegia • Myocardial protection • Energy metabolism • Ultrastructure

INTRODUCTION

Repeated hyperkalaemic blood cardioplegia, considered by many to provide optimal myocardial protection, induces depolarization and re-equilibration of the resting cell membrane potential. This inactivates the voltage-dependent fast Na⁺ channels [1], prevents initiation of the action potential and induces depolarized diastolic arrest. However, this will cause intracellular Na⁺ and Ca²⁺ overload by activation of the Na⁺/H⁺-exchanger and reversal of the Na⁺/Ca²⁺ exchanger; the resulting imbalance in cytosolic ion composition activates energy utilizing compensatory mechanisms [2].

[†]Preliminary results were presented as an abstract at the 8th Joint Scandinavian Conference in Cardiothoracic Surgery, Reykjavik, Iceland, 19 August 2016.

By inducing 'polarized' (non-depolarized) arrest the myocyte membrane potential is maintained at or near the resting membrane potential [3]. In isolated hearts, polarized cardiac arrest reduces myocardial oxygen consumption compared to depolarized arrest, probably as a result of reduced activation of energy-dependent cellular ion channels/pumps, and hence further reduced needs for high-energy phosphates (HEP) during cardiac arrest [4]. The normokalaemic St. Thomas' Hospital polarizing cardioplegic solution (STH-POL) with esmolol/adenosine/magnesium avoids depolarized arrest and reduces the potassium load. A recent experimental study demonstrated comparable myocardial protection and improved postoperative contractility with STH-POL cardioplegia compared to St. Thomas' Hospital cardioplegia

solution No 2 (STH-2) [5]. In the present study, using the same clinically relevant porcine model, we investigated whether cardioplegic arrest with STH-POL offers myocardial protection comparable to a standard depolarizing potassium-based cardioplegic solution (STH-2), with the main focus on tissue levels of HEP and myocardial ultrastructure during aortic clamping and early and late after weaning from cardiopulmonary bypass (CPB).

METHODS

Anaesthesia and instrumentation

The experiments were conducted in accordance with the European Communities Council Directive of 2010 (63/EU) and approved by the Norwegian State Commission for Laboratory Animals (Project 20135835). Twenty-two pigs (Norwegian land race) of either gender, weighing 42 ± 3 (SD) kg were premedicated with an i.m. injection of ketamine, diazepam and atropine. Spontaneous ventilation on mask with oxygen and 3% isoflurane (Rhodia, Bristol, UK) allowed intravenous access through two ear veins. Loading doses followed by continuous infusions of fentanyl, midazolam, pentobarbital and pancuronium secured general anaesthesia and analgesia. This anaesthetic protocol has previously been described and thoroughly evaluated allowing the safe use of neuromuscular blocking agents in young pigs [5, 6]. The animals were tracheotomized, intubated and ventilated (Julian, Drägerwerk, Lübeck, Germany) with nitrous oxide (56–58%) and oxygen. Fluid substitution was Ringers acetate (15 ml/kg/h) with added KCl (20 mmol/l) to maintain normal plasma potassium levels after overnight fasting. In addition, Ringers acetate 5 ml/kg/h was provided after weaning from CPB.

The right femoral artery and vein were cannulated for blood sampling and infusion. An arterial blood gas analysis determined the need for ventilator adjustments (ABL80 FLEX COOX, Radiometer Medical ApS, Brønshøj, Denmark). A surgically inserted catheter measured diuresis and rectal temperature was monitored. A midline sternotomy and pericardiectomy exposed the heart and heparin (125 IU/kg) was given i.v. to prevent catheter clotting. A continuous cardiac output catheter (CCO/EDV 177HF 75, Edwards Lifesciences Inc., Irvine, CA) was floated into the pulmonary artery via the left internal mammary vein. Cardiac output, right ventricular end-diastolic volume, central venous pressure (CVP) and pulmonary artery pressure (PAP) (Vigilance II® and TruWave® transducers, Edwards Lifescience Inc.) were monitored. The proximal aorta was cannulated with a Millar microtip pressure catheter (Millar MPC-500, Houston, TX, USA) through the left internal mammary artery. An identical catheter through the apex of the heart monitored left ventricular pressure. The haemodynamic parameters were recorded by a 16-channel Ponemah (ACQ-7700; Data Sciences International, St. Paul, MN, USA).

Cardiopulmonary bypass and cardioplegia

The heart-lung machine (Stöckert SIII, Munich, Germany) was primed with 1200 ml Ringers acetate. Heparin 500 IU/kg i.v. was given before the brachiocephalic artery (EOPA 18 Fr, Medtronic Inc., Minneapolis, MN, USA) and right atrial appendage (MC2 28/36 Fr, Medtronic Inc.) were cannulated and CPB established with a flow of 90 ml/min per kg and water temperature of 32°C in the heat exchanger. Aortic cross-clamp time was 60 min and a vent

catheter (DLP 13, Medtronic Inc.) temporarily placed through the apex for left ventricular drainage. The body temperature was allowed to drift and CPB flow was reduced to 72 ml/min per kg when rectal temperature reached 35°C or after 20 min. After 40 min of cross-clamping, rewarming was initiated with reset of CPB-flow to 90 ml/min per kg and water temperature at 40°C. Arterial blood gases were obtained before aortic cross-clamping and just before declamping after 60 min. Defibrillation of ventricular fibrillation was the only allowed antiarrhythmic intervention. After 10 min of reperfusion the animals were weaned from CPB and decannulated. The residual blood in the circuit was returned and protamine sulphate 1.5 mg/kg was given.

Cardioplegia was given as either the hyperkalaemic St. Thomas' Hospital cardioplegic solution 2 (STH-2), or the normokalaemic St. Thomas' Hospital polarizing solution (STH-POL). Both solutions were pre-prepared as concentrate and administered as cold (12°C), oxygenated, blood cardioplegia, freshly mixed by a dual-head pump and separate cooling. The cardioplegia was delivered into the aortic root with a flow set to 7% of CPB-flow, following a standardized protocol with an initial 'high-dose' (1.4 concentrate/blood) for 3 min and 2 min of 'low-dose' (1.8 concentrate/blood) given at 20 and 40 min after cross-clamping. The final concentrations of key components in the cardioplegic solutions are presented in the Supplementary Material, Table A.

Experimental protocol

The animals were block-randomized to the STH-POL or STH-2 group (10 per group). After 10 min of stabilization Baseline arterial blood gases and haemodynamic variables were recorded. Two myocardial biopsies from the anterior left ventricular wall were obtained by using 6 and 4 mm biopsy punch (Integra Miltex, York, PA, USA). Both samples included tissue from the epi- and midmyocardium; the 6-mm biopsy was snap-frozen in liquid nitrogen within 5 s and stored at -80°C for later analysis while the 4-mm biopsy was cut and fixed directly in glutaraldehyde.

During CPB the ventilator volume was reduced to 50% and with passive drainage of the left ventricle. Additional heparin (250 IU/kg) was given at 30 min of cross-clamping. After 58 min of cardioplegic arrest, myocardial biopsies were obtained and 2 min later the aortic clamp was removed. The animals were weaned from CPB after 10 min of myocardial reperfusion and decannulated. Twenty and 180 min after declamping myocardial biopsies were taken similar to the Baseline situation. General haemodynamics were recorded every 15 min, from 30 to 180 min after declamping. Finally, the animal was euthanized with intracardiac injection of high dose potassium chloride, the heart removed and samples obtained for complimentary analysis.

Myocardial metabolism and ultrastructure

High energy phosphates [ATP, ADP, AMP and creatine phosphate (CrP)], hypoxanthine and xanthine were measured by high-performance liquid chromatography analysis as previously described [7]. Energy charge (EC) was calculated as:

$$EC = \frac{[ATP] + 0.5 * [ADP]}{[ATP] + [ADP] + [AMP]}$$

Myocardial volume fraction of mitochondria, myofibrils and cytosol were quantified by point counting in 6 randomly selected micrographs ($\times 15000$) from each biopsy, mitochondrial surface

to volume ratio and surface density were calculated by using a Merz grid and the freeware ImageJ [8]. To evaluate inter- and intra-observer variability, the 6 micrographs from 15 randomly selected biopsies were recorded and analysed individually by two observers and by one of the observers twice. For details see Supplementary Material.

Statistical analysis

Data were analysed using SPSS v. 23 (IBM Corp., Armonk, NY, USA) and values given as mean \pm SEM or median (25% percentile; 75% percentile) unless otherwise noted. At Baseline groups were compared by two-sample Student *t*-test on data with normal distribution and with Wilcoxon-Mann-Whitney test on ranks whenever appropriate. Tissue contents of HEPs, degradation products and haemodynamic variables after aortic declamping were compared with two-way ANOVA for repeated measurements (RM-ANOVA) with treatment as group factor (P_g), time as within factor (P_w) and P_i for interaction between time and group. Morphological variables were analysed with nested RM-ANOVA. $P < 0.05$ was considered statistically significant. The intraclass correlation coefficient (ICC) and coefficient of variation (CV%) for inter- and intra-observer variability were calculated for morphometric data. For details see Supplementary Material.

RESULTS

Two animals were excluded. After declamping, one animal in the STH-POL group with profound bleeding and ventricular fibrillation prior to cross-clamp developed severe left heart failure, one animal in the STH-2 group developed severe pulmonary hypertension and right heart failure. Excluded animals were replaced by consecutive experiments. Results are given for 10 animals in each group, except for morphometry where the biopsies from one STH-2 animal were lost. Haemodynamic variables, left ventricular function and arterial blood gases did not differ between groups at Baseline (Fig. 1A–F and Table 1). After 58 min of cardioplegic arrest, the level of serum potassium was significantly increased in the STH-2 compared to the STH-POL group (5.2 ± 0.3 vs 4.1 ± 0.1 mmol/l, $P < 0.001$). During CPB there were no other differences between groups regarding mean arterial pressure, temperatures and arterial blood gases (Supplementary Material, Table B).

Cardiac and haemodynamic variables after weaning

Heart rate increased over time in both groups after weaning (Fig. 1A). In both groups, cardiac index (CI) was initially increased from Baseline but subsequently decreased to a plateau level by 90 min; there were no differences between groups during this period. At 150, 165 and 180 min after declamping, CI was increased in the STH-POL compared to the STH-2 group ($P = 0.036$, $P = 0.026$ and $P = 0.011$, respectively) (Fig. 1B). Left ventricular systolic pressure was unchanged and left ventricular end-diastolic pressure decreased gradually after declamping in both groups (Fig. 1C and D). The first derivative of the left ventricular pressure, $LV-dP/dt_{max}$, did not change significantly over time (Fig. 1E). $LV-dP/dt_{min}$ was less negative in the STH-POL group after 30 min ($P = 0.006$) and 45 min ($P = 0.048$) of reperfusion

compared to corresponding values in the STH-2 group (Fig. 1F). Right ventricular indexed end-diastolic volume (RV-EDV_i) and ejection fraction (RV-EF) did not change over time (Table 2). Indexed stroke volume (RV-SV_i) decreased from 60 to 120 min of reperfusion ($P < 0.001$) for both groups. Central venous pressure (CVP) gradually increased over time ($P_w = 0.030$) in both groups. There were no significant differences between groups regarding mean arterial pressure and pulmonary arterial pressure.

Myocardial high-energy phosphates

At Baseline there were no significant differences between groups for myocardial CrP, adenine nucleotides and the degradation products hypoxanthine and xanthine (Fig. 2A–F). CrP was significantly increased in hearts arrested with STH-POL compared to STH-2 after 58 min of cardiac arrest (59.9 ± 6.4 vs 44.5 ± 7.4 nmol/mg protein; $P < 0.025$) and after 20 min of reperfusion (61.0 ± 6.7 vs 49.0 ± 5.5 nmol/mg protein; $P < 0.05$). However, at 180 min after declamping, the CrP content did not differ between groups (Fig. 2A). At 20 min of reperfusion tissue ATP content was increased in the STH-POL compared to the STH-2 group ($P < 0.05$) (Fig. 2B). Tissue levels of ADP increased from Baseline to 58 min after cardiac arrest in both groups ($P < 0.001$) and decreased to Baseline levels ($P < 0.001$) after 20 and 180 min of reperfusion (Fig. 2C). AMP levels increased in both groups from Baseline to 58 min of cardiac arrest ($P < 0.01$) and did not decrease after reperfusion (Fig. 2D). The level of hypoxanthine increased significantly ($P < 0.001$) in the STH-POL group, and remained increased at the same level at 20 min after declamping (Fig. 2E). After 180 min hypoxanthine levels decreased to Baseline levels ($P < 0.001$). Xanthine levels did not differ between groups and did not change with time (Fig. 2F). There was an overall change in energy charge (EC) over time ($P_w = 0.025$) with no group differences (Table 3). However, multiple contrast tests could not confirm differences between individual time points. The ATP/ADP ratio (pooled means, $n = 20$) decreased from Baseline to 58 min of cross-clamping ($P < 0.001$) and returned to Baseline levels after 20 and 180 min of reperfusion. The CrP/ATP ratio was unchanged.

Mitochondrial ultrastructure

Mitochondrial surface-to-volume ratio ($S_{vratio_{mit}}$) was slightly decreased in the STH-POL compared to the STH-2 group at 20 min after reperfusion (6.74 ± 0.14 vs 7.46 ± 0.13 $\mu\text{m}^2/\mu\text{m}^3$; $P = 0.047$) (Fig. 3A). None of these differences were present at 180 min of reperfusion. Neither mitochondrial surface density (S_{vmit}) nor the myocyte volume fractions of mitochondria, myofibrils and cytosol differed between groups (Fig. 3B and Table 4). For the fractional volumes the interobserver ICC varied between 0.741 and 0.897 with a CV% between 2.48% for myofibrils and 8.14% for sarcoplasm (Table 5). For mitochondrial surface to volume ratio the interobserver ICC was 0.790 with a CV% of 4.05%. Based on ICC calculations, both the inter- and intra-observer variabilities for morphometric data were classified as good to excellent, except for the intra-observer ICC for volume fraction of sarcoplasm [9].

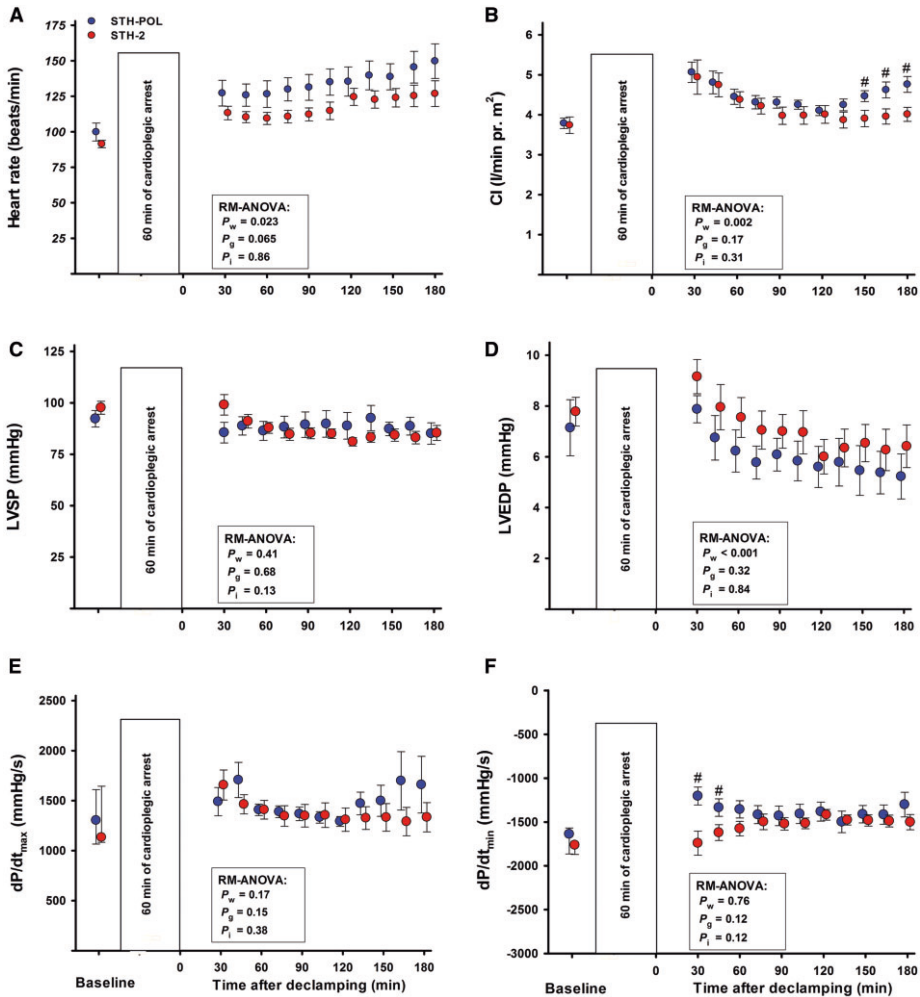


Figure 1: Left ventricular haemodynamic variables, mean (SE) or median (25%; 75%), at Baseline and after CPB and 60 min of cardiac arrest with polarizing (STH-POL; $n = 10$) and depolarizing (STH-2; $n = 10$) cardioplegia. CI: cardiac index; LVSP and LVEDP: left ventricular peak systolic- and end-diastolic pressures; dP/dt_{max} and dP/dt_{min} : peak positive and peak negative of the first derivative of left ventricular pressure; RM-ANOVA: analysis of variance for repeated measurements; P_w , P_g and P_i : P -values for within subjects, between groups and interaction from two-way RM-ANOVA, respectively; #: significantly different from STH-2 at corresponding time after declamping with Bonferroni tests.

DISCUSSION

A transient improvement in energy status with STH-POL cardioplegia was demonstrated as an increase in the myocardial tissue content of CrP after 58 min of cardioplegic arrest and at 20 min after reperfusion and weaning from CPB compared to STH-2 cardioplegia. Also, tissue ATP content was increased at 20 min after reperfusion (Fig. 2A and B).

One of the components of the STH-POL cardioplegia is adenosine, an endogenous purine nucleoside binding to the A_1

receptor. Adenosine reduces cAMP by inhibiting adenylyl cyclase and thereby acts as a K_{ATP} -channel opener. This causes outward K^+ flux and induces polarized cardiac arrest. The polarization effect is especially seen on myocardial conductive tissue such as the atrioventricular node [10]. Esmolol is a cardio-selective β_1 adrenergic receptor blocker with rapid onset by blocking the fast Na^+ and L-type Ca^{2+} -channels initiating polarized arrest [11]. Clinically, esmolol seems to give protection from arrhythmias and is protective in a vulnerable period [12]. In clinically relevant animal studies esmolol as pre-treatment or as adjuvant to

Table 1: Baseline variables before cardiac arrest with polarizing (STH-POL) and depolarizing (STH-2) cardioplegia

Variable	STH-POL	STH-2	Statistics
HR (beats/min)	100 ± 6	91 ± 3	<i>P</i> = 0.23
LV-SP _{max} (mmHg)	92 ± 4	98 ± 3	<i>P</i> = 0.31
LV-EDP (mmHg)	7.1 ± 1.1	7.8 ± 0.7	<i>P</i> = 0.62
LV-dP/dt _{max} (mmHg/s)	1304 (1066; 1611)	1133 (1084; 1645)	<i>P</i> = 0.85
LV-dP/dt _{min} (mmHg/s)	-1638 (-1864; -1568)	-1763 (-1871; -1732)	<i>P</i> = 0.12
CI (L/min per m ²)	3.8 ± 0.1	3.7 ± 0.2	<i>P</i> = 0.85
τ (ms)	31.4 ± 1.1	31.9 ± 1.2	<i>P</i> = 0.76
RV-EDV _i (ml/m ²)	132 ± 5	132 ± 5	<i>P</i> = 0.97
RV-EF (%)	32 ± 2	34 ± 2	<i>P</i> = 0.44
MAP (mmHg)	79 ± 4	88 ± 3	<i>P</i> = 0.092
CVP _{mean} (mmHg)	7.3 ± 0.7	6.7 ± 0.7	<i>P</i> = 0.51
PAP _{mean} (mmHg)	17.8 ± 0.9	17.2 ± 0.8	<i>P</i> = 0.61
Arterial blood gases			
pH	7.50 ± 0.01	7.50 ± 0.01	<i>P</i> = 0.94
pCO ₂ (kPa)	5.42 ± 0.08	5.28 ± 0.08	<i>P</i> = 0.23
HCO ₃ ⁻ (mmol/l)	31.1 ± 0.5	30.1 ± 0.3	<i>P</i> = 0.10
BE (mmol/l)	7.3 ± 0.5	6.4 ± 0.3	<i>P</i> = 0.15
pO ₂ (kPa)	27.0 ± 0.3	27.4 ± 0.3	<i>P</i> = 0.41
Hb (g/dl)	7.7 ± 0.2	8.2 ± 0.5	<i>P</i> = 0.41
s-Na ⁺ (mmol/l)	140 ± 1	141 ± 1	<i>P</i> = 0.22
s-K ⁺ (mmol/l)	3.5 ± 0.1	3.6 ± 0.1	<i>P</i> = 0.74
s-Cl ⁻ (mmol/l)	102 (102; 103)	103 (101; 103)	<i>P</i> = 0.76

Values are mean ± SEM or median (25-percentile; 75-percentile), *n* = 10.

LV and RV: left and right ventricle; HR: heart rate; SP_{max} and EDP: peak systolic and end-diastolic pressure; dP/dt_{max} and dP/dt_{min}: peak positive and peak negative of the first derivative of left ventricular pressure; CI: cardiac index; EF: ejection fraction; EDV_i: end-diastolic volume indexed for body surface area; MAP: mean arterial pressure; CVP_{mean}: mean central venous pressure; PAP_{mean}: mean pulmonary artery pressure; *P*: *P*-values from two-sample *t*-tests or Mann-Whitney Rank Sum Tests.

Table 2: Cardiac and haemodynamic variables 60, 120 and 180 min after aortic declamping following 60 min of polarizing (STH-POL) or depolarizing (STH-2) cardioplegic arrest

Variable	60 min	120 min	180 min	RM-ANOVA statistics
RV-EDV _i (ml/m ²)				
STH-POL	116 ± 5	110 ± 4	105 ± 7	<i>P</i> _w = 0.24, <i>P</i> _g = 0.082, <i>P</i> _i = 0.83
STH-2*	128 ± 5	123 ± 7	121 ± 11	
RV-SV _i (ml/m ²)				
STH-POL	37 ± 2	32 ± 2	34 ± 1	<i>P</i> _w < 0.001, <i>P</i> _g = 0.46, <i>P</i> _i = 0.10
STH-2*	41 ± 2	35 ± 2	32 ± 2	
RV-EF (%)				
STH-POL	32 ± 2	29 ± 2	34 ± 2	<i>P</i> _w = 0.12, <i>P</i> _g = 0.32, <i>P</i> _i = 0.085
STH-2*	33 ± 2	29 ± 2	27 ± 2	
MAP (mmHg)				
STH-POL	67 ± 5	69 ± 8	63 ± 5	<i>P</i> _w = 0.49, <i>P</i> _g = 0.34, <i>P</i> _i = 0.42
STH-2	76 ± 3	69 ± 3	71 ± 4	
CVP _{mean} (mmHg)				
STH-POL	9.1 ± 0.6	9.8 ± 0.9	10.0 ± 0.8	<i>P</i> _w = 0.030, <i>P</i> _g = 0.52, <i>P</i> _i = 0.56
STH-2	8.4 ± 0.8	8.6 ± 1.1	9.7 ± 1.0	
PAP _{mean} (mmHg)				
STH-POL	25 ± 2	26 ± 2	25 ± 2	<i>P</i> _w = 0.25, <i>P</i> _g = 0.50, <i>P</i> _i = 0.74
STH-2	23 ± 2	25 ± 2	24 ± 2	

Values are mean ± SEM for 10 animals in each group (**n* = 9).

RV: right ventricle; _i: value indexed for body surface area; EDV: end-diastolic volume; SV: stroke volume; EF: ejection fraction; MAP: mean arterial pressure; CVP_{mean}: mean central venous pressure; PAP_{mean}: mean pulmonary artery pressure. *P*_w, *P*_g and *P*_i: *P*-values for within subjects, between groups and interaction from two-way RM-ANOVA, respectively.

potassium-based oxygenated blood cardioplegia improves left ventricular contractility after weaning from CPB [13, 14]. Both adenosine (*T*_{1/2}~30s) and esmolol (*T*_{1/2}~9min) have short half-lives and the elimination does not depend on hepatic or kidney

function [15]. These two arresting agents act synergistically, resulting in the desired effect at relatively low but effective concentrations, while minimizing potential adverse effects. Magnesium, included in comparable concentrations both in the STH-POL and

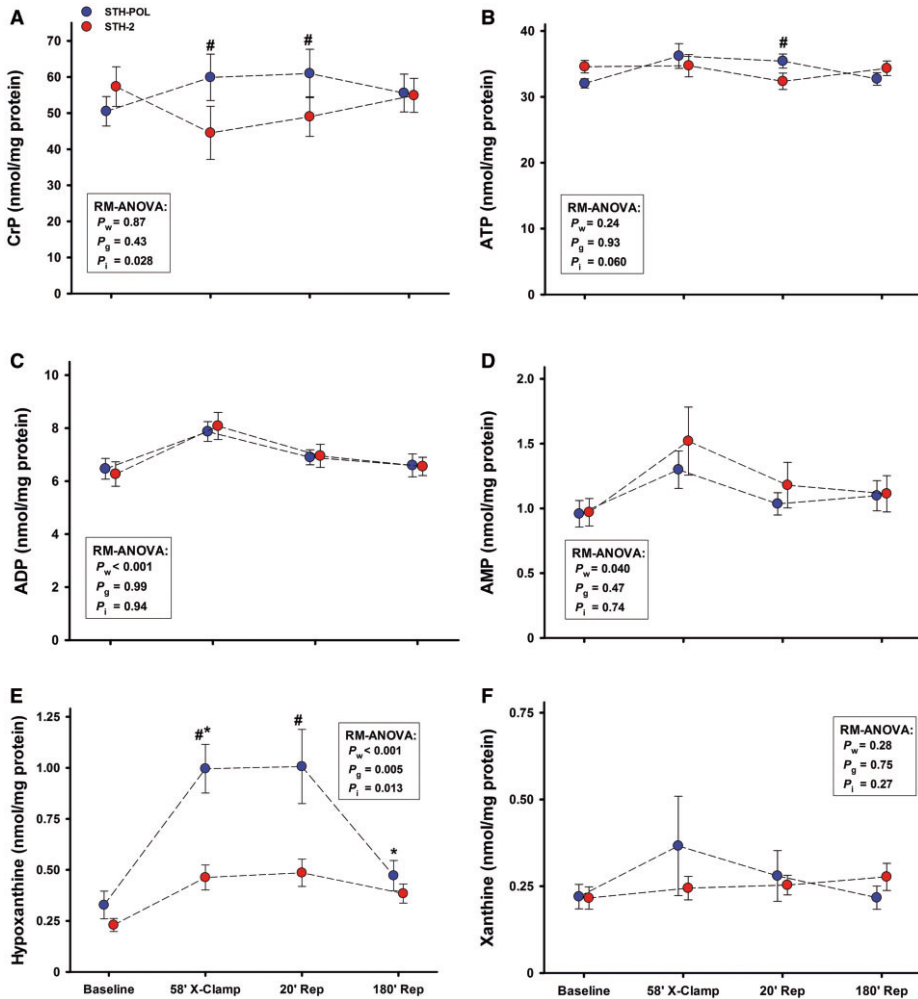


Figure 2: Myocardial tissue levels of creatine phosphate, high energy phosphates and degradation products at Baseline, after 58 min of cardiac arrest with polarizing (STH-POL) and depolarizing (STH-2) cardioplegia, and 20 and 180 min after aortic declamping and reperfusion, $n = 10$ in both groups. CrP: creatine phosphate; ATP, ADP and AMP: adenosine tri-, di- and monophosphate. P_w , P_g and P_i : P -values for within subjects, between groups and interaction from two-way RM-ANOVA, respectively; *: significantly different from the previous value in the STH-POL group; #: significantly different compared to STH-2 at the corresponding time after declamping with *post hoc* multiple contrast tests.

the STH-2 cardioplegia used in the present study suppresses intracellular Ca^{2+} overload during cardioplegia [16].

Mitochondrial creatine kinase present in the mitochondrial intermembrane space regenerates CrP from creatine imported from the cytosol and mitochondrial ADP. In the cytosol CrP serves as an energy reservoir for the rapid buffering and regeneration of ATP *in situ*, as well as for intracellular energy transport by the phosphocreatine shuttle or circuit [17, 18]. Our finding indicates a decrease in consumption of CrP during the 60 min of cardioplegic arrest and early reperfusion in the STH-POL group

(Fig. 2A). When reperfusion and contraction is re-established, the differences between groups fade with time.

Since contraction is ceased during cardioplegic arrest in both groups, the difference in CrP consumption is probably related to reduced energy consumption with polarizing cardioplegia for maintaining intracellular ion balance. For STH-2 cardioplegia intracellular Na^+ and Ca^{2+} overload occurs as a result of extracellular hyperkalaemia. The energy dependent ion channel pumps in the cellular membrane, Na^+/K^+ -ATPase, Ca^{2+} channels and the sarcoplasmic Ca^{2+} channel are active in correcting the imbalance

Table 3: Energy status in myocardial tissue at Baseline, after 58 min of cardioplegic arrest with STH-POL or STH-2 cardioplegia; and 20 and 180 min after declamping and weaning from CPB

	Baseline	58 min Cross-clamp	20 min reperfusion	180 min reperfusion	RM-ANOVA
Energy charge					
STH-POL	0.89 ± 0.01	0.88 ± 0.01	0.90 ± 0.01	0.89 ± 0.01	$P_w = 0.025, P_g = 0.75, P_i = 0.32$
STH-2	0.90 ± 0.01	0.87 ± 0.01	0.88 ± 0.01	0.90 ± 0.01	
ATP/ADP					
STH-POL	5.10 ± 0.29	4.66 ± 0.25	5.25 ± 0.32	5.11 ± 0.30	$P_w = 0.009, P_g = 0.84, P_i = 0.17$
STH-2	5.73 ± 0.35	4.48 ± 0.37	4.82 ± 0.34	5.35 ± 0.27	
CrP/ATP					
STH-POL	1.57 ± 0.11	1.68 ± 0.16	1.69 ± 0.16	1.70 ± 0.15	$P_w = 0.28, P_g = 0.36, P_i = 0.16$
STH-2	1.65 ± 0.15	1.26 ± 0.20	1.48 ± 0.13	1.60 ± 0.12	

Mean ± SEM, $n = 10$.

Energy charge (EC) calculated as: $EC = (ATP + 0.5 ADP)/(AMP + ADP + ATP)$.

ATP and ADP: adenosine tri- and diphosphate; CrP: creatine phosphate. P_w, P_g and P_i : P -values for within subjects, between groups and interaction from two-way RM-ANOVA, respectively.

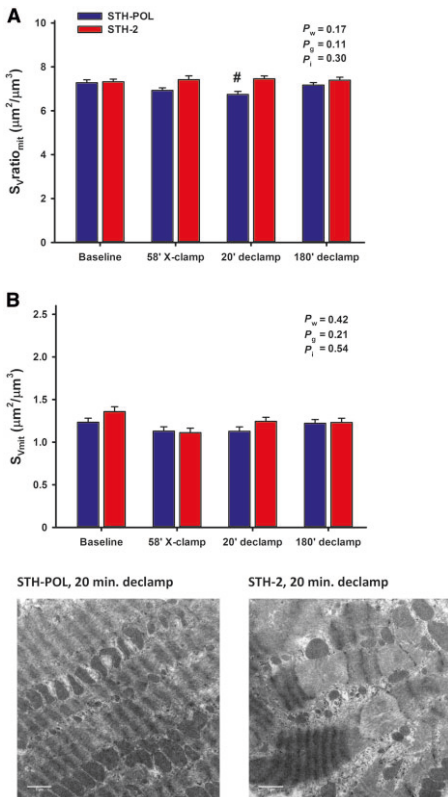


Figure 3: Myocyte mitochondrial surface to volume ratio ($S_{v\text{ratio}_{mit}}$) (A) and surface density (S_{vmit}) (B) in 10 animals in the STH-POL group and 9 animals in the STH-2 group. Bars are mean ± SEM. P_w, P_g and P_i : P -values for within subjects, between groups and interaction from two-way nested ANOVA, respectively; #: significantly different from STH-2 at 20 min after declamping. One micrograph from each group with morphometric readings close to mean values at 20 min after declamping.

in cytosolic ion composition. Since the Na^+ and Ca^{2+} overload is not prominent with polarizing cardiac arrest, these ion pumps are less active during the phase of cardioplegic arrest. As a consequence the requirement for CrP to rephosphorylate ADP to maintain ATP levels is less pronounced (Fig. 2A). In addition, CrP also stabilizes the membrane phospholipid bilayer by binding to the polar heads and decreasing membrane fluidity. Stabilizing the membrane attenuates some of the damage caused by transient ischaemia and hypoxia and helps to prevent cytoplasmic leakage [1, 4, 17].

The consumption of ATP resulted in an increase in both tissue ADP and AMP after 58 min of cardioplegic arrest in both groups. The degradation product hypoxanthine is increased both during arrest and at 20 min after declamping and reperfusion in the STH-POL compared to the STH-2 group. The surplus myocardial hypoxanthine in the STH-POL group is washed out with time during reperfusion and not oxidized to xanthine due to minimal levels of xanthine oxidase in the pig heart [19].

The decrease in surface-to-volume ratio of mitochondria at 20 min after reperfusion and declamping with STH-POL cardioplegia, indicates a temporary mitochondrial swelling (Fig. 3A). Mitochondrial swelling can be observed as early as 10 min after regional myocardial ischaemia [20]. Judged from the tissue levels of HEP, there were no signs of a more severe ischaemia in the STH-POL group than the STH-2 group. We speculate that this could be a result of transient differences in intracellular ionic composition and osmolality. Cytoplasmic volume fractions of cellular components did not differ (Table 4).

Transient differences were observed for energy metabolism and morphology at the end of the ischaemic period and at 20 min after declamping and reperfusion. Cardiac index was increased in the STH-POL compared to the STH-2 group from 150 min of reperfusion and onwards (Fig. 1B). This improved function could be interpreted as a reduction of the ischaemia/reperfusion injury, reduced myocardial stunning or alleviated adrenergic desensitization with STH-POL compared to STH-2 cardioplegia. In the present study myocardial injury was not evaluated. However, with a similar protocol in a recent study showed that STH-POL cardioplegia did not affect the release of troponin-T or myocardial caspase-3 activity as a sign of apoptosis [5]. Whether the transient differences in energy metabolism indicate a reduction of reversible myocardial

Table 4: Myocyte volume fraction (%) of mitochondria, myofibrils and cytosol with STH-POL ($n = 10$) or STH-2 ($n = 9$) cardioplegia before, after 58 min of cardioplegic arrest, and 20 and 180 min after declamping and weaning from CPB

	Baseline	58 min Cross-clamp	20 min Reperfusion	180 min Reperfusion	Nested RM-ANOVA
V_{mit} (%)					
STH-POL	20.86 ± 0.87	20.59 ± 1.02	21.25 ± 0.96	20.43 ± 0.80	$P_w = 0.94, P_g = 0.49, P_i = 0.68$
STH-2	21.30 ± 0.96	18.80 ± 0.99	20.51 ± 0.95	20.58 ± 0.94	
V_{myof} (%)					
STH-POL	62.21 ± 1.14	59.98 ± 1.29	59.45 ± 1.36	61.10 ± 1.36	$P_w = 0.47, P_g = 0.72, P_i = 0.75$
STH-2	61.53 ± 1.28	60.27 ± 1.45	61.56 ± 1.13	60.85 ± 1.13	
V_{cyt} (%)					
STH-POL	16.86 ± 0.93	19.53 ± 1.00	19.02 ± 1.09	18.45 ± 0.84	$P_w = 0.37, P_g = 0.84, P_i = 0.80$
STH-2	17.08 ± 0.80	20.91 ± 1.21	18.09 ± 0.89	18.57 ± 0.91	

Mean ± SEM, 6 randomly selected micrographs from each sample.

V_{mit} , V_{myof} , V_{cyt} : volume fraction of mitochondria, myofibrils and cytosol; P_w , P_g and P_i : P -values for within subjects, between groups and interaction from two-way nested RM-ANOVA, respectively.

Table 5: Intraclass correlation coefficient (ICC) and coefficient of variation (CV%) for inter- and intra-observer variability for morphometry data obtained from 6 electron microscopy pictures from each of 15 randomly selected biopsies

Variable	Inter-observer		Intra-observer	
	ICC	CV (%)	ICC	CV (%)
V_{mit}	0.897	6.04	0.852	5.53
V_{myof}	0.741	2.48	0.719	3.33
V_{sarc}	0.780	8.14	0.566	13.23
$S_v\text{ratio}_{\text{Mit}}$	0.790	4.05	0.853	2.70
S_{VMi}	0.871	5.31	0.816	5.73

V_{mit} : volume fraction; mit : mitochondria; myof : myofibrils; sarc : sarcoplasm; $S_v\text{ratio}_{\text{Mit}}$: mitochondrial surface to volume ratio; S_{VMi} : mitochondrial surface density.

injury appearing as increased cardiac index after 150 min, cannot be answered by this study.

Limitations

The study is performed in young pigs with healthy hearts. Both the ischaemic time of 60 min and the 180 min of observation after declamping and weaning from CPB are relatively short. With regard to the development of myocardial stunning, the observation after weaning may have been extended. On the other hand, the stability of the experimental protocol is also of importance. The results in the present study could be directly compared with a recent and similar study focusing on left ventricular function [5]. The serial tissue biopsies obtained demanded an infrequent need for a haemostatic myocardial suture. For this reason, troponin-T was not evaluated in this study.

CONCLUSION AND IMPLICATIONS

These results demonstrate an improved energy status with polarizing oxygenated blood cardioplegia with esmolol/adenosine/

magnesium (STH-POL) compared to the standard potassium-based depolarizing blood cardioplegia (STH-2) during 60 min of cardioplegic arrest and at early reperfusion. Myocardial function was improved from 150 min after reperfusion and onwards. Comparable results should be obtained in clinical trials before implementation into a new clinical routine.

SUPPLEMENTARY MATERIAL

Supplementary material is available at *EJCTS* online.

ACKNOWLEDGEMENTS

We acknowledge the technical assistance from Lill-Harriet Andreassen, Cato Johnsen, Kjersti Milde, Gry-Hilde Nilsen, Anne Aarsand and the staff at the Vivarium, University of Bergen.

Funding

Financial support was received from the Western Norway Regional Health Authority, the Bergen University Heart Fund, Norwegian Health Association and the Grieg Foundation.

Conflict of interest: none declared.

REFERENCES

- [1] Fallouh HB, Kentish JC, Chambers DJ. Targeting for cardioplegia: arresting agents and their safety. *Curr Opin Pharmacol* 2009;9:220–6.
- [2] Chambers DJ, Fallouh HB. Cardioplegia and cardiac surgery: pharmacological arrest and cardioprotection during global ischemia and reperfusion. *Pharmacol Ther* 2010;127:41–52.
- [3] Snabaitis AK, Shattock MJ, Chambers DJ. Comparison of polarized and depolarized arrest in the isolated rat heart for long-term preservation. *Circulation* 1997;96:3148–56.
- [4] Sternbergh WC, Brunsting LA, Abd-Elfattah AS, Wechsler AS. Basal metabolic energy requirements of polarized and depolarized arrest in rat heart. *Am J Physiol* 1989;256:H846–51.
- [5] Aass T, Stangeland L, Moen CA, Salminen PR, Dahle GO, Chambers DJ *et al.* Myocardial function after polarizing versus depolarizing cardiac

- arrest with blood cardioplegia in a porcine model of cardiopulmonary bypass. *Eur J Cardiothorac Surg* 2016;50:130-9.
- [6] Fannelop T, Dahle GO, Matre K, Segadal L, Grong K. An anaesthetic protocol in the young domestic pig allowing neuromuscular blockade for studies of cardiac function following cardioplegic arrest and cardiopulmonary bypass. *Acta Anaesthesiol Scand* 2004;48:1144-54.
- [7] Stadlbauer V, Stiegler P, Taeubl P, Sereinigg M, Puntchart A, Bradatsch A et al. Energy status of pig donor organs after ischemia is independent of donor type. *J Surg Res* 2013;180:356-67.
- [8] <https://image.nih.gov/ij/> (2 January 2017, date last accessed).
- [9] Cicchetti DV. Guidelines, criteria, and rules of thumb for evaluating normed and standardized assessment instruments in psychology. *Psychol Assessment* 1994;6:284-90.
- [10] Belardinelli L, Giles WR, West A. Ionic mechanisms of adenosine actions in pacemaker cells from rabbit heart. *J Physiol* 1988;405:615-33.
- [11] Fallouh HB, Bardswell SC, McLatchie LM, Shattock MJ, Chambers DJ, Kentish JC. Esmolol cardioplegia: the cellular mechanism of diastolic arrest. *Cardiovasc Res* 2010;87:552-60.
- [12] Turlapaty P, Laddu A, Murthy VS, Singh B, Lee R. Esmolol: a titratable short-acting intravenous beta blocker for acute critical care settings. *Am Heart J* 1987;114:866-85.
- [13] Dahle GO, Salminen PR, Moen CA, Eliassen F, Jonassen AK, Haaverstad R et al. Esmolol added in repeated, cold, oxygenated blood cardioplegia improves myocardial function after cardiopulmonary bypass. *J Cardiothorac Vasc Anesth* 2015;29:684-93.
- [14] Fannelop T, Dahle GO, Matre K, Moen CA, Mongstad A, Eliassen F et al. Esmolol before 80 min of cardiac arrest with oxygenated cold blood cardioplegia alleviates systolic dysfunction. An experimental study in pigs. *Eur J Cardiothorac Surg* 2008;33:9-17.
- [15] Sum CY, Yacobi A, Kartzinel R, Stampfli H, Davis CS, Lai CM. Kinetics of esmolol, an ultra-short-acting beta blocker, and of its major metabolite. *Clin Pharmacol Ther* 1983;34:427-34.
- [16] Ichiba T, Matsuda N, Takemoto N, Ishiguro S, Kuroda H, Mori T. Regulation of intracellular calcium concentrations by calcium and magnesium in cardioplegic solutions protects rat neonatal myocytes from simulated ischemia. *J Mol Cell Cardiol* 1998;30:1105-14.
- [17] Wallimann T, Wyss M, Brdiczka D, Nicolay K, Eppenberger HM. Intracellular compartmentation, structure and function of creatine kinase isoenzymes in tissues with high and fluctuating energy demands: the 'phosphocreatine circuit' for cellular energy homeostasis. *Biochem J* 1992;281:21-40.
- [18] Guimaraes-Ferreira L. Role of the phosphocreatine system on energetic homeostasis in skeletal and cardiac muscles. *Einstein (Sao Paulo)* 2014;12:126-31.
- [19] Muxfeldt M, Schaper W. The activity of xanthine oxidase in heart of pigs, guinea pigs, rabbits, rats, and humans. *Basic Res Cardiol* 1987; 82:486-92.
- [20] Greve G, Rotevatn S, Svendby K, Grong K. Early morphologic changes in cat heart muscle cells after acute coronary artery occlusion. *Am J Pathol* 1990;136:273-83.

Online Table A.

Final molar concentrations in oxygenated blood cardioplegia.

	STH-POL		STH-2	
	High-dose 3 min	Low-dose 2 min	High-dose 3 min	Low-dose 2 min
Esmolol (mM)	1.35	0.68	-	-
Adenosine (mM)	0.50	0.25	-	-
Mg ²⁺ (mM)	20	10	16	9
K ⁺ (mM)	4.3	4.3	22	14
Cl ⁻ (mM)	106	106	134	120
Procaine-HCl (mM)	0.8	0.4	0.8	0.4

STH-POL = St.Thomas' Hospital polarizing cardioplegic solution.

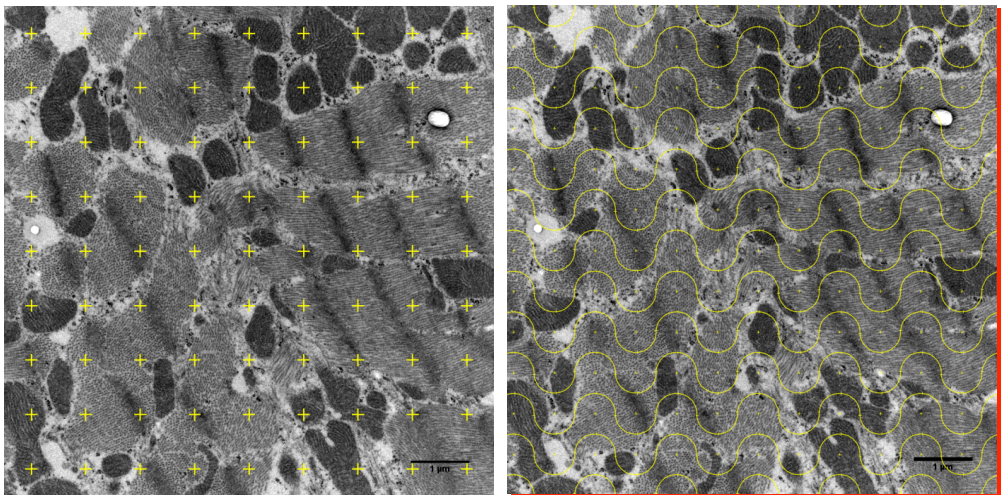
STH-2 = St.Thomas' Hospital cardioplegic solution No 2.

Analysis of myocardial metabolism

Frozen tissue samples averaging 65 mg, were homogenized with a micro-dismembrator and deproteinized with 500µL of 0.4 mol/L perchloric acid. After centrifugation (12000g) 200 µL of the acid extract was neutralized with 20-25 µL of 2 mol/L potassium carbonate (4°C). The supernatant (20µL injection volume) obtained after centrifugation was used for high-performance liquid chromatography (HPLC) analysis. The pellets of the acid extract were dissolved in 1 mL of 0.1 mol/L sodium hydroxide and further diluted 1:10 with physiologic saline for protein determination (BCA Protein Assay, Pierce). High energy phosphates (ATP, ADP, AMP and creatine phosphate), hypoxanthine and xanthine were measured by HPLC. Separation was performed on a Hypersil ODS column (5µm, 250 mm x 4 mm I.D.) using a L-2200 autosampler, two L-2130 HTA pumps and a L-2450 diode array detector (all: VWR Hitachi, Radnor, PA). Detector signals (absorbance at 214 nm and 254 nm) were recorded and the program EZchrom Elite (VWR Hitachi) was used for data acquisition and analysis.

Analysis of ultrastructure

Myocardial biopsies were fixed overnight in 0.1 mol/L Na-cacodylate buffer with 2.5% glutaraldehyde, washed, post-fixated with 1% OsO₄, dehydrated and stored in 70% ethanol, sectioned and stained with uranyl acetate. Sections were visualized by transmission electron microscope (JEM-1230, Jeol, Tokyo, Japan) and images acquired using a 1 MP gatan camera. The scanning electron microscopy images were acquired with microscope (JSM-7400F, Jeol). Myocardial volume fraction of mitochondria, myofibrils and cytosol were quantified by point counting with a grid (9 x 9 points, random offset) in 6 randomly selected micrographs (x 15.000) from each biopsy, mitochondrial surface to volume ratio and surface density were calculated by counting mitochondrial points and membrane crossings using a Merz grid (random offset, random phase) and the freeware ImageJ.



The results are based on a total of 456 micrographs and 36936 points (crosses for illustration) counted to calculate of volume fractions (left). For mitochondrial surface-to-volume ratio and surface density calculations, a total of 34629 points within the mitochondria and 44310 line crossings of the mitochondrial outer membrane were counted (right). For the Merz grid mitochondria crossing beyond the lower horizontal and the right vertical edges (red) of the micrographs were not included.

Statistical analysis

At Baseline groups were compared by two-sample Student t-test on data with normal distribution and with Wilcoxon-Mann-Whitney test on ranks if the Kolmogorov-Smirnov test or the Levene equal variance tests were significant. Variables describing tissue contents of HEPs, degradation products and haemodynamic variables after aortic declamping were compared with two-way ANOVA for repeated measurements (RM-ANOVA) with time as within factor (P_w) and cardioplegia with STH-POL or STH-2 as grouping factor (P_g) and post hoc Bonferroni contrasts. If Mauchly's test of sphericity was significant ($P < 0.05$), the Greenhouse-Geisser adjustment of degrees of freedom was used for the evaluation of main effects. If a significant interaction ($P_i < 0.10$) was found, new ANOVA's for simple main effect were performed with adjustment of degrees of freedom. Cell means were finally compared with Neumann-Keuls multiple contrast tests when justified by the preceding ANOVA. The morphological variables were analysed with a nested RM-ANOVA with 6 micrographs from each biopsy and 4 different biopsies (time) from each animal. $P < 0.05$ was considered statistically significant. The Intraclass correlation coefficient (ICC) and Coefficient of variation (CV%) for inter- and intra-observer variability was calculated for morphometric data.

Online Table B.

Mean arterial pressure, temperature, haemoglobin, arterial blood gases and electrolytes during cardiopulmonary bypass in two groups of pigs with 60 min of polarizing (STH-POL) or depolarizing (STH-2) cardioplegic arrest. Values are mean \pm SEM, n = 10.

Variable	1 min before X-clamp (A)	30 min X-clamp (B)	58 min X-clamp (C)	RM-ANOVA statistics
MAP (mmHg)				
STH-POL	55 \pm 6	45 \pm 5	41 \pm 4	$P_w = 0.39, P_g = 0.64, P_i = 0.14$
STH-2	48 \pm 6	47 \pm 3	52 \pm 3	
Temp_{rect} ($^{\circ}$C)				
STH-POL	38.2 \pm 0.2	34.5 \pm 0.2	37.4 \pm 0.3	$P_w < 0.001, P_g = 0.68, P_i = 0.62$
STH-2	38.5 \pm 0.2	34.4 \pm 0.1	37.4 \pm 0.2	
Arterial blood gases (n = 9 + 9)				
Hb (g/dL)				
STH-POL	6.0 \pm 0.3		7.1 \pm 0.4	$P_w < 0.001, P_g = 0.29, P_i = 0.32$
STH-2	6.1 \pm 0.3		7.9 \pm 0.4	
pH				
STH-POL	7.45 \pm 0.01		7.41 \pm 0.01	$P_w = 0.024, P_g = 0.23, P_i = 0.19$
STH-2	7.42 \pm 0.01		7.41 \pm 0.01	
pO₂ (kPa)				
STH-POL	16.5 \pm 2.0		18.0 \pm 2.0	$P_w = 0.19, P_g = 0.29, P_i = 0.49$
STH-2	13.2 \pm 1.6		18.0 \pm 1.9	
pCO₂ (kPa)				
STH-POL	5.6 \pm 0.1		6.5 \pm 0.2	$P_w = 0.003, P_g = 0.76, P_i = 0.06$
STH-2	6.0 \pm 0.3		6.2 \pm 0.2	
HCO₃⁻ (mmol/L)				
STH-POL	28.6 \pm 0.7		30.1 \pm 0.5	$P_w = 0.037, P_g = 0.43, P_i = 0.21$
STH-2	28.5 \pm 0.6		28.9 \pm 0.7	
s-K⁺ (mmol/L)				
STH-POL	4.0 \pm 0.1		4.1 \pm 0.1	$P_w = 0.005, P_g = 0.010, P_i = 0.013$
STH-2	4.2 \pm 0.2		5.2 \pm 0.3 ^{a#}	
s-Na⁺ (mmol/L)				
STH-POL	139 \pm 1		139 \pm 1	$P_w = 0.80, P_g = 0.85, P_i = 0.94$
STH-2	139 \pm 1		139 \pm 1	

MAP = mean aortic pressure; Temp_{rect} = rectal temperature; s = serum levels; P_w, P_g, P_i = p-values for within subjects, between groups and for interaction from two-way RM-ANOVA, respectively; ^a = significant different within the same group mean from value in columns with corresponding capital letter; # = significantly different from STH-POL at 58 min of X-clamp.

PAPER III

with Supplemental Material

Left ventricular dysfunction after two hours of polarizing or depolarizing cardioplegic arrest in a porcine model

Perfusion

2019, Vol. 34(1) 67–75

© The Author(s) 2018




Article reuse guidelines:

sagepub.com/journals-permissions

DOI: 10.1177/0267659118791357

journals.sagepub.com/home/prf



Terje Aass,^{1,2}  Lodve Stangeland,² Christian Arvei Moen,¹ Atle Solholm,¹ Geir Olav Dahle,² David J. Chambers,³ Malte Urban,¹ Knut Nesheim,¹ Rune Haaverstad,^{1,2} Knut Matre² and Ketil Grong²

Abstract

Introduction: This experimental study compares myocardial function after prolonged arrest by St. Thomas' Hospital polarizing cardioplegic solution (esmolol, adenosine, Mg²⁺) with depolarizing (hyperkalaemic) St. Thomas' Hospital No 2, both administered as cold oxygenated blood cardioplegia.

Methods: Twenty anaesthetized pigs on tepid (34°C) cardiopulmonary bypass (CPB) were randomised to cardioplegic arrest for 120 min with antegrade, repeated, cold, oxygenated, polarizing (STH-POL) or depolarizing (STH-2) blood cardioplegia every 20 min. Cardiac function was evaluated at Baseline and 60, 150 and 240 min after weaning from CPB, using a pressure-conductance catheter and epicardial echocardiography. Regional tissue blood flow, cleaved caspase-3 activity and levels of malondialdehyde were evaluated in myocardial tissue samples.

Results: Preload recruitable stroke work (PRSW) was increased after polarizing compared to depolarizing cardioplegia 150 min after declamping (73.0±3.2 vs. 64.3±2.4 mmHg, p=0.047). Myocardial tissue blood flow rate was high in both groups compared to the Baseline levels and decreased significantly in the STH-POL group only, from 60 min to 150 min after declamping (p<0.005). Blood flow was significantly reduced in the STH-POL compared to the STH-2 group 240 min after declamping (p<0.05). Left ventricular mechanical efficiency, the ratio between total pressure-volume area and blood flow rate, gradually decreased after STH-2 cardioplegia and was significantly reduced compared to STH-POL cardioplegia after 150 and 240 min (p<0.05 for both).

Conclusion: Myocardial protection for two hours of polarizing cardioplegic arrest with STH-POL in oxygenated blood is non-inferior compared to STH-2 blood cardioplegia. STH-POL cardioplegia alleviates the mismatch between myocardial function and perfusion after weaning from CPB

Keywords

adenosine; esmolol; potassium; cardioplegic arrest; cardiac function; ventricular dysfunction

Introduction

Depolarized cardioplegic arrest with repeated administration of hyperkalaemic solutions has been used for decades in cardiothoracic surgery.¹ Hyperkalaemic crystalloid solutions with intracellular (low sodium) or extracellular (high sodium) composition administered once are also established routines in clinical practice.^{2,3} The most widely used cardioplegia worldwide is hyperkalaemic solutions given intermittently as cold crystalloid or oxygenated blood cardioplegia.^{4,5} Various normokalaemic, substrate-enriched cardioplegic solutions have been evaluated after continuous, intermittent or single-dose

¹Section of Cardiothoracic Surgery, Department of Heart Disease, Haukeland University Hospital, Bergen, Norway

²Department of Clinical Science, Faculty of Medicine, University of Bergen, Bergen, Norway

³Cardiac Surgical Research, The Rayne Institute (King's College London), Guy's and St Thomas' NHS Foundation Trust, St Thomas' Hospital, London, United Kingdom

Corresponding author:

Terje Aass, Section of Cardiothoracic Surgery, Department of Heart Disease, Haukeland University Hospital, P.O. Box 1400, 5021 Bergen, Norway.

Email: terje.aass@uib.no

administration. This alternative concept, polarized arrest, has several potential advantages, proven in both experimental and clinical studies.⁶⁻⁹ Still, the use of polarized cardioplegic arrest is not widely established clinically.

In a porcine study, the normokalaemic St. Thomas' Hospital polarizing cardioplegic solution (STH-POL), formulated with a mixture of the short-acting β -adrenergic blocker esmolol, adenosine and Mg^{2+} , improves myocardial contractility after 60 min of cardioplegic arrest compared to the standard depolarizing St. Thomas' Hospital cardioplegic solution No 2 (STH-2).¹⁰ Esmolol, adenosine and Mg^{2+} each target ion channels in the myocyte cellular membrane, thus, preventing rapid depolarization and triggering of the action potential.¹¹ Furthermore, STH-POL blood cardioplegia improves myocardial energy status compared to STH-2 blood cardioplegia just before and early after aortic declamping following 60 min of cardioplegic arrest.¹² The aim of the present study was to compare STH-POL and STH-2 oxygenated blood cardioplegia in an experimental setting with prolonged (120 min) myocyte membrane polarization or depolarization, with clear differences in total potassium load. In this clinically relevant animal study, left ventricular function was evaluated and compared up to 4 hours after 120 min of cardioplegic arrest. We hypothesize that the experimental STH-POL cardioplegic solution is non-inferior compared to STH-2 with respect to myocardial function in the early hours after aortic declamping.

Methods

The experiments were conducted in accordance with the European Communities Council Directive of 2010 (63/EU) and approved by the Norwegian State Commission for Laboratory Animals (Project 20135835). Twenty-eight anaesthetized young pigs (Norwegian Landrace) of either gender, weighing 42 ± 3 (SD) kg were used. The protocol for premedication and anaesthesia has been evaluated (for details see Supplementary Material).¹³ Prophylactic antibiotic therapy with cefalotin 1.0 g IV followed by 0.5 g during CPB and 1.0 g after weaning was administered. Fluid substitution, Ringer's acetate 15 mL/kg/h with 20 mmol/L KCl added, was given throughout the experiment. Additional Ringer's acetate 5 mL/kg/h was administered after weaning from CPB.

Instrumentation and evaluation

The right femoral artery and vein were cannulated for blood sampling and infusion. An early arterial blood gas analysis determined the need for ventilator adjustments. Rectal temperature was monitored and an open suprapubic

cystotomy with insertion of a catheter measured diuresis. After midline sternotomy and pericardiotomy, heparin (125 IU/kg) was given IV to prevent catheter clotting. A continuous cardiac output catheter (CCO/EDV 177HF 75, Edwards Lifesciences Inc., Irvine, CA, USA), advanced from the left internal mammary vein into the pulmonary artery, monitored cardiac output, right ventricular end-diastolic volume (EDV), central venous pressure (CVP) and pulmonary artery pressure (PAP) (Vigilance II® and TruWave® transducers, Edwards Lifescience Inc.). A microtip pressure catheter (Millar MPC-500, Houston, TX, USA) was inserted into the proximal aorta through the left internal mammary artery. The haemodynamic parameters were digitised and later analysed (Ponemah ACQ-7700 and Ponemah Physiology Platform v. 5.2, Data Sciences International, St. Paul, MN, USA). A dual-field pressure-conductance catheter (CA71083-PL, CDLeycom, Hengelo, the Netherlands) connected to a Sigma-M signal conditioner (CDLeycom) was inserted through the apex and into the left ventricle (LV). The distal part was positioned above the aortic valve, verified by epicardial echocardiography (Vivid E9, GE Vingmed Ultrasound, Horten, Norway). An infant feeding tube inserted into the left atrium was used for microsphere injections and a tourniquet placed around the inferior vena cava allowed brief intermittent dynamic preload reductions.

Baseline variables were obtained: arterial blood gases (OPTI CCA-TS2, OPTI Medical Systems, Atlanta, GA), serum troponin-T (Troponin-T hs, Roche Diagnostics GmbH, Mannheim, Germany), haemodynamic variables and the first injection of 15 μ m fluorescent microspheres (Dye-Trak "F"; Triton Technology Inc., San Diego, CA, USA). After a short period of pre-oxygenation and respirator shut-off in the end expirium, LV pressure-volume loops were registered before and during a brief period of inferior vena cava occlusion. During a bolus of 5 mL hypertonic saline (10%) injected into the pulmonary artery, pressure-volume loops were recorded three times for the estimation of parallel conductance.^{14,15} Echocardiographic recordings were obtained for evaluation of strain and strain rate during brief periods of respiratory shut-off. Pulsed-wave Doppler signals in the aortic outflow tract, speckle tracking echocardiography (STE) in the 4-chamber and the short-axis views and tissue Doppler imaging (TDI) of the anterior left ventricular wall in short-axis view were recorded (for details see Supplementary Material).

Experimental protocol

The animals were block-randomised to either the STH-POL or the STH-2 group (10 per group). The heart-lung machine was primed with 1200 mL Ringer's acetate. Systemic heparinization (500 IU/kg) was followed by cannulation of the brachiocephalic artery (EOPA 18 Fr,

Table 1. Final molar concentrations in oxygenated blood cardioplegia.

	STH-POL		STH-2	
	High-dose 3 min	Low-dose 2 min	High-dose 3 min	Low-dose 2 min
Esmolol (mM)	1.35	0.68	–	–
Adenosine (mM)	0.50	0.25	–	–
Mg ²⁺ (mM)	20	10	16	9
K ⁺ (mM)	4.3	4.3	22	14
Cl ⁻ (mM)	106	106	134	120
Procaine-HCl (mM)	0.8	0.4	0.8	0.4

STH-POL: Modified St.Thomas' Hospital polarizing cardioplegic solution; STH-2: Modified St.Thomas' Hospital cardioplegic solution No 2.

Medtronic Inc., Minneapolis, MN, USA) and the right atrial appendage (MC2 28/36 Fr, Medtronic Inc.). Cardiopulmonary bypass (CPB) was established with a flow of 90 mL/min/kg and a water temperature of 32°C in the heat exchanger. After aortic cross-clamping, cardioplegia was induced, either with normokalaemic STH-POL or hyperkalaemic STH-2 cardioplegia. Both solutions were pre-prepared as concentrate, modified with procaine and administered as cold (12°C), oxygenated, blood cardioplegia, freshly mixed by a dual-head pump with separate cooling. The cardioplegia was given into the aortic root, with the flow set to 7% of CPB flow, following a standardised protocol with an initial 'high-dose' for 3 min and 2 min of 'low-dose' at 20, 40, 60, 80 and 100 min after cross-clamping. The final concentrations of key components in the cardioplegic solutions are presented in Table 1. The aortic cross-clamp time was 120 min. A left heart vent catheter (DLP 13, Medtronic Inc.), temporarily replacing the pressure-conductance catheter, was placed through the apex and allowed passive drainage of the heart during the arrest. The body temperature drifted towards 34°C and CPB flow was reduced to 72 mL/min/kg when the rectal temperature reached 35°C or after 20 min. After 100 min of cross-clamping, systemic rewarming was initiated, with CPB flow reset to 90 mL/min/kg and the water temperature at 40°C. Arterial blood gases were obtained before cross-clamping, after 60 min and prior to declamping after 120 min. During CPB, the ventilator volume was reduced to 50%. Additional heparin (250 IU/kg) was given after 60 min of cross-clamping. Defibrillation was the only allowed anti-arrhythmic intervention if ventricular fibrillation occurred at declamping. After 10 min of reperfusion, the animals were weaned from CPB and the residual blood in the circuit infused followed by decannulation. Protamine sulphate 2 mg/kg was given for heparin reversal.

After weaning from CPB, general haemodynamics were continuously recorded for 240 min. As for Baseline, measurements of LV pressures, volumes, systolic and diastolic function, regional tissue blood flow and echocardiographic recordings were repeated at 60, 150 and

240 min after reperfusion. Finally, the animal was euthanized with an intracardiac injection of high-dose potassium chloride, the heart was explanted and samples were obtained for regional tissue blood flow measurements, tissue water content, caspase-3 activity and levels of malondialdehyde (MDA).

Global and regional left ventricular function

Associated data files obtained by the pressure-conductance catheter (1 for evaluation of function, 3 for parallel conductance) were coded and analysed as 80 independent entities with custom-made software. The mean of 5-8 cardiac cycles during the stable situations and load-independent variables obtained during dynamic preload reductions were calculated. Absolute volumes were estimated by correcting for parallel conductance and cardiac output. Volumes were indexed by body surface area calculated as BSA (m²) = (BW^{2/3} x k)/100, where BW is body weight in kg and k for pigs is 9 m²/kg^{-2/3}.¹⁶ The LV mechanical efficiency (Joules/mL/g) was calculated as a ratio between the total pressure-volume area (PVA) and the blood flow rate by the formula; Mechanical efficiency = (PE+SW) x HR/BFR, where PE and SW are pressure-volume areas for the LV potential energy and stroke work in Joules, HR is heart rate and BFR is LV blood flow rate per gramme of tissue.

Regional myocardial strain and strain rate were recorded with STE and TDI. Peak systolic strain in the circumferential, radial and longitudinal direction and radial peak ejection strain rate were measured with appropriate software (EchoPAC BT12, GE Vingmed Ultrasound).

Myocardial tissue samples and analyses

Multiple tissue samples were obtained from the LV endo-, mid- and epicardium and the right ventricle (RV). Myocardium, snap-frozen and stored in liquid nitrogen, was analysed for apoptosis by caspase-3

activity (K105-400, BioVision Inc., Milpitas, CA, USA) and for oxidative stress by MDA (K739-100, BioVision Inc.). Samples were homogenised, lysed and analysed according to the manufacturer's instructions. Samples from the left and right ventricles and reference blood were weighed, hydrolysed, microspheres isolated, colours dissolved and quantified by fluorospectrophotometry. Blood flow rate was calculated as earlier described.¹⁷ Tissue water content was calculated as a fraction of the wet weight after drying samples for three weeks at 60°C.

Statistical analysis

Data analyses were performed by SPSS v. 23 (IBM Corp., Armonk, NY) and the values given as mean±SEM or median (25% percentile; 75% percentile) unless otherwise noted. Groups were compared at Baseline by two-sample Student t-test and Wilcoxon-Mann-Whitney test on ranks, whenever appropriate. Haemodynamic variables during and after CPB were compared with two-way analysis of variance for repeated measures (RM-ANOVA). For details see Supplementary Material.

Results

Characteristics at Baseline and during CPB

Eight animals were excluded due to reasons other than technical failure during surgery or instrumentation. Of these, seven animals, two in the STH-POL and five in the STH-2 group, developed severe pulmonary hypertension and right heart failure soon after declamping and weaning from CPB. The concomitant reduction of LV filling and systemic hypotension ended in myocardial ischemia and LV failure. One animal in the STH-POL group developed severe tachyarrhythmia at reperfusion, making further evaluation futile. Excluded animals were replaced by the subsequent experiment and results are given for 10 animals in each group.

At Baseline, the STH-POL and STH-2 groups were similar regarding variables describing general haemodynamics, left ventricular and myocardial function, tissue blood flow rate, temperature, blood gases and serum troponin-T levels (Supplement Table A, Figures 2-4). Mean arterial pressure (MAP) was significantly lower in the STH-POL at 60, 80 and 100 min of cardioplegic arrest compared to the STH-2 group (Figure 1). Serum potassium did not differ before cross-clamping while gradually increasing over time in both groups, but was more pronounced with STH-2 cardioplegia. At declamping, the serum potassium averaged 4.4 ± 0.1 mmol/L in the STH-POL vs. 5.5 ± 0.2 mmol/L

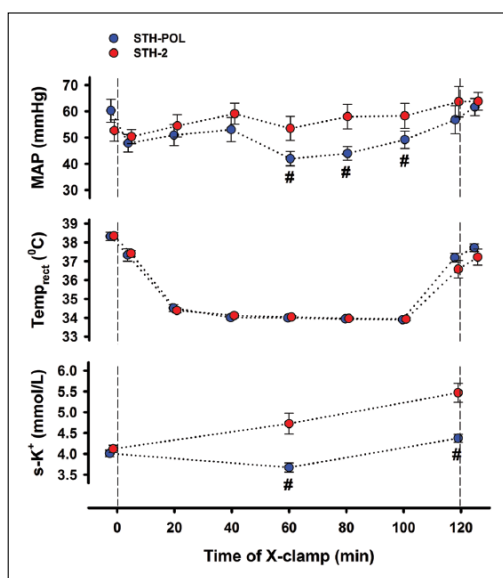


Figure 1. Mean arterial pressure (MAP), temperature and serum potassium (mean±SEM) during 120 min of cardioplegic arrest with polarizing (STH-POL; n=10) and depolarizing (STH-2; n=10) cardioplegia. #: p<0.05 vs. STH-2 at the corresponding point in time.

in the STH-2 group ($p < 0.001$). Arterial blood gases, haemoglobin and other electrolytes did not differ between the groups during cross-clamping (Supplement Table B). Electrical cardioversion of ventricular fibrillation at declamping was needed in 2 out of 10 animals in the STH-POL vs. 8 out of 10 in the STH-2 group ($p=0.025$).

Haemodynamic and cardiac variables after CPB

The heart rate (HR) gradually increased in both groups over time while the left ventricular systolic pressure (LVSP) decreased after weaning from CPB (Figure 2). The left ventricular end-diastolic pressure (LVEDP) was unchanged. The peak positive derivative of LV pressure, dp/dt_{max} , decreased from 90 min and onwards, while peak negative dp/dt_{min} increased. Cardiac index (CI) decreased gradually in the first 90 min after declamping, levelled out around 175 min and then stabilised at levels comparable to the Baseline in both groups. The slope of the LV end-systolic pressure-volume relation ($ESPVR_{slope}$) increased in both groups during reperfusion (Figure 3). At 240 min after declamping, there was a borderline difference between the groups ($p=0.088$). PRSW was significantly increased in the STH-POL compared to the

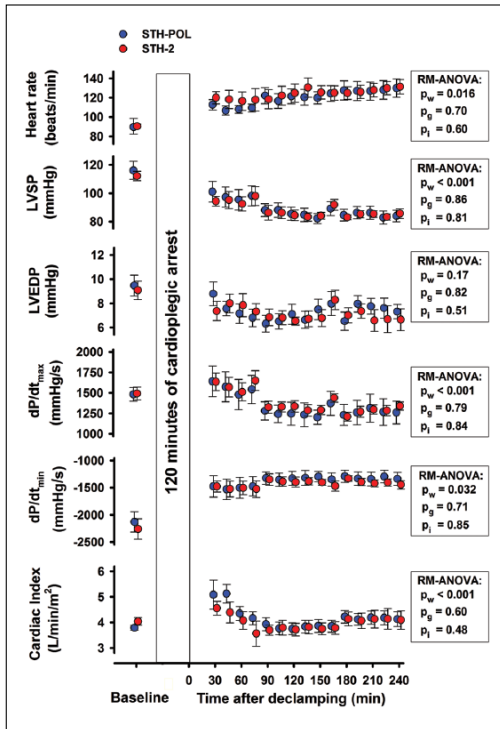


Figure 2. Haemodynamic variables, mean (SEM) or median (25%; 75%), at Baseline and every 15 min of reperfusion after CPB and 120 min of cardiac arrest with polarizing (STH-POL; $n=10$) and depolarizing (STH-2; $n=10$) cardioplegia. LVSP and LVEDP: left ventricular peak systolic- and end-diastolic pressures; dP/dt_{max} and dP/dt_{min} : peak positive and peak negative of the first derivate of the left ventricular pressure; RM-ANOVA: analysis of variance for repeated measurements; p_w , p_g and p_i : p-values for within subjects, between groups and interaction from two-way RM-ANOVA, respectively.

STH-2 group 150 min after declamping (73.0 ± 3.2 vs. 64.3 ± 2.4 mmHg, $p=0.047$), but did not differ after 240 min. The LV isovolumic relaxation time constant τ and the logarithmic end-diastolic pressure-volume relation β did not differ over time or between groups. Both peak systolic strain in the longitudinal direction (STE) and radial peak ejection strain rate (TDI) decreased over time in both groups (Supplement Figure A and B).

The LV end-diastolic volume (LVEDV), stroke volume and stroke work decreased in both groups from 60 min to 150 min after aortic declamping and reperfusion, paralleled by a borderline significant ($p_w=0.052$) decrease in the RV end-diastolic volume (Supplement Table C).

Myocardial blood flow and mechanical efficiency

Regional tissue blood flow rate in the RV wall did not differ between the groups after declamping, decreased from 60 min to 150 min after declamping ($p = 0.001$) and did not change further (Supplement Table C). LV tissue blood flow rate was high in both groups compared to levels seen at Baseline (Figure 4). Blood flow decreased significantly in the STH-POL group only ($p < 0.005$) from 60 min to 150 min after declamping and was essentially unchanged in the STH-2 group. At 240 min after declamping, LV blood flow was significantly reduced in the STH-POL compared to the STH-2 group ($p < 0.05$). The ratio between LV mechanical energy gain and blood flow rate was reduced by approximately 50% 60 min after aortic declamping compared to Baseline (Figure 4). Left ventricular mechanical efficiency gradually decreased in the STH-2 group only and was significantly lower than in the STH-POL group after 150 and 240 min.

Myocardial oxidative stress, apoptosis and ischemic injury

Apoptotic activation evaluated by caspase-3 activity was more pronounced in the RV and subepicardial LV tissue compared to the myocardium in the mid- and subendocardial left ventricle, but with no differences between the treatment groups (Figure 5). Oxidative stress evaluated by MDA did not differ between different regions of the left and the right ventricle. Serum troponin-T levels accumulated over time from 60 to 240 min after declamping, but did not differ between groups (Supplement Table C). The levels of serum potassium were increased throughout the reperfusion period in the STH-2 compared to the STH-POL group (Supplement Table D).

Discussion

This porcine study indicates better myocardial contractile efficiency, demonstrated as a reduced mismatch between myocardial function and flow after weaning from CPB following 120 min of cardioplegic arrest with St. Thomas' Hospital polarizing solution compared to standard blood cardioplegia. The pressure-volume loop area of the LV potential energy and mechanical performance strongly correlates with myocardial oxygen consumption and, hence, with myocardial blood flow rate.¹⁸⁻²¹ In the present study, both cardioplegic protocols demonstrate a mismatch between performance and myocardial blood flow rate compared to Baseline after 120 min of cardiac arrest (Figure 4). However, cardiac function did not differ between the groups evaluated by

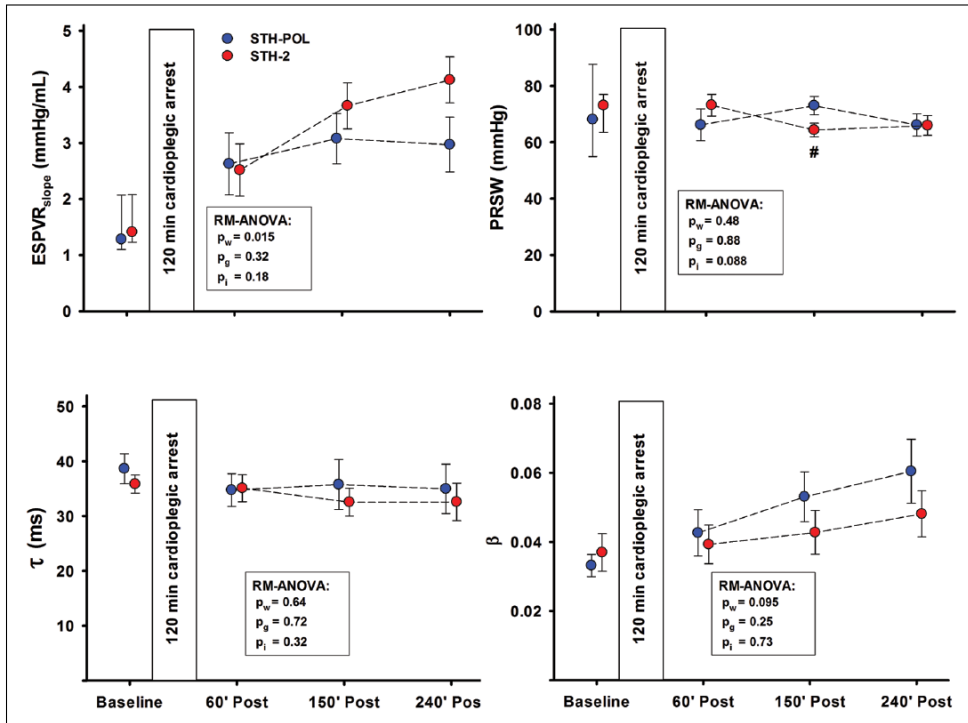


Figure 3. Left ventricle functional variables mean (SEM) or median (25%; 75%) at Baseline and 60, 150 and 240 min after CPB and aortic declamping following 120 min of cardiac arrest with polarizing (STH-POL) and depolarizing (STH-2) cardioplegia, $n=10$ in both groups. Statistics as in Figure 2. ESPVR_{slope}: slope of the end-systolic pressure volume relationship; PRSW: slope of preload recruitable stroke work; Tau (τ): isovolumic relaxation constant; Beta (β): the logarithmic end-diastolic pressure-volume relationship. #: significantly different from STH-POL at 150 min of reperfusion.

variables like CI and ejection fraction after reperfusion and weaning (Figure 2, Supplement Table C). Myocardial blood flow rate was reduced in the STH-POL compared to the STH-2 group at 240 min after declamping. This could be interpreted as a reduction of myocardial stunning following polarizing compared to depolarizing cardioplegia.^{22,23} Depolarizing cardioplegia exposes the myocardium to high levels of potassium during cardioplegic arrest. Several studies have demonstrated that hyperkalaemic cardiac arrest contributes to myocardial stunning.^{6,24,25}

In a previous study, creatine phosphate and adenosine triphosphate (ATP) levels were temporary increased just before and 20 min after declamping following 60 min of cardioplegic arrest with STH-POL compared to STH-2 cardioplegia.¹² Creatine phosphate exerts both anti-oxidant and anti-apoptotic effects.²⁶ One could speculate if these factors might contribute to the improved mechanical efficiency (Figure 4) also seen after 120 min of cardioplegic arrest.

Myocardial blood flow rate is influenced by factors such as preload, afterload, heart rate and resistance in myocardial vessels.²⁷ Neither LVEDP, LVEDV, HR nor MAP differed between the groups after weaning from CPB (Figure 2, Supplement Table C). Both adenosine and esmolol are short-acting and probably do not influence myocardial vascular resistance after reperfusion and weaning.^{11,28,29} In the STH-2 group, hyperkalaemia was present at 60, 150 and 240 min after declamping compared to the STH-POL group (Supplement Table D). Hyperkalaemic cardioplegic solutions may induce vasoconstriction by direct depolarization of vascular smooth muscle or the underlying endothelium in coronary arteries.^{30,31} Conversely, hyperkalaemia does not directly reduce myocardial vascular resistance following dilatation and, hence, relative hyperaemia.³²

In the STH-POL group, two of 10 animals required defibrillation for ventricular fibrillation after declamping compared to eight out of 10 in the STH-2 group, probably related to increased potassium levels in the

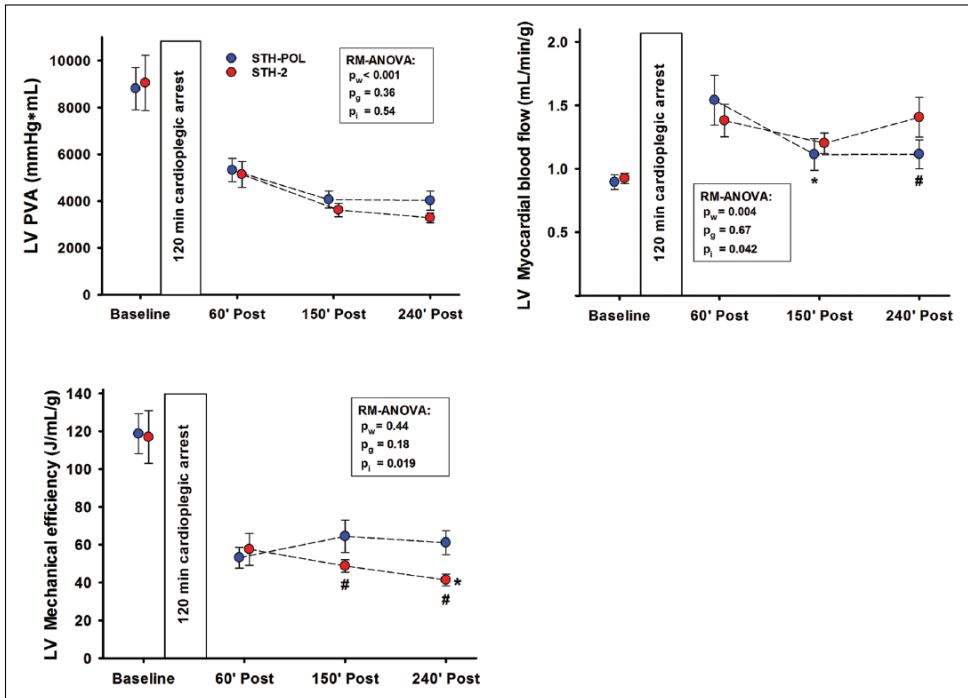


Figure 4. Left ventricular (LV) pressure-volume area (PVA), myocardial blood flow rate and mechanical efficiency at Baseline and 60, 150 and 240 min after CPB and aortic declamping following 120 min of cardioplegic arrest, $n=10$ in both groups. Statistics as in Figure 2. *: significantly different from 60 to 150 or 240 min of reperfusion within group; #: significantly different between groups at corresponding point of time.

latter (Figure 1). Evidence of increased myocardial damage and apoptotic activity in the STH-2 group compared to the STH-POL group was not found in the present study, based on activated caspase-3 or s-troponin-T release (Figure 5, Supplement Table C). There is no evidence of myocardial damage caused by elective external cardioversion in patients, evaluated by the release of s-troponin-T.^{33,34}

Myocardial levels of xanthine oxidase are found to be low in both pigs and in humans.³⁵ Temporary high levels of hypoxanthine are to be expected in the STH-POL group due to degradation of the adenosine component.¹² However, no difference in tissue levels of MDA was found, demonstrating that degradation of hypoxanthine to uric acid by xanthine oxidase did not cause an extra myocardial oxidative stress in the present study.³⁶

Contractility, evaluated as PRSW, was increased 150 min after declamping with STH-POL cardioplegia, but did not differ from the STH-2 group after 240 min (Figure 3). In a previous study comparing STH-POL and STH-2 cardioplegia, LV contractility and myocardial strain rate were better maintained 180 min after

weaning following 60 min of cardioplegic arrest.¹⁰ With an ischemic period of 120 min of cardioplegic arrest in this present study, group differences with regard to contractility faded after 240 min.

Limitations

The present study was performed in young, porcine hearts without clinically relevant pathology. Both the ischemic time and the observation period after declamping were limited. In our experience, 120 min of cardioplegic arrest following weaning from CPB and 240 min of reperfusion is close to the limit of what is feasible and reproducible for a translational animal study design in pigs. The replacement of three vs. five animals in the STH-POL and the STH-2 groups could introduce a selection bias. However, irrespective of cardioplegic solution, the frequency of arrhythmias and pulmonary hypertension after myocardial ischaemia/reperfusion and CPB is high in this model. For the purpose of standardisation, treatment interventions in this protocol were limited, which is reflected in a high mortality rate.

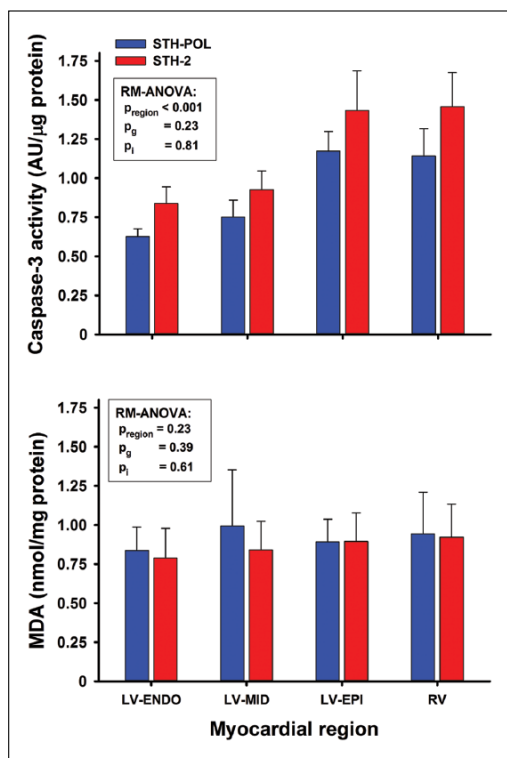


Figure 5. Caspase-3 activity and levels of MDA in myocardial tissue samples obtained at 240 min after reperfusion following CPB and 120 min of cardioplegic arrest with polarizing (STH-POL) or depolarizing (STH-2) cardioplegia, $n=10$ in both groups. MDA: malondialdehyde; LV: left ventricle; RV: right ventricle. p_{region} , p_{g} and p_{i} : p-values for regions within hearts, between groups and interaction from two-way RM-ANOVA, respectively.

Clinical implications

Results from the present study demonstrate polarizing cardioplegia with esmolol, adenosine and magnesium to be non-inferior to standard depolarizing, potassium-based, repeated, oxygenated, blood cardioplegia. Clinical trials determining safety should be conducted before implementation into a new clinical routine. In theory, the use of STH-POL could be beneficial, especially in patients with preoperative left ventricular dysfunction and/or in patients requiring a long period of cardioplegic arrest.

Conclusion

Two hours of cardioplegic arrest with St.Thomas' Hospital polarizing solution in oxygenated blood allevi-

ates mismatch between myocardial function and perfusion after weaning from CPB compared to St.Thomas' Hospital No 2 blood cardioplegia.

Acknowledgements

The technical assistance from Cato Johnsen, Kjersti Milde, Gry-Hilde Nilsen and the staff at the Vivarium, University of Bergen is greatly appreciated.


Declaration of Conflicting Interests

The authors declared the following potential conflicts of interest with respect to the research, authorship, and/or publication of this article: Co-author David J. Chambers declares a conflict of interest in that he is co-inventor of a novel cardioplegic solution in which esmolol and adenosine are essential components. A European patent has been granted for this cardioplegia; a US patent application is filed. All other authors declare no conflict of interest.

Funding

The authors disclosed receipt of the following financial support for the research, authorship, and/or publication of this article: Financial support was received from the Western Norway Regional Health Authority, the University of Bergen Heart Fund, the Norwegian Health Association and the Grieg Foundation.

ORCID iD

Terje Aass  <https://orcid.org/0000-0003-4207-3454>

References

1. Yamamoto H, Yamamoto F. Myocardial protection in cardiac surgery: a historical review from the beginning to the current topics. *Gen Thorac Cardiovasc Surg* 2013; 61: 485–496.
2. Braathen B, Jeppson A, Schersten H, et al. One single dose of histidine-tryptophan-ketoglutarate solution gives equally good myocardial protection in elective mitral valve surgery as repetitive cold blood cardioplegia: a prospective randomized study. *J Thorac Cardiovasc Surg* 2011; 141: 995–1001.
3. Ramanathan R, Parrish DW, Armour TK, et al. Use of del Nido cardioplegia in adult cardiac surgery. *Thorac Cardiovasc Surg* 2015; 63: 624–627.
4. Ferguson ZG, Yarbrough DE, Jarvis BL, et al. Evidence-based medicine and myocardial protection—where is the evidence? *Perfusion* 2015; 30: 415–422.
5. Zeng J, He W, Qu Z, et al. Cold blood versus crystalloid cardioplegia for myocardial protection in adult cardiac surgery: a meta-analysis of randomized controlled studies. *J Cardiothorac Vasc Anesth* 2014; 28: 674–681.
6. Dobson GP, Faggian G, Onorati F, et al. Hyperkalemic cardioplegia for adult and pediatric surgery: end of an era? *Front Physiol* 2013; 4: 228.
7. Mehlhorn U, Sauer H, Kuhn-Regnier F, et al. Myocardial beta-blockade as an alternative to cardioplegic arrest during coronary artery surgery. *Cardiovasc Surg* 1999; 7: 549–557.

8. Dobson GP, Letson HL. Adenosine, lidocaine, and Mg²⁺ (ALM): from cardiac surgery to combat casualty care—teaching old drugs new tricks. *J Trauma Acute Care Surg* 2016; 80: 135–145.
9. Malhotra A, Wadhawa V, Ramani J, et al. Normokalemic nondepolarizing long-acting blood cardioplegia. *Asian Cardiovasc Thorac Ann* 2017; 25: 495–501.
10. Aass T, Stangeland L, Moen CA, et al. Myocardial function after polarizing versus depolarizing cardiac arrest with blood cardioplegia in a porcine model of cardiopulmonary bypass. *Eur J Cardiothorac Surg* 2016; 50: 130–139.
11. Chambers DJ, Fallouh HB. Cardioplegia and cardiac surgery: pharmacological arrest and cardioprotection during global ischemia and reperfusion. *Pharmacol Ther* 2010; 127: 41–52.
12. Aass T, Stangeland L, Chambers DJ, et al. Myocardial energy metabolism and ultrastructure with polarizing and depolarizing cardioplegia in a porcine model. *Eur J Cardiothorac Surg* 2017; 52: 180–188.
13. Fannelop T, Dahle GO, Matre K, et al. An anaesthetic protocol in the young domestic pig allowing neuromuscular blockade for studies of cardiac function following cardioplegic arrest and cardiopulmonary bypass. *Acta Anaesthesiol Scand* 2004; 48: 1144–1154.
14. Steendijk P, Staal E, Jukema JW, et al. Hypertonic saline method accurately determines parallel conductance for dual-field conductance catheter. *Am J Physiol Heart Circ Physiol* 2001; 281: H755–763.
15. Szwarz RS, Mickleborough LL, Mizuno S, et al. Conductance catheter measurements of left ventricular volume in the intact dog: parallel conductance is independent of left ventricular size. *Cardiovasc Res* 1994; 28: 252–258.
16. Hawk C, Leary SL, Morris TH. *Formulary for laboratory animals*. 3rd Edition. Ames: Blackwell Publishing Professional, 2005, p.203.
17. Kowallik P, Schulz R, Guth BD, et al. Measurement of regional myocardial blood flow with multiple colored microspheres. *Circulation* 1991; 83: 974–982.
18. Gibbs CL. Mechanical determinants of myocardial oxygen consumption. *Clin Exp Pharmacol Physiol* 1995; 22: 1–9.
19. Knaapen P, Germans T, Knutti J, et al. Myocardial energetics and efficiency: current status of the noninvasive approach. *Circulation* 2007; 115: 918–927.
20. Suga H. Ventricular energetics. *Physiol Rev* 1990; 70: 247–277.
21. Vinten-Johansen J, Duncan HW, Finkenber JG, et al. Prediction of myocardial O₂ requirements by indirect indices. *Am J Physiol* 1982; 243: H862–868.
22. Heusch G, Schulz R. Perfusion-contraction match and mismatch. *Basic Res Cardiol* 2001; 96: 1–10.
23. Kassiotis C, Rajabi M, Taegtmeier H. Metabolic reserve of the heart: the forgotten link between contraction and coronary flow. *Prog Cardiovasc Dis* 2008; 51: 74–88.
24. Damiano RJ, Jr., Cohen NM. Hyperpolarized arrest attenuates myocardial stunning following global surgical ischemia: an alternative to traditional hyperkalemic cardioplegia? *J Card Surg* 1994; 9: 517–525.
25. Anselmi A, Abbate A, Girola F, et al. Myocardial ischemia, stunning, inflammation, and apoptosis during cardiac surgery: a review of evidence. *Eur J Cardiothorac Surg* 2004; 25: 304–311.
26. Gaddi AV, Galuppo P, Yang J. Creatine phosphate administration in cell energy impairment conditions: a summary of past and present research. *Heart Lung Circ* 2017; 26: 1026–1035.
27. Schremmer B, Dhainaut JF. Regulation of myocardial oxygen delivery. *Intensive Care Med* 1990; 16 Suppl 2: S157–163.
28. Belardinelli L, Shryock JC, Song Y, et al. Ionic basis of the electrophysiological actions of adenosine on cardiomyocytes. *FASEB J* 1995; 9: 359–365.
29. Sum CY, Yacobi A, Kartzinel R, et al. Kinetics of esmolol, an ultra-short-acting beta blocker, and of its major metabolite. *Clin Pharmacol Ther* 1983; 34: 427–434.
30. Han JG, Yang Q, Yao XQ, et al. Role of large-conductance calcium-activated potassium channels of coronary arteries in heart preservation. *J Heart Lung Transplant* 2009; 28: 1094–1101.
31. He GW. Endothelial function related to vascular tone in cardiac surgery. *Heart Lung Circ* 2005; 14: 13–18.
32. Goodwill AG, Dick GM, Kiel AM, et al. Regulation of coronary blood flow. *Compr Physiol* 2017; 7: 321–382.
33. Cemin R, Rauhe W, Marini M, et al. Serum troponin I level after external electrical direct current synchronized cardioversion in patients with normal or reduced ejection fraction: no evidence of myocytes injury. *Clin Cardiol* 2005; 28: 467–470.
34. Lund M, French JK, Johnson RN, et al. Serum troponins T and I after elective cardioversion. *Eur Heart J* 2000; 21: 245–253.
35. Muxfeldt M, Schaper W. The activity of xanthine oxidase in heart of pigs, guinea pigs, rabbits, rats, and humans. *Basic Res Cardiol* 1987; 82: 486–492.
36. Kim YJ, Ryu HM, Choi JY, et al. Hypoxanthine causes endothelial dysfunction through oxidative stress-induced apoptosis. *Biochem Biophys Res Commun* 2017; 482: 821–827.

Animals and anaesthesia

The pigs, weighing 42 ± 3 (SD) kg, were premedicated with an intramuscular injection of a mixture of ketamine (20 mg/kg), diazepam (10 mg) and atropine (1 mg) followed by a short period of spontaneous mask ventilation with oxygen and 3% isoflurane (Rhodia, Bristol, UK), allowing cannulation of two ear veins. Loading doses of fentanyl (0.02 mg/kg), midazolam (0.3 mg/kg), pancuronium (0.063 mg/kg) and pentobarbital (15 mg/kg) were given IV, followed by continuous infusion of fentanyl (0.02 mg/kg/h), midazolam (0.3 mg/kg/h), pancuronium (0.2 mg/kg/h) and pentobarbital (4 mg/kg/h). The animals were tracheotomised and ventilated (Julian, Drägerwerk, Lübeck, Germany) with a mixture of nitrous oxide (56-58%) and oxygen. Tidal volume was set to 11 mL/kg and the frequency adjusted, aiming at an end-tidal $p\text{CO}_2$ ranging from 5.0 to 5.6 kPa. This anaesthetic protocol has been thoroughly evaluated previously, allowing the use of a neuromuscular blocking agent in young pigs.^A

Epicardial echocardiography

The echocardiographic recordings were performed with a Vivid E9 scanner and a 6S cardiac probe (GE Vingmed Ultrasound, Horten, Norway). The respirator was disconnected during recordings. A soft silicon pad (4×4×3 cm) served as an offset between the epicardium and the sector probe.^B B-mode cine-loops of the short-axis view at the equator were recorded and used for speckle tracking analysis (STE) of radial and circumferential strain. In the same view a high frame-rate recording focusing on the anterior left ventricular wall was obtained with Tissue Doppler Imaging (TDI) for strain and strain rate measurements. From the apical view pulsed-wave Doppler velocity recordings from the aortic valve were obtained for timing purposes. Still in the long-axis view, 4-chamber B-mode cine-loops of the left ventricle were obtained for STE analysis of longitudinal strain. All analyses were performed off-line using EchoPac BT12 (GE Vingmed Ultrasound). End-diastole was defined as the beginning of the first deflection of the QRS complex on electrocardiogram, whereas the end-systole was defined as the time of aortic valve closure on corresponding pulsed-wave Doppler spectral recordings. For TDI analysis, strain length (SL) was set to 6 mm and the region of interest (ROI) to 6×6 mm. The ROI was

placed within a distance of $\frac{1}{2}$ SL from the epicardium and $\frac{1}{2}$ SL from the endocardium. Regional STE-strain in the circumferential and radial direction was recorded in the Antero-Septal segment, longitudinal strain in the Mid-Septal segment. Both radial peak systolic strain and peak ejection strain rate in the anterior left ventricular wall were obtained from the TDI recordings.

Statistical analysis

Data analyses were performed by SPSS v. 23 (IBM Corp., Armonk, NY, USA) and values given as mean \pm SEM or median (25% percentile; 75 % percentile) unless otherwise noted. The Baseline variables were compared by two-sample Student t-test and Wilcoxon-Mann-Whitney test on ranks, whenever appropriate. Hemodynamic variables during CPB and after aortic declamping were compared with two-way analysis of variance for repeated measures (RM-ANOVA) with STH-POL or STH-2 as group factor (p_g) and time as within factor (p_w) with post hoc Bonferroni contrasts when appropriate.^c The Greenhouse-Geisser adjustment of degrees of freedom was used for the evaluation of main effects when Mauchly's test of sphericity was significant ($p < 0.05$). If a significant interaction ($p_i < 0.10$) was found, new ANOVAs for simple main effect were performed with adjustment of degrees of freedom. Cell means were finally compared with Neumann-Keuls multiple contrast tests when justified by the preceding ANOVA. The Intraclass Correlation Coefficient (ICC) for 20 randomly selected TDI recordings was calculated.

A:

Fannelop T et al. Acta Anaesthesiol Scand 2004; 48(9): 1144-54. PMID: 15352961.
<https://onlinelibrary.wiley.com/doi/abs/10.1111/j.1399-6576.2004.00464.x>

B:

Moen CA et al. Eur Heart J Cardiovasc Imaging. 2013; 14(1): 24-37. PMID: 22531463
<https://academic.oup.com/ehjcardio/article/14/1/24/2947830>

C:

Tybout A et al. Journal of Consumer Psychology 2001; 10(1-2): 5-35.
<https://www.sciencedirect.com/science/article/pii/S1057740801702446>

Supplement Table A.

Baseline variables before cardioplegic arrest in two groups of pigs randomized to 120 min of polarizing (STH-POL) or depolarizing (STH-2) cardioplegic arrest.

Variable	STH-POL	STH-2	p-statistics
LV-EDV _i (mL/m ²)	77 ± 3	82 ± 4	0.38
LV-ESV _i (mL/m ²)	35 ± 1	37 ± 3	0.42
LV-SV _i (mL/m ²)	43 ± 2	45 ± 1	0.58
LV-EF (%)	55 ± 1	55 ± 2	0.91
LV-SW _i (mmHg*mL/m ²)	4230 ± 361	4389 ± 385	0.77
LV-flow-Epi (mL/min/g)	0.83 ± 0.05	0.86 ± 0.04	0.67
LV-flow-Mid (mL/min/g)	0.96 ± 0.5	0.98 ± 0.05	0.73
LV-flow-Endo (mL/min/g)	1.00 ± 0.06	1.03 ± 0.05	0.70
RV-EDV _i (mL/m ²)	130 (119; 165)	125 (110; 149)	0.21
RV-EF (%)	25 (22; 26)	27 (24; 33)	0.20
RV-flow (mL/min/g)	0.62 ± 0.05	0.67 ± 0.05	0.53
AOP _{mean} (mmHg)	98 ± 6	97 ± 4	0.90
CVP _{mean} (mmHg)	7.0 ± 0.7	7.2 ± 0.7	0.89
PAP _{mean} (mmHg)	17.8 (15.4; 19.5)	18.8 (16.1; 21.2)	0.39
pH	7.49 (7.45; 7.52)	7.51 (7.49; 7.53)	0.43
pCO ₂ (kPa)	5.2 (4.5; 5.4)	5.3 (5.0; 5.4)	0.60
pO ₂ (kPa)	25.2 ± 0.6	26.1 ± 0.4	0.19
BE (mmol/L)	6.6 (0.3; 8.0)	7.3 (5.5; 9.1)	0.33
HCO ₃ ⁻ (mmol/L)	30.2 (23.8; 31.6)	30.8 (28.9; 32.7)	0.33
Hb (g/dL)	8.8 ± 0.2	8.9 ± 0.1	0.60
Hct (%)	26.5 ± 0.5	26.9 ± 0.3	0.56
s-Na ⁺ (mmol/L)	139 (138; 140)	140 (139; 140)	0.45
s-K ⁺ (mmol/L)	3.9 (3.8; 4.1)	3.9 (3.8; 4.2)	0.82
s-Cl ⁻ (mmol/L)	102 ± 1	102 ± 1	0.62
s-troponin-T (ng/L)	46 (39; 61)	60 (40; 110)	0.43
Temperature _{rectal} (°C)	38.4 ± 0.2	38.4 ± 0.2	0.85
Diuresis (mL/kg/h)	2.3 (1.6; 3.6)	2.7 (1.7; 3.9)	0.68

Values are mean ± SEM or median (25-percentile; 75-percentile), n = 10.

LV and RV = left and right ventricle; _i = value indexed for body surface area; ESV and EDV = end-systolic and end-diastolic volume; SV = stroke volume; EF = ejection fraction; SW = stroke work; Epi-, Mid- and Endo- = subepi-, midmyo- and subendocardium. AOP, CVP and PAP = aortic, central venous and pulmonary artery pressure; p-values from two-sample t-tests or Mann-Whitney Rank Sum Tests.

Supplemental Table B.

Arterial blood gases, haemoglobin and electrolytes during cardiopulmonary bypass in two groups of pigs with 120 min of polarizing (STH-POL) or depolarizing (STH-2) cardioplegic arrest.

Variable	1 min before X-clamp (A)	60 min X-clamp (B)	118 min X-clamp (C)	RM-ANOVA statistics
pH				
STH-POL	7.42 ± 0.01	7.39 ± 0.01	7.39 ± 0.02	$p_w < 0.001, p_g = 0.19, p_i = 0.042$
STH-2	7.42 ± 0.01	7.35 ± 0.01 ^{a,#}	7.38 ± 0.01 ^{a,b}	
pO ₂ (kPa)				
STH-POL	15.7 ± 1.5	27.7 ± 2.1	17.3 ± 1.1	$p_w < 0.001, p_g = 0.42, p_i = 0.68$
STH-2	14.0 ± 1.0	25.5 ± 2.0	17.6 ± 1.7	
pCO ₂ (kPa)				
STH-POL	5.5 ± 0.2	6.3 ± 0.2 ^a	6.4 ± 0.3 ^a	$p_w < 0.001, p_g = 0.52, p_i = 0.082$
STH-2	5.7 ± 0.2	6.9 ± 0.3 ^{a,#}	6.1 ± 0.2 ^{a,b}	
HCO ₃ ⁻ (mmol/L)				
STH-POL	26.7 ± 0.8	28.1 ± 0.8	27.6 ± 1.0	$p_w = 0.13, p_g = 0.81, p_i = 0.40$
STH-2	27.1 ± 0.9	27.8 ± 1.0	26.6 ± 1.2	
BE (mmol/L)				
STH-POL	2.1 ± 0.8	3.0 ± 0.8	2.4 ± 1.1	$p_w = 0.29, p_g = 0.65, p_i = 0.24$
STH-2	2.5 ± 0.8	2.1 ± 0.8	1.3 ± 1.1	
Hb (g/dL)				
STH-POL	6.5 ± 0.2	7.6 ± 0.2	7.7 ± 0.3	$p_w < 0.001, p_g = 0.078, p_i = 0.27$
STH-2	6.6 ± 0.2	8.4 ± 0.3	8.5 ± 0.3	
s-Na ⁺ (mmol/L)				
STH-POL	138 ± 1	139 ± 1	139 ± 1	$p_w = 0.59, p_g = 0.72, p_i = 0.17$
STH-2	139 ± 1	139 ± 1	138 ± 1	
s-Cl ⁻ (mmol/L)				
STH-POL	103 ± 1	103 ± 1	104 ± 1 ^{a,b}	$p_w < 0.001, p_g = 0.13, p_i = 0.098$
STH-2	103 ± 1	105 ± 1 ^{a,#}	105 ± 1 ^{a,b}	

Values are mean ± SEM, n = 10.

s = serum levels; p_w, p_g, p_i = p-values for within subjects, between groups and for interaction from two-way RM-ANOVA, respectively; ^a and ^b = significantly different within the same group mean from value(s) in columns with corresponding capital letter; # = significantly different from STH-POL at 60 min of aortic cross-clamping (X-clamp).

Supplement Table C.

Cardiac and haemodynamic variables, tissue blood flow and serum troponins 60, 150 and 240 min after aortic declamping following 120 min of polarizing (STH-POL) or depolarizing (STH-2) cardioplegic arrest.

Variable	60 min	150 min	240 min	RM-ANOVA statistics
LV-ESV _i (mL/m ²)				
STH-POL	24 ± 4	22 ± 2	22 ± 1	p _w = 0.81, p _g = 0.76, p _i = 0.75
STH-2	23 ± 3	23 ± 3	24 ± 4	
LV-EDV _i (mL/m ²)				
STH-POL	63 ± 5	54 ± 5	55 ± 2	p _w = 0.046, p _g = 0.99, p _i = 0.79
STH-2	61 ± 5	54 ± 3	57 ± 5	
LV-SV _i (mL/m ²)				
STH-POL	39 ± 3	32 ± 2	34 ± 2	p _w < 0.001, p _g = 0.75, p _i = 0.89
STH-2	37 ± 3	32 ± 1	33 ± 2	
LV-EF (%)				
STH-POL	62 ± 3	60 ± 2	61 ± 2	p _w = 0.52, p _g = 0.72, p _i = 0.93
STH-2	62 ± 2	60 ± 3	59 ± 4	
SW _i (mmHg*mL/m ²)				
STH-POL	3046 ± 278	2520 ± 273	2468 ± 255	p _w < 0.001, p _g = 0.58, p _i = 0.84
STH-2	2983 ± 290	2297 ± 142	2252 ± 201	
RV-EDV _i (mL/m ²)				
STH-POL	150 ± 7	136 ± 5	134 ± 5	p _w = 0.052, p _g = 0.71, p _i = 0.25
STH-2	139 ± 11	138 ± 9	134 ± 6	
RV-EF (%)				
STH-POL	29 ± 2	27 ± 1	29 ± 2	p _w = 0.35, p _g = 0.69, p _i = 0.94
STH-2	28 ± 2	26 ± 2	29 ± 2	
RV blood flow rate (mL/min/g)				
STH-POL	1.65 ± 0.19	1.18 ± 0.09	1.23 ± 0.12	p _w = 0.006, p _g = 0.089, p _i = 0.76
STH-2	1.96 ± 0.23	1.46 ± 0.12	1.69 ± 0.23	
MAP (mmHg)				
STH-POL	75 ± 8	59 ± 4	60 ± 4	p _w < 0.001, p _g = 0.68, p _i = 0.66
STH-2	75 ± 5	64 ± 4	63 ± 4	
CVP _{mean} (mmHg)				
STH-POL	8.6 ± 0.7	9.4 ± 0.6	10.6 ± 0.7	p _w = 0.054, p _g = 0.093, p _i = 0.39
STH-2	10.9 ± 1.2	11.5 ± 1.0	11.6 ± 0.8	
PAP _{mean} (mmHg)				
STH-POL	26 ± 2	25 ± 2	25 ± 1	p _w = 0.027, p _g = 0.19, p _i = 0.18
STH-2	31 ± 3	29 ± 2	27 ± 2	
s-troponin-T (ng/L)				
STH-POL	519 ± 98	527 ± 76	802 ± 114	p _w < 0.001, p _g = 0.35, p _i = 0.33
STH-2	743 ± 155	707 ± 140	907 ± 169	

Values are mean ± SEM for 10 animals in each group.

LV and RV = left and right ventricle; _i = value indexed for body surface area; ESV and EDV = end-systolic and end-diastolic volume; SV = stroke volume; EF = ejection fraction; SW = stroke work; MAP, CVP and PAP = mean arterial-, central venous- and pulmonary artery pressure; s- = serum. p_w, p_g and p_i = p-values for within subjects, between groups and interaction from two-way RM-ANOVA, respectively.

Supplement Table D.

Arterial blood gases, haemoglobin, electrolytes, temperature and diuresis in pigs 60, 150 and 240 min after weaning from 120 min of polarizing (STH-POL) or depolarizing (STH-2) cardioplegic arrest.

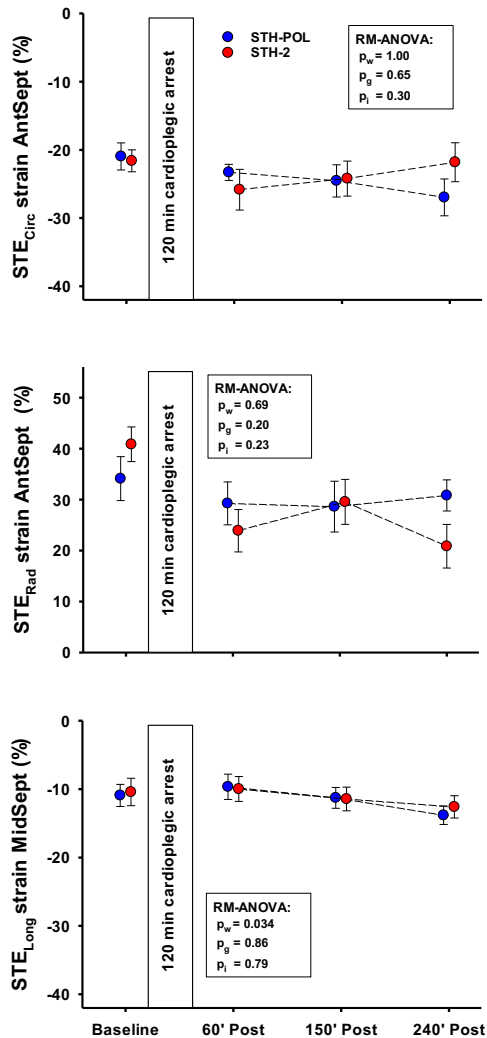
Variable	60 min	150 min	240 min	RM-ANOVA statistics
pH				
STH-POL	7.42 ± 0.01	7.43 ± 0.01	7.43 ± 0.02	$p_w = 0.005, p_g = 0.74, p_i = 0.056$
STH-2	7.41 ± 0.02	7.44 ± 0.02	7.45 ± 0.01 ^a	
pCO ₂ (kPa)				
STH-POL	5.4 ± 0.2	5.4 ± 0.2	5.4 ± 0.3	$p_w = 0.19, p_g = 0.58, p_i = 0.14$
STH-2	5.8 ± 0.2	5.5 ± 0.2	5.4 ± 0.2	
pO ₂ (kPa)				
STH-POL	17.0 ± 2.1	19.8 ± 1.3	20.9 ± 2.1	$p_w < 0.001, p_g = 0.89, p_i = 0.73$
STH-2	16.0 ± 2.0	19.4 ± 1.7	21.3 ± 1.2	
HCO ₃ ⁻ (mmol/L)				
STH-POL	25.9 ± 1.3	26.2 ± 1.5	26.6 ± 1.5	$p_w = 0.24, p_g = 0.57, p_i = 0.84$
STH-2	27.0 ± 1.3	27.6 ± 1.5	27.6 ± 1.4	
BE (mmol/L)				
STH-POL	1.5 ± 1.3	1.8 ± 1.5	2.1 ± 1.5	$p_w = 0.036, p_g = 0.56, p_i = 0.54$
STH-2	2.2 ± 1.4	3.4 ± 1.5	3.3 ± 1.4	
Hb (g/dL)				
STH-POL	9.0 ± 0.3	8.5 ± 0.2	7.8 ± 0.2	$p_w < 0.001, p_g = 0.098, p_i = 0.53$
STH-2	8.4 ± 0.2	7.8 ± 0.3	7.4 ± 0.2	
Hct (%)				
STH-POL	27.1 ± 0.8	25.7 ± 0.7	23.5 ± 0.7	$p_w < 0.001, p_g = 0.11, p_i = 0.53$
STH-2	25.3 ± 0.8	23.7 ± 0.9	22.4 ± 0.7	
s-Na ⁺ (mmol/L)				
STH-POL	141 ± 1	142 ± 1	142 ± 1	$p_w = 0.67, p_g = 0.001, p_i = 0.47$
STH-2	139 ± 1	138 ± 1	138 ± 1	
s-K ⁺ (mmol/L)				
STH-POL	4.5 ± 0.1	4.8 ± 0.1	5.0 ± 0.1	$p_w < 0.001, p_g = 0.013, p_i = 0.45$
STH-2	5.1 ± 0.2	5.6 ± 0.3	5.5 ± 0.3	
s-Cl ⁻ (mmol/L)				
STH-POL	104 ± 1	105 ± 1 ^a	105 ± 1 ^a	$p_w = 0.17, p_g = 0.14, p_i = 0.006$
STH-2	104 ± 1	103 ± 1	104 ± 1	
Temp _{rect} (°C)				
STH-POL	37.7 ± 0.1	37.8 ± 0.2	37.8 ± 0.2	$p_w = 0.026, p_g = 0.98, p_i = 0.097$
STH-2	37.4 ± 0.2	37.8 ± 0.2 ^a	38.0 ± 0.2 ^a	
Diuresis (mL/kg/h)				
STH-POL	12.5 ± 2.8	5.9 ± 1.2	3.4 ± 0.8	$p_w < 0.001, p_g = 0.37, p_i = 0.56$
STH-2	9.8 ± 1.5	4.1 ± 0.8	3.3 ± 0.4	

Values are mean ± SEM, n = 10.

s- = serum; Temp_{rect} = rectal temperature. p_w, p_g, p_i = p-values for within subjects, between groups and for interaction from two-way RM-ANOVA, respectively. ^a denotes significantly different from 60 min.

Supplement Figure A

Regional peak systolic strain by Speckle Tracking Echocardiography (STE).



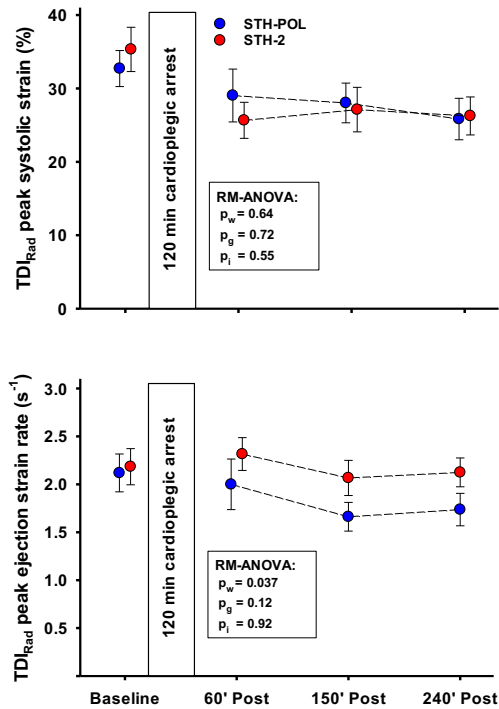
Values are mean \pm SEM for 10 experiments in each group.

Regional strain by Speckle Tracking Echocardiography in the circumferential (STE_{Circ}) and radial (STE_{Rad}) directions from the short-axis view in the antero-septal (AntSept) segment, and in the Longitudinal direction (STE_{Long}) from the four-chamber view in the mid-septal (MidSept) segment. STH-POL and STH-2 = polarizing and depolarizing cardioplegia. RM-ANOVA = analysis of variance for repeated measurements; p_w , p_g , p_i = p-values for within subjects, between groups and for interaction from two-way RM-ANOVA, respectively.

Frame rates for the STE recordings were 74 ± 5 (SD) (range 63 – 88) frames/s, in the short-axis view and 74 ± 8 (range 63 – 93) frames/s in the four-chamber view.

Supplement Figure B

Peak systolic strain and peak ejection strain rate by Tissue Doppler Imaging (TDI).



Values are mean \pm SEM for 10 experiments in each group.

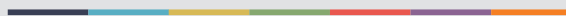
Radial peak systolic strain and peak ejection strain rate in the left ventricular anterior wall by Tissue Doppler Imaging from the short-axis view. STH-POL and STH-2 = polarizing and depolarizing cardioplegia. RM-ANOVA = analysis of variance for repeated measurements; p_w, p_g, p_i = p-values for within subjects, between groups and for interaction from two-way RM-ANOVA, respectively.

Frame rate for the TDI recordings were 619 ± 67 (SD) (range 327 - 749) frames/s.

Two independent observers analysed 20 randomly selected TDI recordings. The Intraclass Correlation Coefficient for inter-observer variability was 0.783 for peak systolic strain and 0.874 for peak ejection strain rate.



Graphic design: Communication Division, UIB / Print: Skjipes Kommunikasjon AS



uib.no

ISBN: 978-82-308-3572-2